Project Report

Combining Mineral Fines with Chemical Dispersants to Disperse Oil in Low Temperature and Low Mixing Environments, Including the Arctic

Contract No. E12PC00006

Submitted to:

Frank Bennett, Contracting Officer
and
Hung Nguyen, Contracting Officer Representative

Procurement Operations Branch
Department of the Interior, Bureau of Safety and Environmental Enforcement (BSEE)
381 Elden Street (MS 2101)
Herndon VA 20170

Submitted by:

Kenneth Lee[1]*, Ying Zheng[2], François Xavier Merlin[3], Zhengkai Li[1], Haibo Niu[1], Thomas King[1], Brian Robinson[1], P.E. Kepkay[1], G.D. Wohlgeschaffen[1] and R. Doane[1]

[1]Centre for Offshore Oil, Gas and Energy Research; Fisheries and Oceans Canada
1 Challenger Drive, PO Box 1006, Dartmouth, NS, Canada, B2Y 4A2

[2]Department of Chemical Engineering, University of New Brunswick
Fredericton, New Brunswick, Canada, E3B 5A3

[3]Center of Documentation, Research and Experimentation on Accidental Water Pollution
Rue Alain Colas/BP 20413, Brest Cedex 29604, France

*Corresponding Author: Phone: (902) 426-7344; E-mail: ken.lee@dfo-mpo.gc.ca

May 31, 2012

Table of Contents

List of Tables

List of Figures

1. Introduction

In February, 2010 the U.S. Department of the Interior, Bureau of Safety and Environmental Enforcement (BSEE) (at the time the Minerals Management Service – MMS) awarded research funding under MMS Contract No. E12PC00006 (formerly MMS #M10PC00071) to the Centre for Offshore Oil, Gas and Energy Research (COOGER) of the Department of Fisheries and Oceans Canada. The funding was made available to carry out a two-year research program, the scope of which included: bench studies on the formation and oil dispersion efficacy of Oil-Mineral-Aggregates (OMA) using different types of mineral fines; laboratory tests to determine how mineral fines affect chemical dispersant efficiency; and wave tank experiments to validate laboratory results at the meso-scale.

The research is managed by COOGER (Bedford Institute of Oceanography, Dartmouth, Nova Scotia), and conducted by its scientists as well as those in the Department of Chemical Engineering, University of New Brunswick (UNB) (Fredericton, New Brunswick), and the Center of Documentation, Research and Experimentation (CEDRE) on Accidental Water Pollution (Brest, France). The primary objective of the study is to assess the feasibility of a cold water and Arctic marine oil spill countermeasure strategy based on the stimulation of OMA formation in combination with chemical dispersant. Both of these treatment technologies have been proven to enhance the dispersion of oil spilled at sea. This study is designed to assess the possibility of enhanced dispersion based on the synergistic effects of chemical dispersants and mineral fine particles on oil dispersion efficiency. Experiments were conducted in both laboratory and wave tank systems under controlled conditions to evaluate the potential effectiveness of the treatment method on oil spills from shipboard and rig operations. Mathematical models have also been used to assess the environmental risks of the proposed operational strategy, and to assess the effectiveness of the field application of the developed technique as a means to provide guidance for field operations. The study aims to evaluate the applicability of combining a dispersant with common mineral fines to treat oil slicks in low energy regimes that are typical in cold water and ice-prone environments such as the Arctic.

The primary tasks undertaken in the study include:

- Conducting laboratory baffled flask tests (BFT) on the formation of OMA with addition of chemical dispersants in dispersion of oil at low temperature conditions;
- Conducting Institut Français du Pétrole (IFP) laboratory tests on the feasibility of stimulating oil dispersion at low temperature and under low mixing energy conditions by using a combination of dispersants and mineral fines derived from drilling operations;

- Performing wave tank testing on the influence of factors such as wave conditions and the presence of chemical dispersants on the formation and transport of OMA at low temperature.
- Preliminary modeling of the fate and biological effects of OMA formation as an oil spill response option.

Three oils were used in laboratory tests using EPA standard baffled flask tests and the flow-through wave tank facility. The oils are weathered Alaska North Slope (ANS), weathered Arabian Light Crude (ALC), and a Fuel Oil (IFO-40). These represent the commonly encountered oils that might be transported, and may be candidate oils requiring oil spill response in cold waters, including the Arctic. A fourth crude oil, Alberta Sweet Blend, was used in the modified IFP test by CEDRE. Chemical dispersants in baffled flask tests included Corexit 9500 and Corexit 9527, the two most commonly stocked commercial chemical dispersants in North America. A European chemical oil dispersant formulation, GAMLEN OD 4000, was used in the modified IFP tests conducted by CEDRE.

Mineral fine products of kaolin were used in the baffled flask tests. These products were selected based on previous research that has shown kaolin to be the most effective among a number of mineral fine particles in forming oil-mineral aggregates (Lee, 2002; Stoffyn-Egli and Lee, 2002), and allow for comparison of the results with those obtained from a previous OMA study at normal temperature (Lee et al., 2009; Zhang et al., 2010). CEDRE included bentonite and sepiolite in their screening of mineral fine particles for subsequent systematic tests (see Section 3). In the event of emergency spill response operations, these mineral fine particles are readily available as commercial products for use by the offshore oil and gas industry for the formulation of drilling muds on-site. The study was designed to test the feasibility of adding mineral fines to promote and enhance the dispersion of oil in a calm environment, and to prevent the oil from re-coalescing and rising to the sea surface. To facilitate a comparison of results, the same mineral fine (kaolin) and dispersant formulations were used by the laboratories.

2. Baffled Flask Laboratory Experiments: Formation of OMA with Chemical Dispersants under Low Temperature Conditions

2.1. Materials and Methods

2.1.1 Measurement of Crude Oil and Mineral Properties

The reference test oils, dispersants, and mineral fines were selected for use in this study following consultation with BSEE's Scientific Authority for the project. The physical and chemical properties of the materials used for the baffled flask experiments are summarized in Table 1. The Saturate, Aromatic, Resin and Asphaltene (SARA) content of the oil was determined using thin layer chromatography coupled to flame ionization detection (Iatroscan Mk 6, Shell-USA, Virginia, USA). Crude oil density was measured by a portable densimeter (DMA 35N, Anton Paar GmbH, Graz, Austria) at 22˚C. The boiling points for different components in the oils were measured following ASTM-2887 using the simulation distillation method (Shimadzu GC-2010). Viscosities of crudes were assessed using a viscosimeter (Bohlin Geminin HR Nano Rheometer manufactured by Malvern Instrument) following ASTM D445-06.

Kaolin, mined as kaolin in numerous parts of the world, is a layered silicate mineral with the chemical composition $Al_2Si_2O_5(OH)_4$. For comparative purposes within this study, modified kaolin with an increased level of hydrophobicity (more than the commercial product) was prepared using a methodology described in the literature (Molphy et al. 1994). The following procedures were taken to modify kaolin particles. First, 120 mL toluene was added to a 3 neck flask and preheated to 60^{o}C. Then 2 grams of the original kaolin was added, followed by 30 µL toluene diisocyanate (TDI) and stirring for 3 hours. Subsequently, the temperature was increased to 80, 85, and 87^{o}C to obtain different hydrophobic amounts. Then, 30 mL butanol was added and stirred for another 3 hours. Finally, the reaction was stopped and the modified kaolin was washed with deionized water and dried overnight.

The size distribution of the modified minerals was measured by a laser particle size analyzer (Analysette 22 compact, Fritsch Gmbh, Idar-Oberstein, Germany) and surface area was determined by BET nitrogen adsorption (Belsorp-max, Bel, Japan). The hydrophobicity was determined based on the static contact angle that was measured using a JC200A instrument (PowerEach, China) with a digital photo analyzer, imaging at 3 s after the water contacted the sample pellet. The coatings of alkyl groups on the modified kaolin were identified on the infrared spectra (IRS), generated by a Nicolet 6700 (Thermo Scientific, USA).

Table 1: Test materials used

Properties of oils							
	Saturates %	**Aromatics %**	**Resins %**	**Asphaltenes %**	**Weathered %**	**Density (g/ml)**	**Viscosity cSt at 20°C**
Alaska North Slope (ANS)	**32.0**	**39.3**	**24.4**	**4.3**	**10**	**0.8607**	**17.5**
Arabian Light Crude (ALC)	**32.7**	**18.9**	**46.9**	**1.5**	**7**	**0.8691**	**15.5**
Fuel Oil 40 (IFO-40)	**23.7**	**39.2**	**31.5**	**10.1**	**no**	**0.9393**	**210**

Properties of minerals				
	Formation temperature (^{o}C)	**Average particle size (µm)**	**Surface area (m^2/g)**	**Contact angle (°C)**
Original Kaolin	**-**	**5.8**	**10.0**	**11.0**
Modified Kaolin (MK1)	**75**	**5.8**	**10.0**	**38.0**
Modified Kaolin (MK2)	**80**	**5.8**	**10.0**	**58.0**
Modified Kaolin (MK3)	**85**	**5.8**	**10.2**	**65.0**
Modified Kaolin (MK4)	**87**	**5.8**	**n/a**	**71.0**

Properties of dispersants				
	Specific gravity	**Density (lb/gal, g/mL)**	**Viscosity**	**Boiling point (°C)**
Corexit 9500	**0.95**	**7.91, 0.9478**	**22.5 cst at 40 ° C**	**147**
Corexit 9527	**0.98 - 1.02**	**8.2 - 8.5, 0.9826 - 1.018**	**160 cst @ 0 °C**	**171**

2.1.2 Experimental Design

A full factorial design has been used to investigate the effects of different operational factors on the OMA formation (Tables 2 and 3) and stability of the OMA particles formed in the water column. The dispersed oil and OMA particles have been assessed by two criteria: (1) the amount of oil that is removed from the surface through formation of OMA or small

droplets that may be suspended in the water column, and; (2) the size distribution of the formed drops of oil and/or OMA.

The experiments were conducted using a modified version of the standard EPA baffled flask test protocol (Sorial et al. 2004; Venosa et al. 2002). A minimum of three tests were carried out for each experimental set. The temperature of samples was maintained at 2^{o}C by a temperature controller and monitored by a thermocouple. To conduct experiments under a salinity gradient similar to seawater, a saline test solution (30 ppt) was prepared by the addition of sea salts to de-ionized water. The pH value of 6.8 was maintained for all the experiments. For each test, a 120 mL aliquot of the saline solution was added to a baffled flask (Fisher Scientific), prior to the addition of 32 or 16 mg of mineral fines, depending on the treatment. The baffled flask was then placed on an orbital shaker (VWR DS 500e) at 250 rpm for 10 minutes. Subsequently, 100 µL of oil was added to each baffled flask, followed by addition of either 4 or 2 µL of dispersant. The contents of the baffled flask were then agitated again on an orbital shaker at 250 rpm for 30 minutes, followed by a reduced shaker speed of 100 rpm for another 30 minutes. After mixing, 2 mL of sample was drained from the stopcock and was discarded, and then 30 ml of sample was collected and analyzed to quantify the percentage of oil removed from the water surface. The total oil concentration was analyzed using the EPA standard UVS method (Mapada UV-1800 PC).

The effect of the various treatment factors (dispersant type/amount; mineral type/amount) on the dispersion of ANS, ALC and IFO-40 was evaluated in terms of Oil Removal Percentage (ORP), calculated as:

$$Oil\ Removal\ Percentage\ (ORP) = \frac{Amount\ of\ oil\ in\ the\ water\ column}{Total\ oil\ added}(100\%) \qquad (1)$$

Table 2: Four-factor two-level full factorial experimental design (Box et al. 1978) to investigate OMA formation and stability in the baffled flasks at low temperature.

Treatment	Factors			
	Fine Type	Dispersant Type	Mineral to Oil Ratio	Dispersant to Oil Ratio
1	-	-	-	-
2	+	-	-	-
3	-	+	-	-
4	+	+	-	-
5	-	-	+	-
6	+	-	+	-
7	-	+	+	-
8	+	+	+	-
9	-	-	-	+
10	+	-	-	+
11	-	+	-	+
12	+	+	-	+
13	-	-	+	+
14	+	-	+	+
15	-	+	+	+
16	+	+	+	+

Table 3: Factorial levels for the full factorial experimental design (MOR = mineral to oil ratio; DOR = dispersant to oil ratio).

Treatment level	Factor level			
	Fine Type	Dispersant Type	MOR	DOR
-	Kaolin	Corexit 9500	1:3	1:25
+	Modified Kaolin	Corexit 9527	1:6	1:50

2.1.3 Size Distribution of OMA by Microscopy

Size distributions of OMA were measured in samples taken from mixtures using IFO-40 dispersed with Corexit 9500. Analyses were conducted on samples over a range of dispersant to oil ratios (DORs), while maintaining a constant mineral to oil ratio (MOR). In each case the baffled flask was allowed to stand for 15 minutes to allow the OMA to form and settle prior to sampling.

The OMA size distribution was measured using a Leica DM4000M microscope. Samples were collected from two different sections of the flasks, one from the bottom, the other from the middle about 2 cm above the bottom. The results of the samples taken from the middle section were evaluated using the free mineral to total mineral percentage (MTP) and free oil

to total oil percentage (OTP). The fractions of free minerals and oil droplets to the original total were calculated in terms of volume of minerals and oil droplets. The oil droplets and mineral particles were considered to be cylindrical when the mean diameter was greater than 10 μm, because the gap between the microscope slides was 10 μm, otherwise the free oil droplets and minerals are considered to be spherical.

The frequency distribution of OMA was calculated using the following equation:

$$Frequency = \frac{The\ Number\ of\ Particles\ of\ the\ Size\ Interval}{Total\ Number\ of\ Particles} \quad (2)$$

2.2 Results and Discussion

2.2.1 Characterization of the three oils

The results from the boiling point analysis are shown in Figure 1. ANS and ALC have similar boiling point distributions while IFO-40 is heavier with about 15% yield at 300 and at 350°C, but most of the yield coming off at >500°C. Both ANS and ALC contain approximately 20%wt hydrocarbons that have a boiling point higher than 500 °C, whereas IFO-40 has about 40%wt.

The results from the viscosity analysis are shown in Figure 2. The viscosity of all the three oils increased dramatically as temperature decreased. IFO-40 was more viscous than the other two crudes within the measured temperature range. In particular, from 0 to 4^{o}C (the range at which all of the experiments were conducted), IFO-40 showed a two-fold increase in viscosity over the other two crudes. The viscosity distribution indicates that temperature may impact dispersant efficiency.

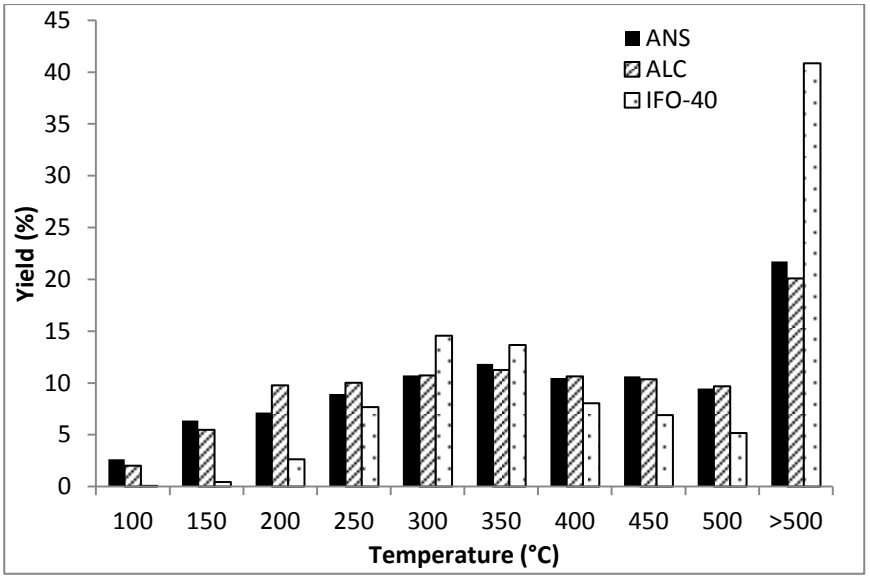

Figure 1: Simulation distillation results for three petroleum crudes.

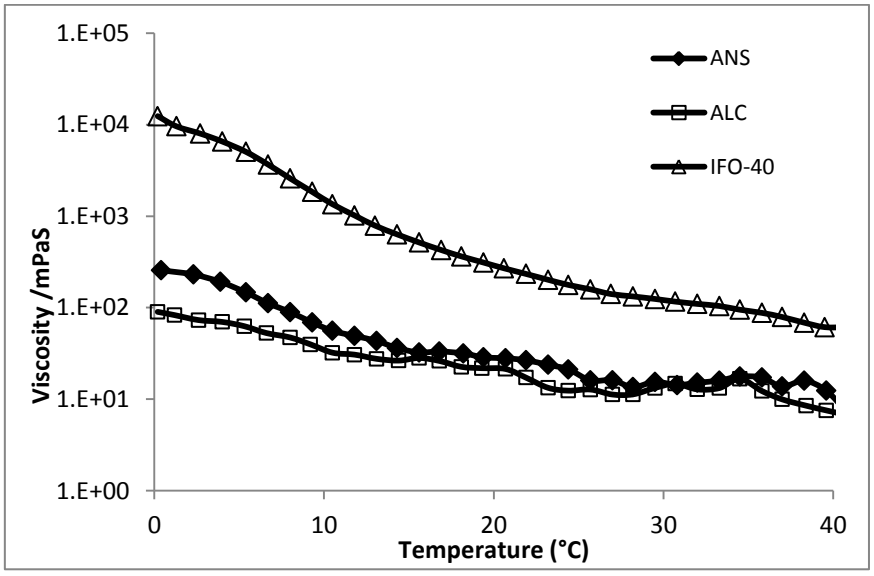

Figure 2: Dynamic viscosity of the oils at various temperatures

2.2.2 The effect of temperature on the formation of OMA

The effect of temperature on the formation of OMA was studied in the absence of dispersant (Figure 3). At room temperature (20°C), similar oil removal performances (ORP of 68-70%) were observed for ANS and ALC, whose viscosities are nearly the same. The IFO-40 having greater viscosity appeared to have a lower ORP (about 62%) than its lighter counterparts, ANS and ALC. At 0°C the ORPs for all the three crudes decreased. The decrease in ORP was proportional to increase in crude viscosity (Figures 2 and 3a). The viscosity of oil appears to play a key role in oil removal performance by mineral fines.

The effect of temperature was further studied by varying the ratio of mineral fines and IFO-40 (Figure 3b). An increase in the mineral to oil ratio from 1:12 to 1:6 can enhance ORP by 20% at 20°C or 10% at 2°C. Further additions of minerals did not enhance the performance (Figure 3b).

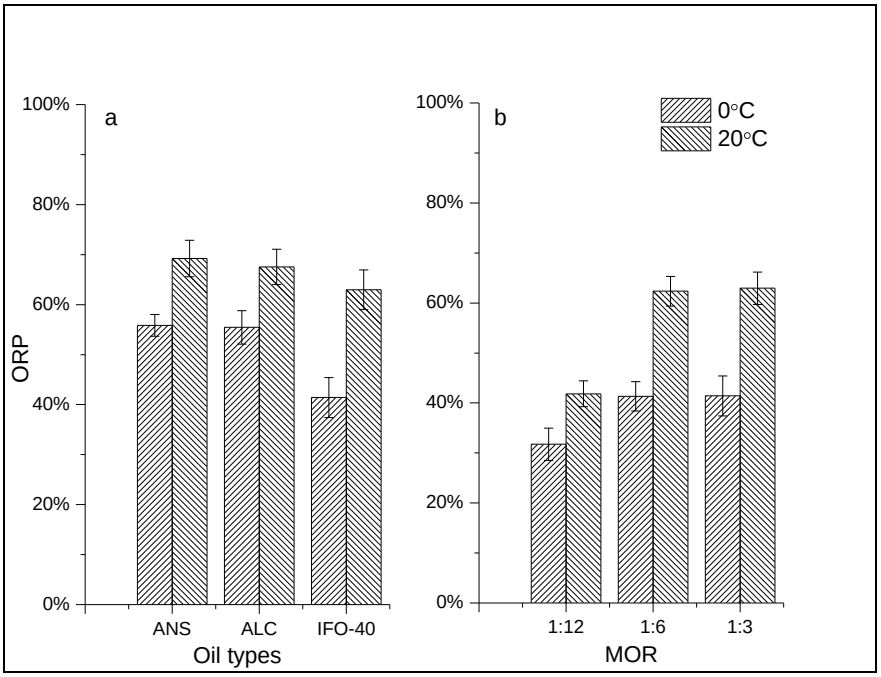

Figure 3: Effect of temperature on oil removal performance (ORP) using (a) various oils at a mineral to oil ratio (MOR) = 1:3, and (b) various MORs with IFO-40.

2.2.3 Effect of Mineral-to-oil Ratio on Oil Dispersion

The effects of dispersant and minerals on oil dispersion were investigated following the full factorial design (Table 2 and Table 3). Five levels of MOR were examined for Corexit 9500 at a DOR of 1:25. Oil removal was higher than 70% for all three crude oils (Figure 4). The results support the hypothesis that the combined use of minerals and dispersant may be an efficient means to enhance the transport of oil from surface water. The highest ORP occurred at MOR = 1:3 for all three oils. A preliminary inspection of the data suggests that an increase or decrease in MOR can lead to a lower oil removal percentage. For lower MOR (1:12 to 1:3), the ORP increased as a function of MOR; more oil was removed from the water surface. This indicates that minerals can enhance the formation of OMA and/or sequester oil. However, the opposite result was obtained when the MOR exceeded 1:3. Excessive minerals developed more OMA, some of which rose to the water surface instead of settling to the bottom of the flask. The floatation of OMAs resulted in lower ORPs. This observation is consistent with previous observations made by (Omotoso et al., 2002). As a result, during an operational response, this phenomenon could result in an accumulation of oil at the sea surface.

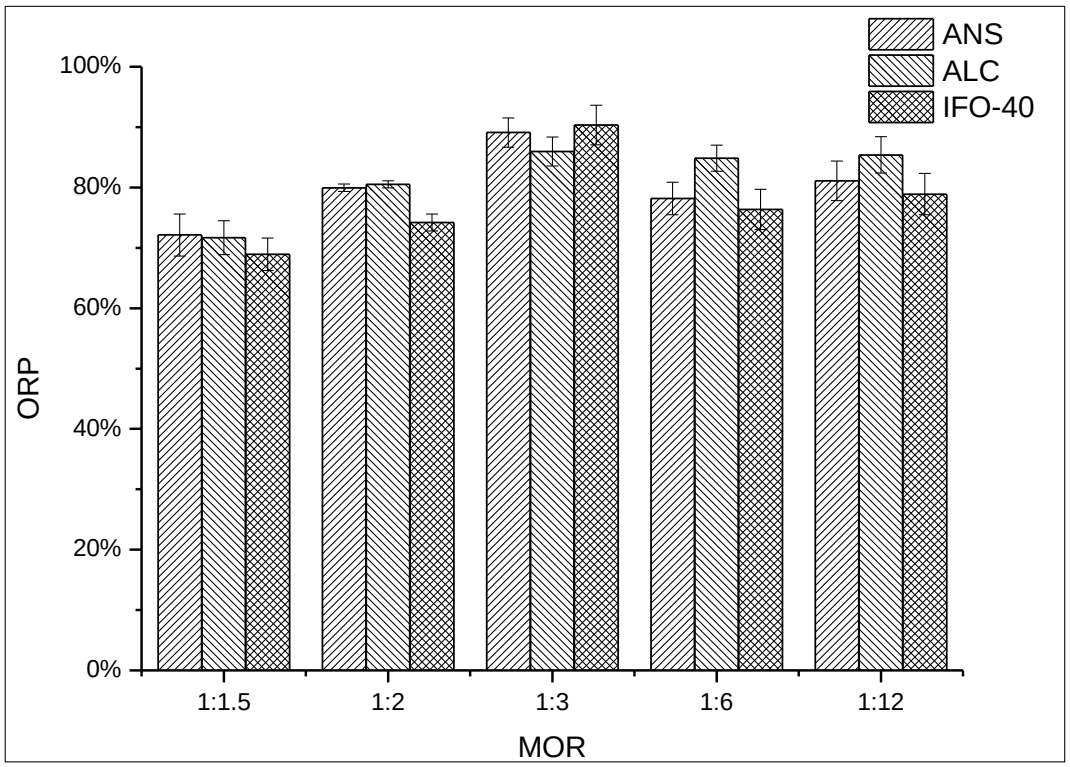

Figure 4: Effects of mineral to oil ratio (MOR) on dispersion efficiency of oil in the BFT (Corexit 9500; DOR=1:25).

2.2.4 Effect of Dispersant-to-oil Ratio on Oil Dispersion

The trend for the effect of DOR is shown in Figure 5. At a MOR of 1:3 (Figure 5a), high DOR led to a higher oil removal percentage for IFO-40, but the increased DOR had little effect on the ORP for ANS and ALC. A low ORP was observed for IFO-40 at DOR = 1:50 indicating that insufficient dispersant was used. IFO-40 is more viscous than the other two oils and thus requires more dispersant. This is consistent with the report that heavy oil (i.e., low API gravity) and weathered oils are more resistant to dispersion and may require a higher DOR (Lessard and Demarco, 2000). Introduction of more minerals to the system where MOR reached 1:1.5 (Figure 5-b) resulted in only slightly lower ORP at higher DOR when compared with MOR = 1:3 (Figure 5 a).

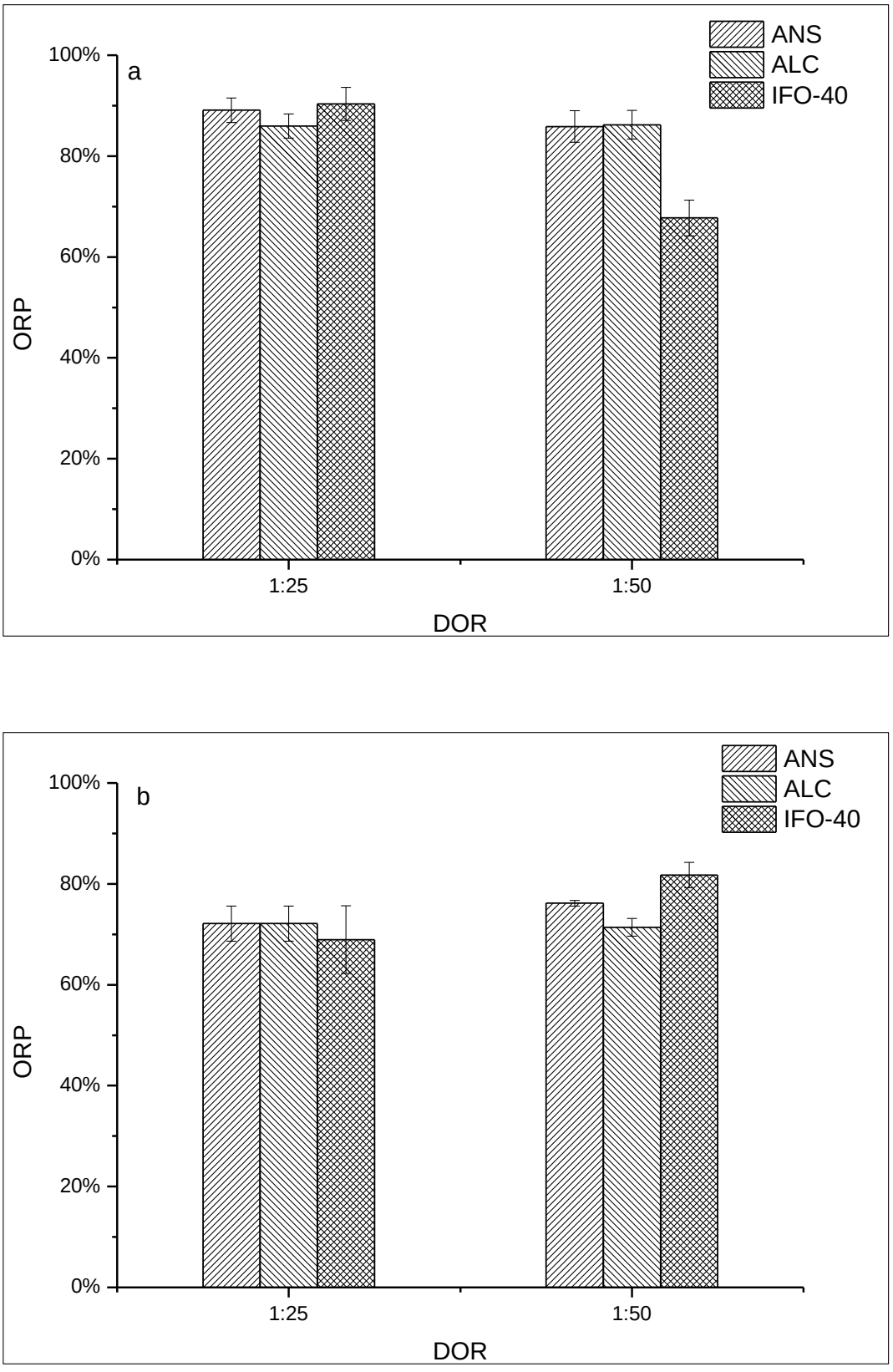

Figure 5: Effect of dispersant to oil ratio (DOR) on oil removal percentage (ORP) using Corexit 9500 at MOR = 1:3 (a) and MOR = 1:1.5 (b)

2.2.5 Effect of Dispersant Type on Oil Dispersion

The effect of dispersant type on crude oil dispersion was also evaluated. Two formulations of the commercial product Corexit were tested, and the results can be found in Figure 6 and 7. Under all treatment conditions, Corexit 9500 was more effective in dispersing ALC and IFO-40. Dispersant type seemed to have no effect on ANS.

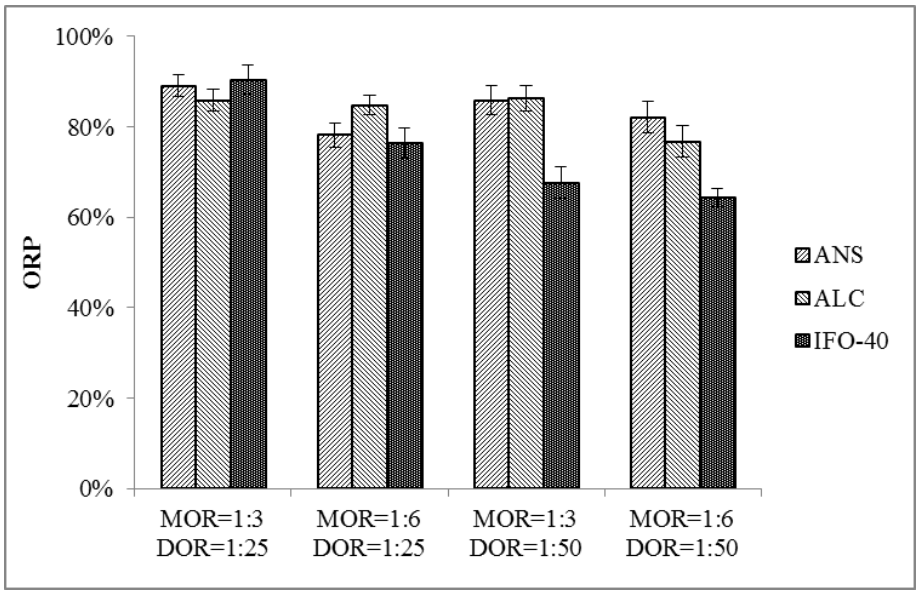

Figure 6: Effect of dispersant to oil ratio and mineral to oil ratio on ORP using Corexit 9500.

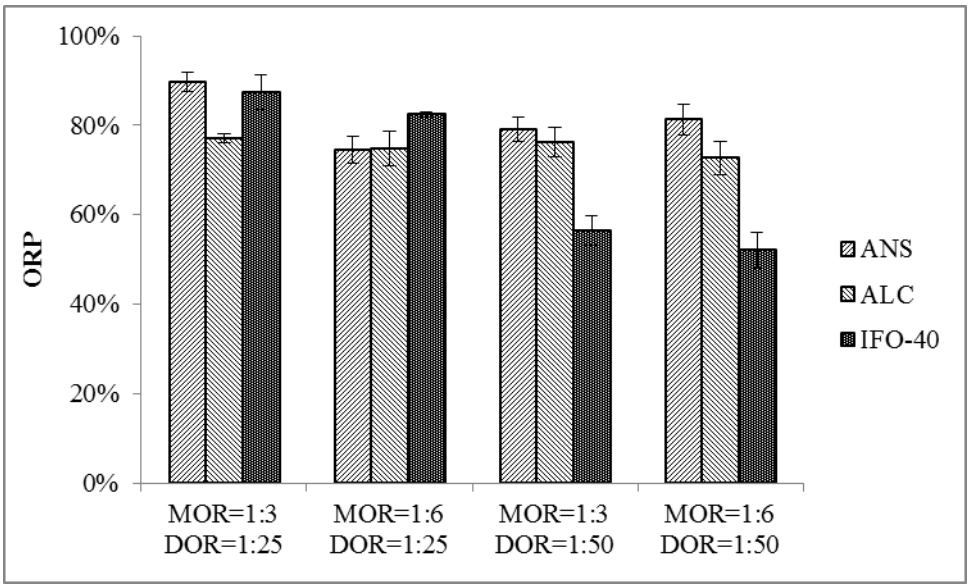

Figure 7: Effect of dispersant to oil ratio and mineral to oil ratio on ORP using Corexit 9527.

2.2.6 Morphology of OMA

Samples were taken from the surface, middle and bottom of the flask for microscopic examination, and the results are shown in Figure 8. IFO-40 was chosen in this experiment due to its high viscosity which provides a more dramatic response to dispersant compared with the other two oils. Corexit 9500 was the dispersant used in this test. MOR and DOR were set at 1:2 and 1:50, respectively. The results showed that OMA at the bottom of the flask were dense and large (Figure 8a), while smaller, less dense OMA and free suspended oil were observed in the middle water column and floating on the water surface (Figure 8b, c). Oil droplets contacted each other to form larger droplets, and oil droplets also interacted with minerals to form OMAs, which stabilize droplets by preventing coalescence. The minerals used in this work are hydrophilic in nature. The presence of dispersant can lower the hydrophobic nature of oil droplets and improve the interaction between hydrophilic minerals and oil droplets. Given this reasoning, it is understandable that insufficient dispersant can result in decreased OMA formation and thus lead to a lower ORP for a highly viscous oil such as IFO-40 (Figure 5-left).

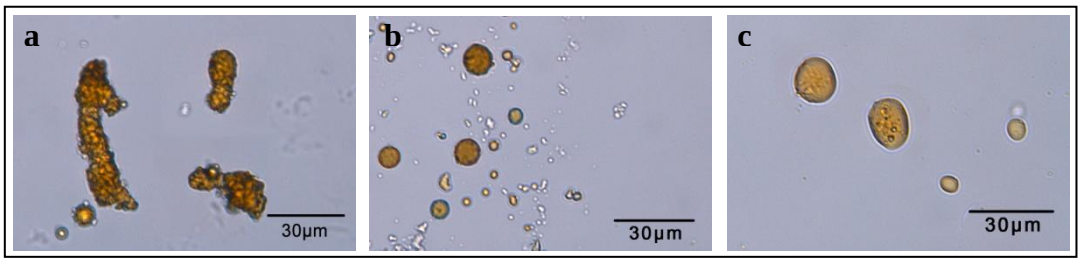

Figure 8: Morphology of OMA for IFO-40, Corexit 9500, DOR = 1:50 and MOR = 1:2 at the bottom (a), middle (b), and surface (c) of the baffled flask.

Figure 9 shows the effect of dispersant on the morphology of OMAs. Samples were taken from the middle part of the solution where the dispersed oil was concentrated. In the absence of dispersant, the oil droplets were round with smooth edges (Figure 9a) and OMA were barely observed. Introduction of dispersant (Figure 9b-c) led to irregular shapes of oil droplets due to lowered surface tension of the droplets. This is consistent with the observations of others (Li et al., 2007), and indicates that the addition of dispersant may enhance the formation of OMA and slightly increase the OMA size.

Figure 10 shows the effect of the amount of minerals on the morphology of OMA. Samples were taken from the bottom of the solution where the OMA were concentrated. An increase in minerals was is more likely to form large, dense OMA, in which more oil would be trapped. However, the addition of higher mineral concentrations may not be cost effective.

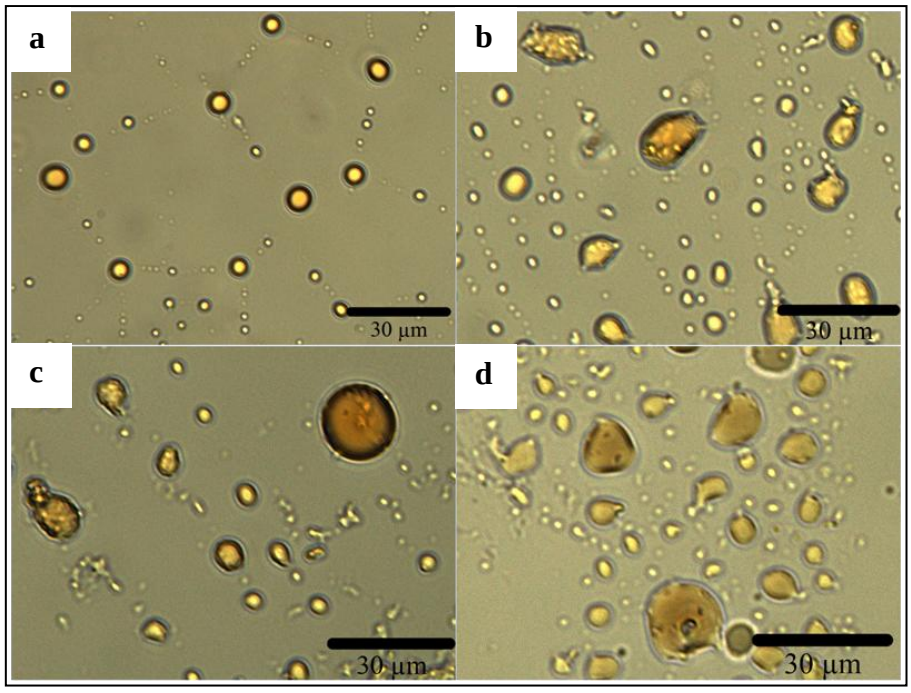

Figure 9: Effect of Corexit 9500 on OMA morphology from samples taken in the middle of the baffled flask for IFO-40 at a MOR of 1:3; DOR: a = 0; b = 1:100; c = 1:50; d = 1:25

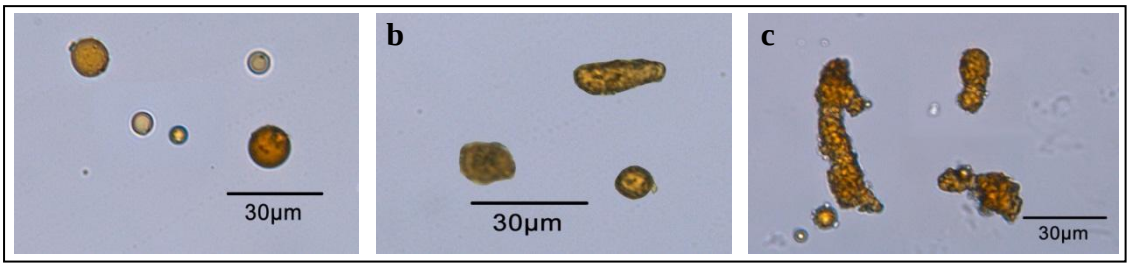

Figure 10: Effect of MOR on OMA morphology at the bottom of the flask for IFO-40 and Corexit 9500; DOR = 1:50; MOR = 1:12 (a), 1:3 (b) and 1:2 (c)

Figure 11 shows a statistical analysis of the results represented in Figure 10. The free oil and minerals refer to those that were not involved in the formation of OMA. Without dispersant, both the free mineral total percentage (MTP) and the free oil total percentage (OTP) approached 100%, indicating that the majority of mineral fines did not form OMA. With the addition of dispersant, however, both MTP and OTP decreased significantly (from almost 100% to 21.7% and 20.1%, respectively), indicating that roughly 80% of the mineral fines and oil droplets were taken up in the formation of OMA. Increasing the DOR resulted in increased OMA formation. When the DOR reached 1:25, almost no free minerals were left in water, suggesting that dispersants can enhance the formation of OMA. Conversely, the ratio of free oil droplets to total oil increased from 20.1% to 67.8% when the DOR increased from 1:100 to 1:25 suggesting that the higher DOR of 1:25 may be lowering the oil surface tension

so much that oil droplet dispersion is favoured more than OMA formation. This suggests that there exists an optimal DOR for enhancing chemically dispersed OMA formation. For MOR of 1:3, the optimal dispersant to oil ratio lies between 1:50 and 1:25.

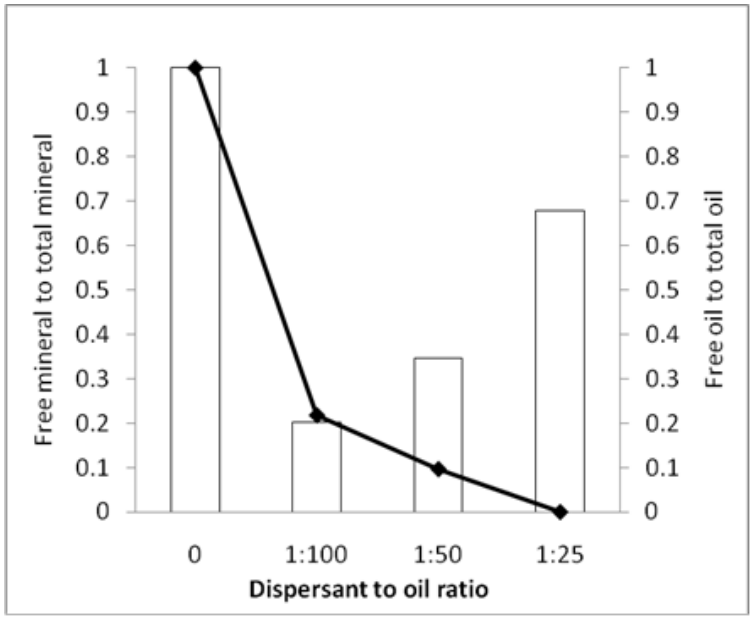

Figure 11: Fractions of free minerals to total minerals used (solid line), and fraction of free oil to total oil (bars), as a function of DOR (for IFO-40 and Corexit 9500).

In summary, the combined use of chemical dispersant (Corexit 9500 and Corexit 9527) and mineral fines has shown that the oil removal rate increased when more dispersant and minerals were applied. Corexit 9500 seemed to enhance dispersion to a larger degree than Corexit 9527 for all three crude oils. The dispersant to oil ratio (DOR) and mineral to oil ratio (MOR) are cross-influential. Statistical study of microscopic images of OMA produced in the flasks suggested that there may be an optimal ratio of dispersant to minerals for OMA formation.

2.2.7 Particle Size Distributions

Size distributions were calculated for the OMA in the microscopic images. Figure 12 shows the size distribution for the original kaolin. Double peaks were observed and the mean sizes for the peaks were 1.6 µm and 10 µm, respectively. The effect of MOR is shown in Figure 13. Samples for microscopy were first taken from the bottom of the solution (Figure 13a). At MOR = 1:12 a narrow peak appeared, centered at 2 µm. Only fine minerals interacted with oil droplets to form small aggregates. An increased amount of minerals resulted in larger mean sizes and a broader size distribution of OMA. The mineral-oil interaction extended from fines to all sizes of mineral particles. The shift in peak diameter also indicates that small OMA are likely to aggregate into large ones with the addition of more minerals.

Figure 13b shows the size distribution for the samples taken from the middle part of the baffled flask. For all MORs tested, the size distribution appeared to be similar (2.4 μm), suggesting that it is the buoyancy of the aggregates that causes them to remain in the water column. Size distribution of samples taken from the surface is shown in Figure 13c. As MOR shifted from 1:12 to 1:2, the peaks became asymmetric and the mean sizes of OMAs were slightly increased. This finding confirms the conclusion obtained from Figure 6 that large OMAs float back to the water surface.

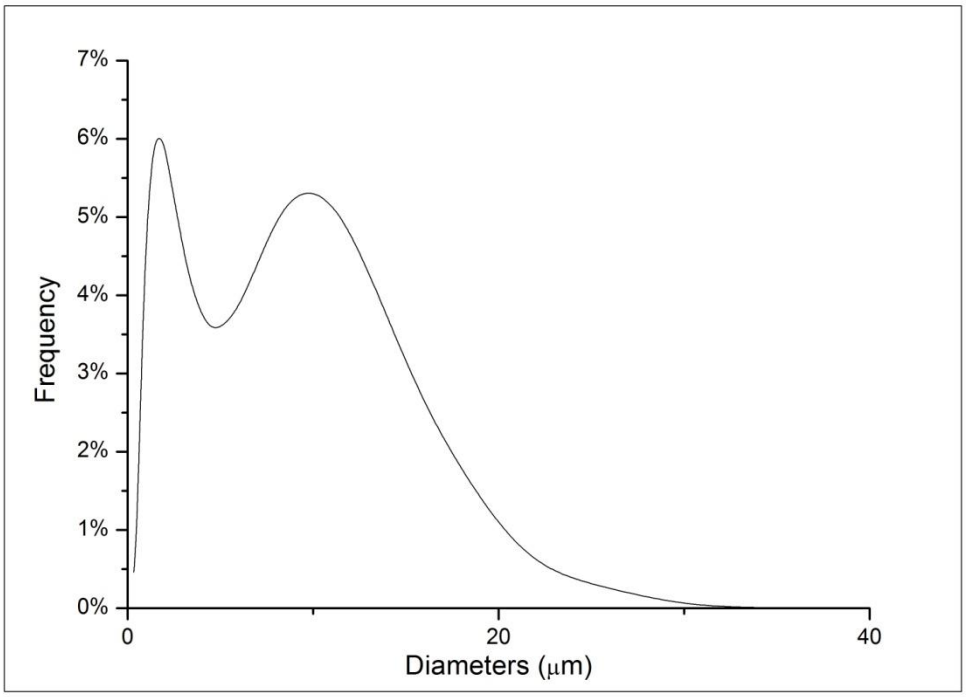

Figure 12: Particle size distribution of original kaolin mineral fines.

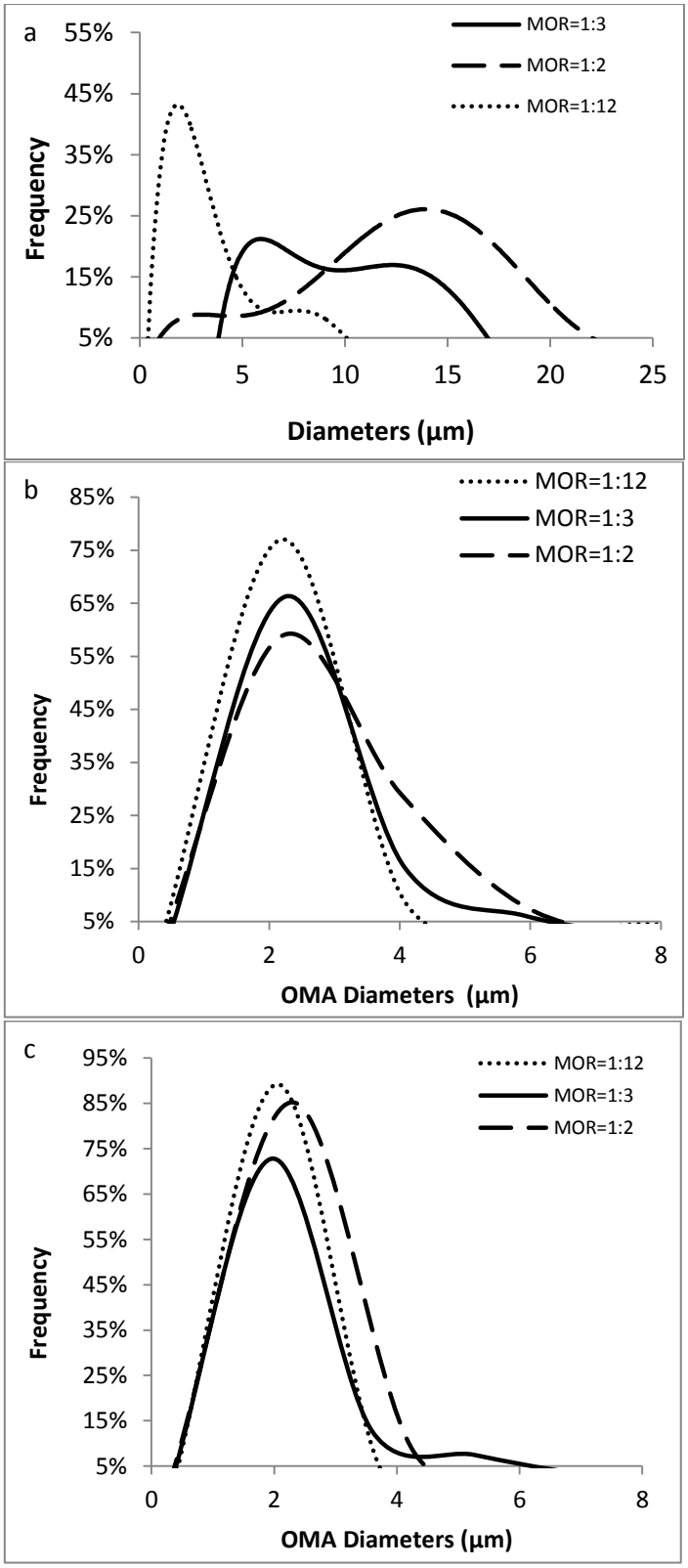

Figure 13: Effect of MOR on particle size distribution of OMA for IFO-40 and Corexit 9500 at a DOR of 1:50. Samples taken from the (a) bottom, (b) middle, and (c) surface of the flask.

The size distributions of the formed OMA's for a range of DOR's are presented in Figure 14 for IFO-40, using a MOR of 1:3 and Corexit 9500 as the dispersant. Samples were taken from the bottom of the baffled flask. Without application of dispersant, the peak of the size distribution was at 0.83μm with a frequency of 56%. When dispersant was introduced, the peak shifted to 1.3μm with a frequency of 39%. When more dispersant was introduced (1:50), the peak shifted back to 0.83 μm and the curve flattened, indicating a wider size distribution of OMA sizes. At the highest DOR (1:25), the peak rose to a frequency of 81.2%, and the distribution of particle sizes narrowed. This finding supports the observation of the effect of dispersant on reducing OMA size.

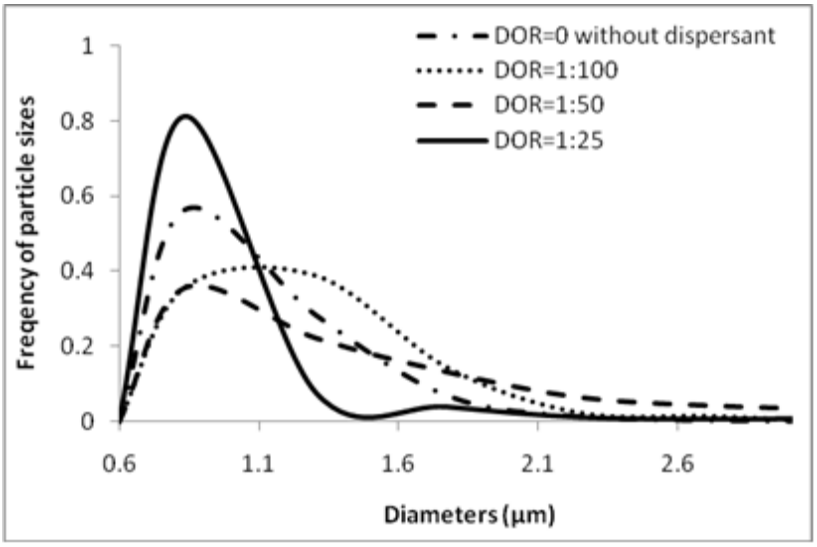

Figure 14: OMA size distributions for IFO-40 and Corexit 9500 at MOR of 1:3 (samples were taken from the bottom of the flasks).

2.2.8 Modification of original kaolin

The success of modification of original kaolin is identified by FTIR spectra (Nicolet 6700, Thermo Scientific, US) shown in Figure 15. Kaolin and modified kaolin are displayed for comparison. The characteristic vibration of the NH group at 1550 cm-1 suggests that kaolin was successfully covalent with Toluene 2, 4-diisocyanate. The peaks at 2952 and 2884cm^{-1} verified the existence of CH_2, a functional group from aliphatic alcohol. The modified kaolin has a much higher hydrophobicity than original kaolin as indicated by the contact angle shown in Table 1. There was no change in surface area.

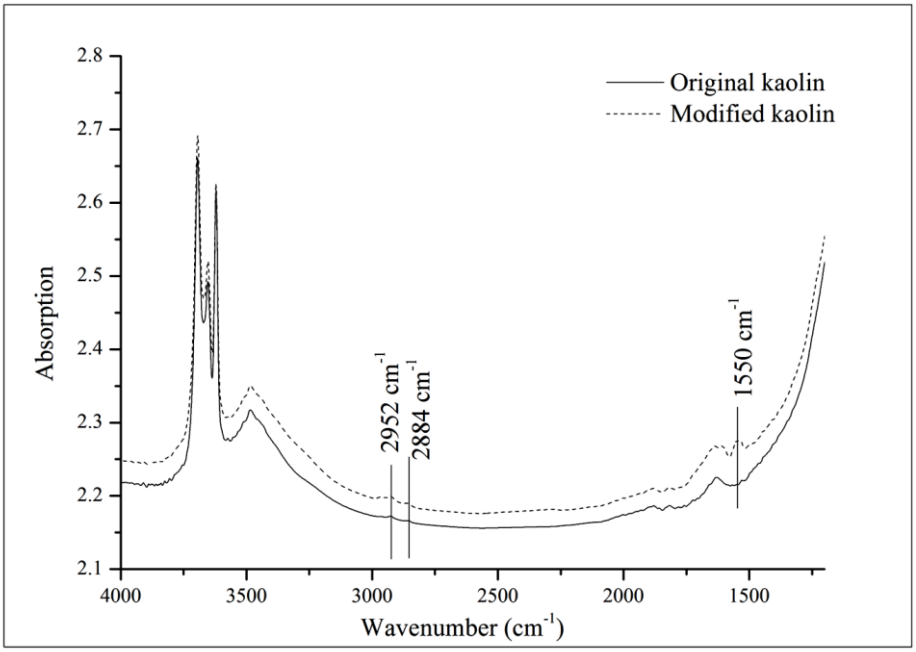

Figure 15: FTIR result of modified kaolin.

2.2.9 Oil Removal Performance of modified kaolin

The formation of OMAs involves interactions between oil droplets and minerals. Hydrophilic kaolin may have little affinity to interact with hydrophobic crude oil. Therefore, the original kaolin was modified to increase its hydrophobicity. The oil removal performance with different modified kaolin particles is shown in Figure 16. ANS was used as the crude oil and no dispersant was used for this run. The four types of modified kaolin with different contact angles exhibited different oil removal efficiencies compared with the original kaolin (Figure 16). When the kaolin particles Mk-1 and Mk-2 with lower contact angles (38^o and 58^o) were used, an oil removal rate of approximately 75% was achieved. This ORP is about 20% higher than the original kaolin. Further increasing the hydrophobicity (contact angle from 58° to 71°) resulted in the modified kaolin particles (MK-3 and MK-4) agglomerating together rather than interacting with the oil, and subsequently the ORP dropped dramatically. This suggests that there is an optimal hydrophobicity for OMA formation and oil removal performance. Modified kaolin (MK1) was thus selected for further study. Reference to "modified kaolin" in the subsequent figures of this chapter refers to MK1.

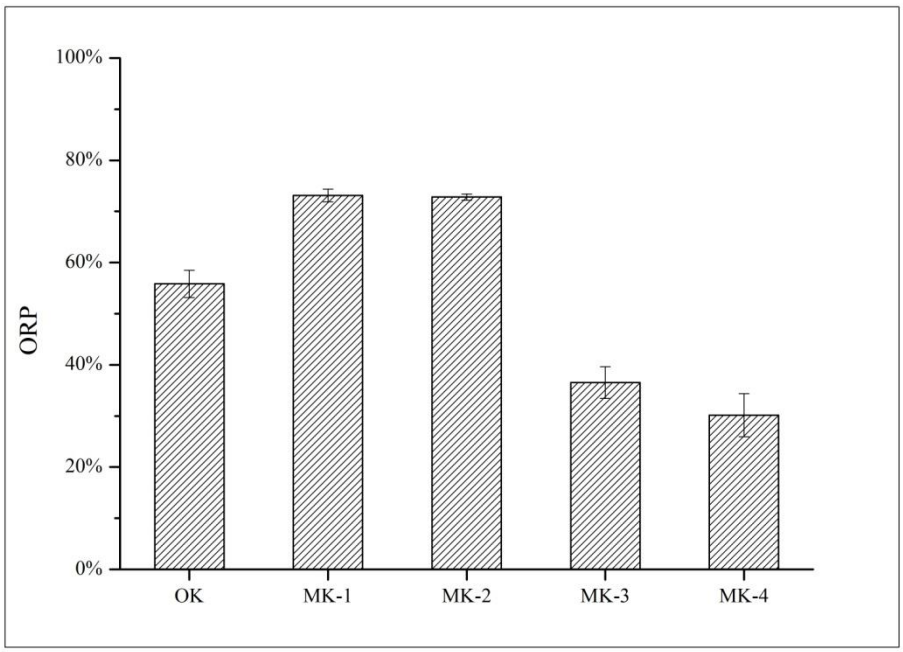

Figure 16: Effect of hydrophobicity on the oil removal rate.

2.2.10 OMA formation with modified kaolin particles

The performance of modified kaolin particles (MK1) on oil removal were evaluated using the three oils (Figure 17). The original kaolin particles were also examined under the same experimental conditions. Without dispersant, modified kaolin particles exhibited higher oil removal performance (18%, 18% and 35% increase in ORP for ANS, ALC, and IFO-40, respectively) than the original kaolin. The increase in ORP suggests hydrophobicity of mineral particles plays an important role in the formation of OMA.

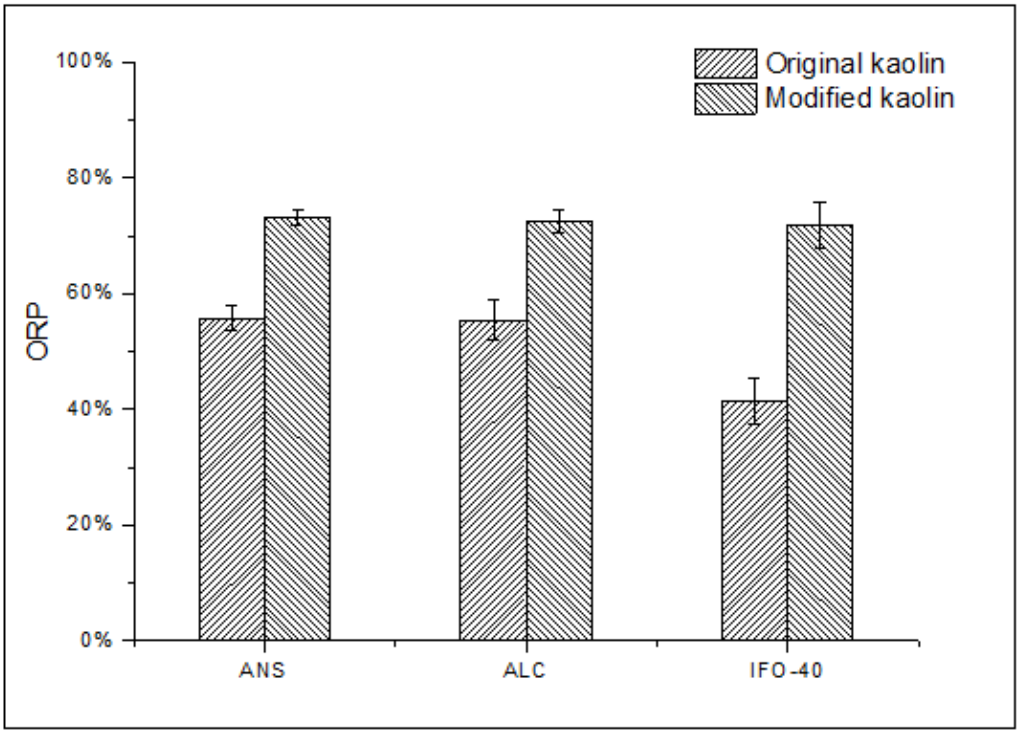

Figure 17: Comparison of original kaolin and modified kaolin on the oil removal performance (without dispersant).

Figure 18 compares the ORPs at different MOR using ANS as the oil and Corexit 9500 as the dispersant with a DOR of 1:25. The performance of the modified kaolin remained almost the same regardless of the presence of dispersant. On the other hand, the dispersant can significantly improve the oil removal rate for the original kaolin. In the presence of dispersant, the modified kaolin particles remove approximately 2 to 16% less oil than the original kaolin. Containing hydrophilic heads and hydrophobic tails, dispersant can serve as a "bridge" to connect hydrophilic kaolin particles to hydrophobic oil droplets. By increasing the hydrophobic properties of the kaolin, the modified particles can better interact with oil droplets without the need for dispersant.

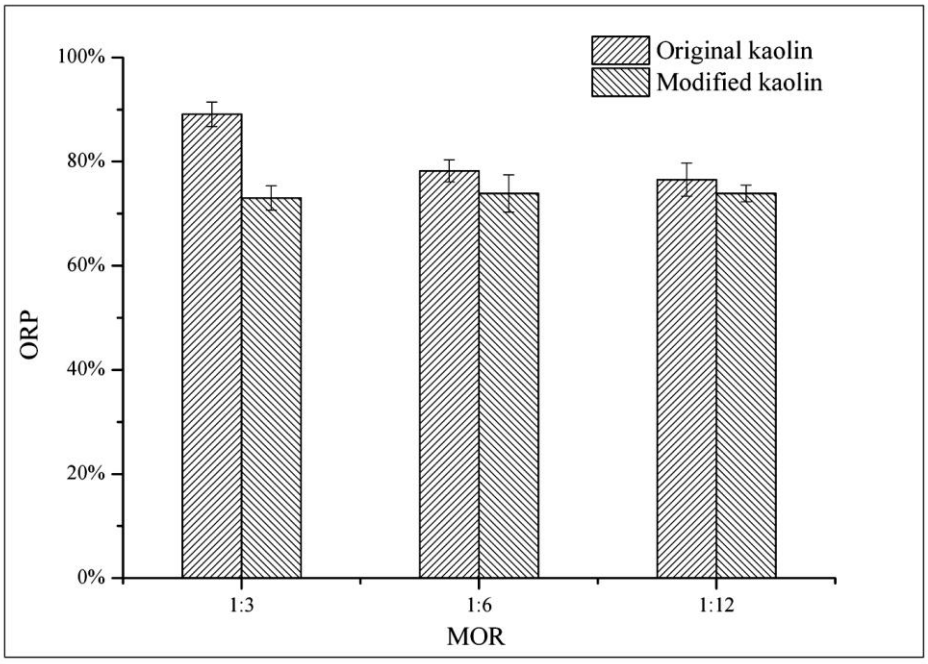

Figure 18: Effect of dispersant (Corexit 9500 at a dispersant to oil ratio of 1:25) with different mineral to oil ratios (MOR)

Figure 19 shows the effect of DOR on the performance of the modified kaolin. Comparing the three dispersant to oil ratios, the values of ORP appear similar, which confirms that dispersant does not play an important role in the interaction between modified kaolin and oil droplets.

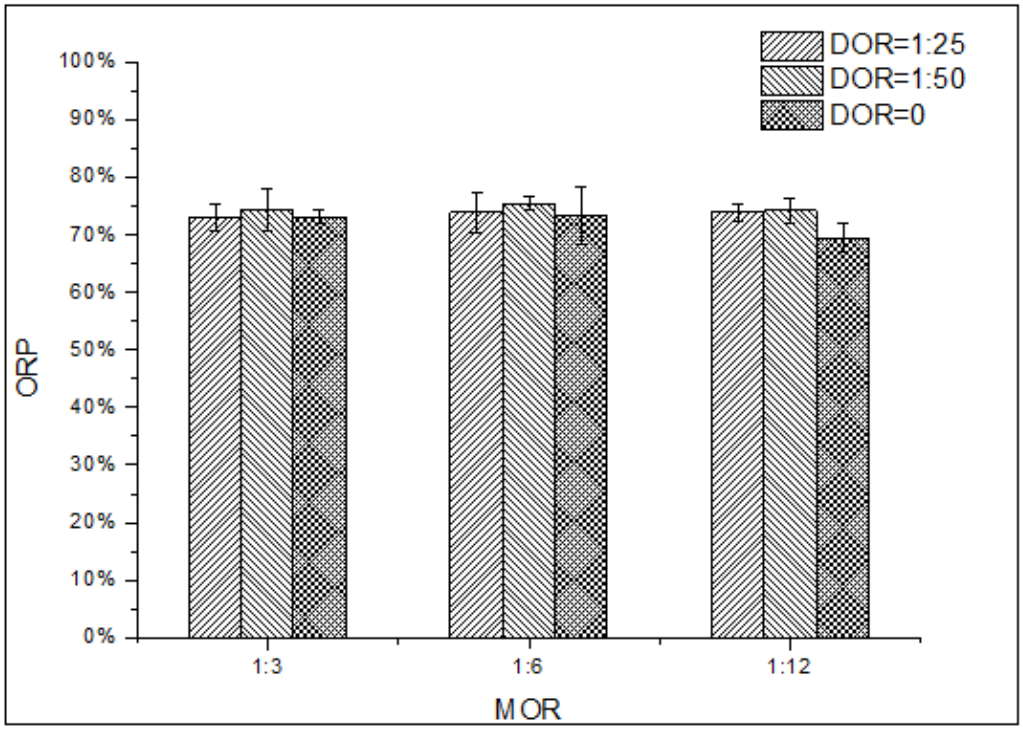

Figure 19: Effect of modified kaolin with and without dispersant.

A detailed comparison of the effect of dispersant and the type of crudes on the oil removal performance of modified kaolin revealed that all the ORPs fell within the range of 70 to 80%, and no significant difference was identified with different mineral to oil ratios Figure 20. It is shown that all the ORPs fall in the range of 70% and 80% and no significant difference is identified with different mineral to oil ratios. Neither did the mineral to oil ratio have much impact on the oil removal ratio, which suggests that a small amount of modified kaolin can be just as effective as a large amount.

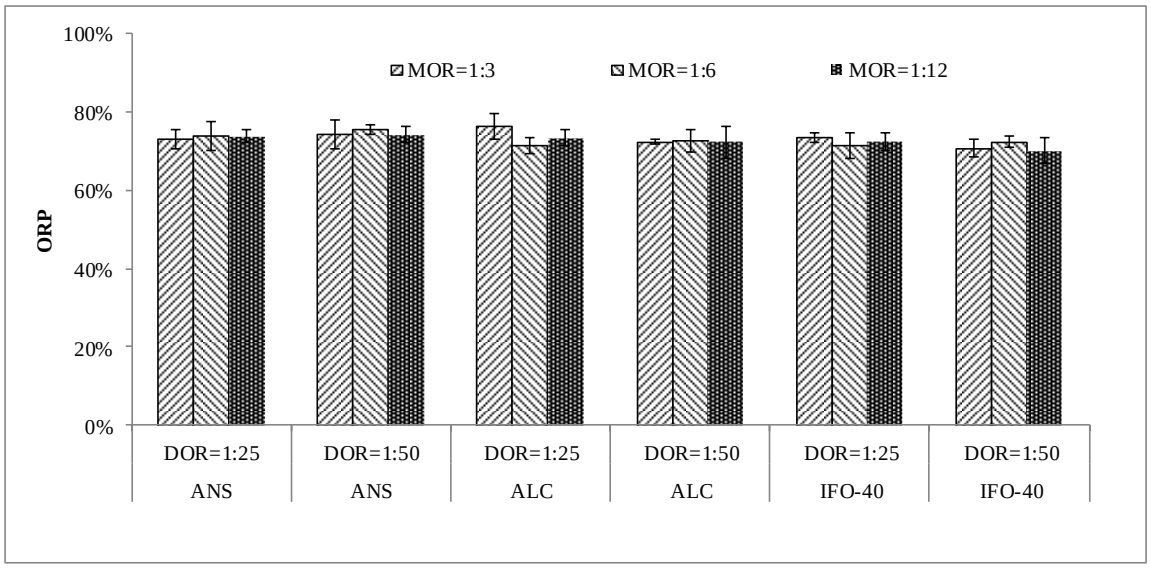

Figure 20: Effect of mineral to oil ratio on the oil removal percentage.

In summary, the modified kaolin perform much better than the original kaolin without the presence of dispersant. But similar performance was observed under the various conditions when dispersant was introduced.

2.2.11 Morphology of OMAs using modified kaolin

The morphology of OMAs formed with modified kaolin with and without dispersant was recorded using a microscope (Figure 21). Samples were taken from the bottom of the flask using IFO-40 in a mineral to oil ratio of 1:12. Figure 21a shows that in the absence of dispersant, large OMAs were observed, which indicates that there was a strong interaction between the modified kaolin and the oil droplets. The presence of dispersant dramatically decreased the size of OMAs (Figure 21b). In the presence of dispersant, the average size of the OMA was significantly reduced, with a maximum peak at 4 µm (Figure 22).

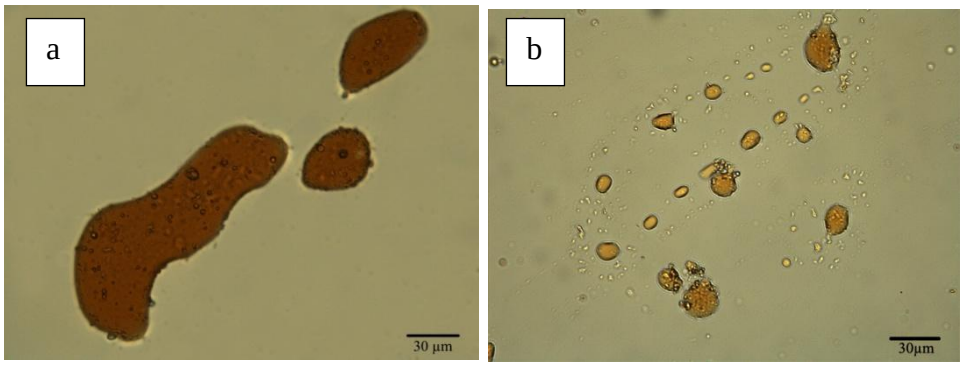

Figure 21: Morphology of OMAs using modified kaolin and: (a) no dispersant; (b) Corexit 9500 DOR= 1:50

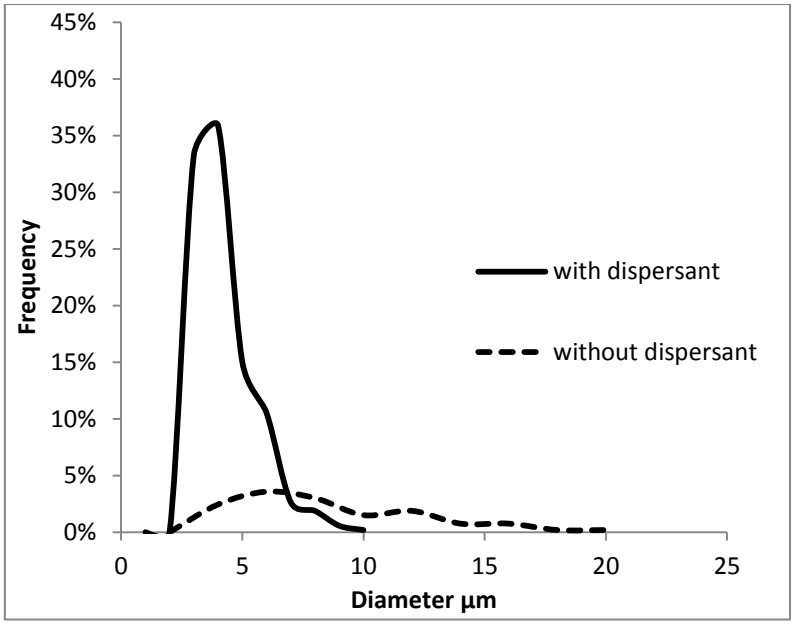

Figure 22: Size distribution of modified kaolin OMA with and without dispersant.

2.3 Conclusion

The roles of both dispersant and minerals in the removal of oil in cold water environments were investigated using a series of baffled flask experiments. The results confirmed that a combination of dispersant and mineral fines is an effective approach to remediate oil spills in cold environments. The data show that there is an optimal mineral-to-oil ratio and dispersant-to-oil ratio whereby the introduction of an appropriate amount of minerals and dispersant can result in improved oil removal performance. OMA morphology and size distributions show that the use of more minerals can lead to the formation of more and larger OMA. Modified kaolin exhibits a stronger interaction with oil droplets compared to the original kaolin, and there is an optimal hydrophobicity for kaolin. Dispersant can reduce the size of OMA and can enhance the effectiveness of the original kaolin, but cannot improve the interaction between modified kaolin and the tested oils. A smaller amount of modified kaolin can be used in removing oil in the absence of dispersant than would be required if the original kaolin were used.

3. Modified Institut Français du Pétrole (IFP) Test: The Influence of Chemical Oil Dispersant and Mineral Fine Additions on the Dispersion of Oil under Low Temperature and Mixing Energy Conditions

3.1 Introduction

The objective of this program component was to investigate the feasibility of an oil spill countermeasure in low energy, cold and icy water conditions based on the application of chemical dispersant and the addition of mineral particles to enhance the dispersion of oil in the water column, and increase the stability of suspended oil droplets in a low energy environment (preventing coalescence and the reformation of a surface slick) by the formation of oil-mineral aggregates (OMA). Dispersants and mineral particles were applied in a combined fashion (1) to break up oil into droplets, (2) to sustain small oil mineral aggregates particles in the water column as discreet oiled particles, (3) to dissipate the oiled particles in water, and (4) to dilute oil to a threshold concentration lower than the toxic level.

3.2 Study Design

Laboratory tests were conducted at Cedre, France in the laboratory of Francois Xavier Merlin using a modified IFP (Institut Français du Pétrole) dilution test apparatus. The IFP test is a standard protocol used for the approval of dispersant products in France. Recently the IFP test was modified to account for low mixing energy to simulate calm conditions by varying the stroke and speed of the electric motor used to generate waves, and tests were run at low temperature comparable to ice infested marine waters. The efficiency of dispersion was studied with different mineral products used by the oil industry, and added at different concentrations. Measurements were made of the amount of oil dispersed, and the stability of the dispersion. In order to study the particle size distribution during formation of OMA, a LISST-100X laser particle analyzer from DFO/COOGER was incorporated into the test system.

This experiment was designed to improve our knowledge on: 1) the behaviour of oil mineral aggregates (OMA) in the water at different energy levels within the test tank system (i.e., do they settle in the tank?), 2) the influence of mixing energy on the efficacy of dispersants, 3) the influence of mineral fine additions on oil dispersion under low energy conditions.

The experimental test matrix included different oils and different clay particle types with and without dispersants in order to assess the effects of the presence of clay particles on the efficiency and stability of the dispersion. The evaluation was made through measurements of the concentrations of dispersed oil in the water column of the test tank as well as the fate of

the dispersed oil, whether coalescing or remaining buoyant in the water phase. Additional measurements of aggregate size were used to assess the efficacy of the dispersion process.

3.3 Materials and Methods

3.3.1 Oils and Dispersants

Three oils were initially selected for testing in Cedre, France: weathered Arabian Light Crude (ALC); Albert Sweet Mix Blend, and IFO 40 fuel oil. Of these, continued testing was carried out on Alberta Sweet Mix Blend (viscosity = 5.5 mPa.s at 20°C and 12.5 mPa.s at 5°C), and an IFO 40 mixture of 64.5% heavy fuel oil (FO2) and 33.5% diesel oil, so that the mixture had a viscosity of 526 mPa.s at 5°C. The dispersants tested were Corexit 9500 from NALCO and a European product, GAMLEN OD 4000 from INOSPEC. The mineral particles to be used should be readily available in the field, and in this sense, minerals that are used for drilling mud seemed appropriate. CEDRE considered bentonites and sepiolites.

The test temperature was $\leq 5^{o}$C and the salinity of the seawater was 30 ppt.

3.3.2 Jar Tests

Candidate clays

Four samples of minerals used in drilling muds were sent by IFP but without any technical information:

Bentonite MR
Bentonite W100
Bentonite Greenbond
Sepiolite

Subsequently, 4 samples with technical data sheets (Appendix 1 of this report), were obtained from the "Société Française des Bentonites et derives."

ATC/NA
C2t
Geko 5
Greenbond 453t

Preliminary tests and selection of clays

Preliminary tests were carried out in order to select the desired products for further evaluation. These preliminary tests included mixing a known quantity of oil with mineral particles, with and without dispersant in water in a beaker, in order to observe, visually after a one hour settling period, the behaviour of the dispersion, such as coalescence and resurfacing,

the tendency to settle on the bottom, or stabilisation of the dispersion in the water column (Figure 23).

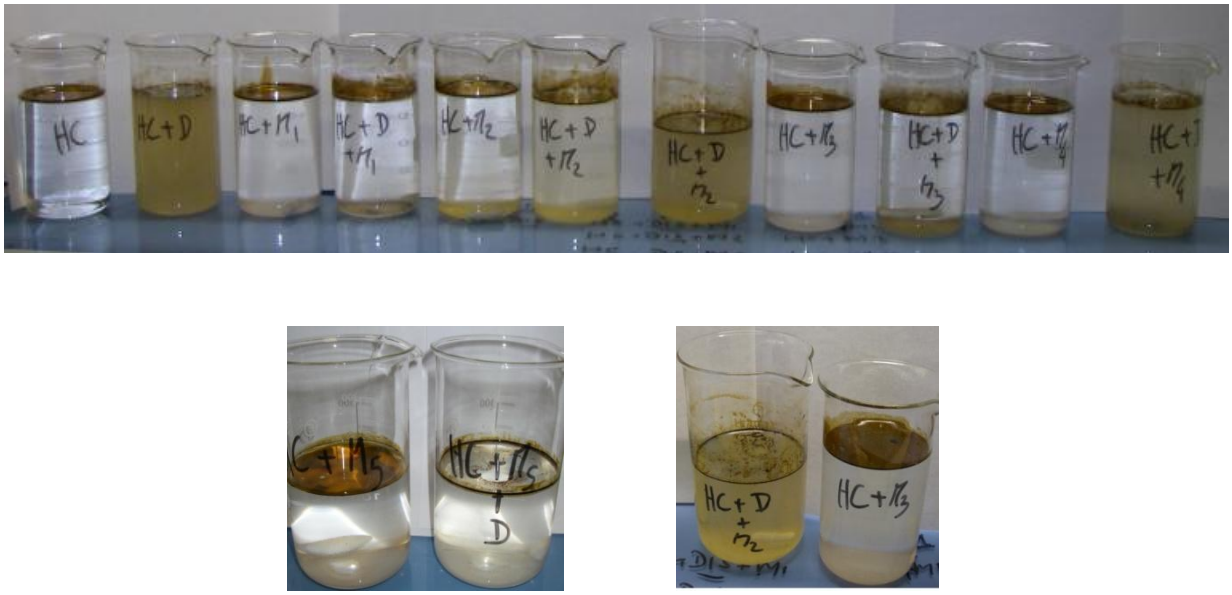

Figure 23: Photos illustrating preliminary tests of dispersed oil behaviour with and without mineral particles

The minerals known as ATC/NA and C2t were selected as they resulted in minimum recoalescence and resurfacing of oil, and promoted a better dispersion efficiency of oil in the water column. In order to link this work with the other parts of the project conducted in Canada by COOGER and UNB, kaolin was included with the two commercial products for laboratory tests.

3.4 Laboratory Experiments

3.4.1 Description of the IFP test

The laboratory tests consisted of measuring the efficiency of the dispersion using the IFP laboratory test (flow-through test / standard test method NF 90 345, Fig. 24) which is used for the approval of dispersants in France. For this particular study, the equipment was modified to allow fine tuning of the mixing energy during the test to promote dispersion.

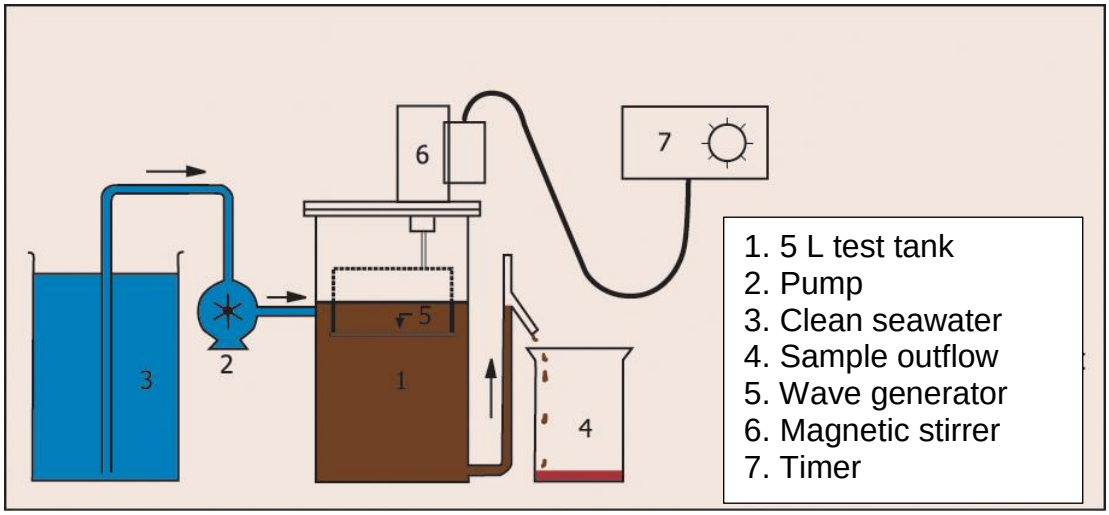

Figure 24: Schematic of the IFP test standard NFT 90 345

The IFP test method was originally designed to compare dispersant products in order to select the more efficient ones. To be realistic, the test method attempted to reproduce open ocean processes (wave action and dilution). However, the standard test conditions have been set to delineate the greatest differences among dispersants rather than reflecting a particular sea state. In this study, the test was used to compare the behaviour of the different mixtures of oil, dispersant and mineral particles, especially their stability in the water column after one hour of settling time.

The test took place in a 5 litre test tank equipped with water inlet and outlet (Fig. 24). A continuous dilution was created in the test tank by an inflow of 0.5 litres per hour. The test tank solution was moderately agitated by a wave generator producing vertical oscillations. In the modified equipment used for our tests, the wave beater was driven by an electric motor, and both speed (rpm) and stroke (cm) were adjustable.

At the beginning of the test, the flow of sea water was allowed to stabilize. The oil was then added followed one minute afterward by the dispersant. The mixture of oil and dispersant was then allowed to rest for one additional minute. Subsequently, the agitator was activated for one hour. During this time, as water flows out, the dispersed oil was progressively evacuated through the outflow and collected in a separatory funnel. For this study, a magnetic stirring bar was added and rotated slowly at the bottom of the test tank to avoid any settling.

After one hour, the sea water pump was stopped and the oil in the separatory funnel was allowed to stand for one additional hour. In order to measure the sizes of the oil droplets and aggregates coming out the test tank, a LISST-100X particle size analyser was installed between the test tank and the separatory funnel. Figures 25 and 26 illustrate the experimental setup of the testing equipment with the LISST. The LISST was set with the cell equipped

with the magnetic stirrer (turning at low speed) to avoid the settling of aggregates in the counting cell.

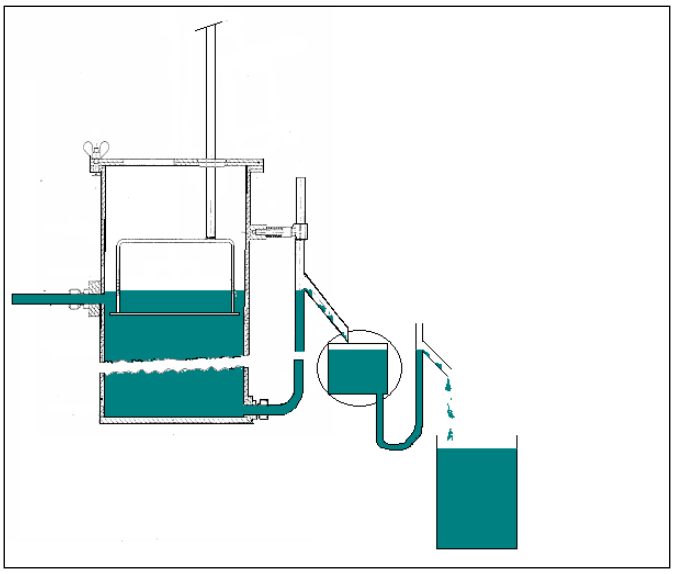

Figure 25: Schematic of test tank equipped with LISST counting cell (circled) and final separatory funnel

Figure 26: Test tank at the rear with the black LISST

Conventionally in the IFP test, the efficiency represents the relative amount of oil dispersed and eliminated in the overflow during the one hour period. The efficiency value ranges

between 0 and 100, where 100 corresponds to a maximum theoretical quantity that would be eliminated in the case of a totally dispersed substance. In this study, all the oil which was flushed out of the test tank was considered as dispersed and was used to calculate the overall dispersion efficiency of each test. Preliminary tests examined the energy level to apply after dispersant application and during mineral introduction. The magnetic stirrer ensured that all of the dispersed oil, with or without minerals, passed through the LISST to be monitored for size. To assess the dispersed oil, it was collected in a separatory funnel in three fractions: the decanted fraction from the bottom (settled), middle suspended fraction in the water column, and the coalesced fraction on or near the surface. These permitted assessment of oil mass balance.

Figure 27 is a schematic representation of the modified IFP dilution test, and Figure 28 shows the IFP system in the laboratory at CEDRE.

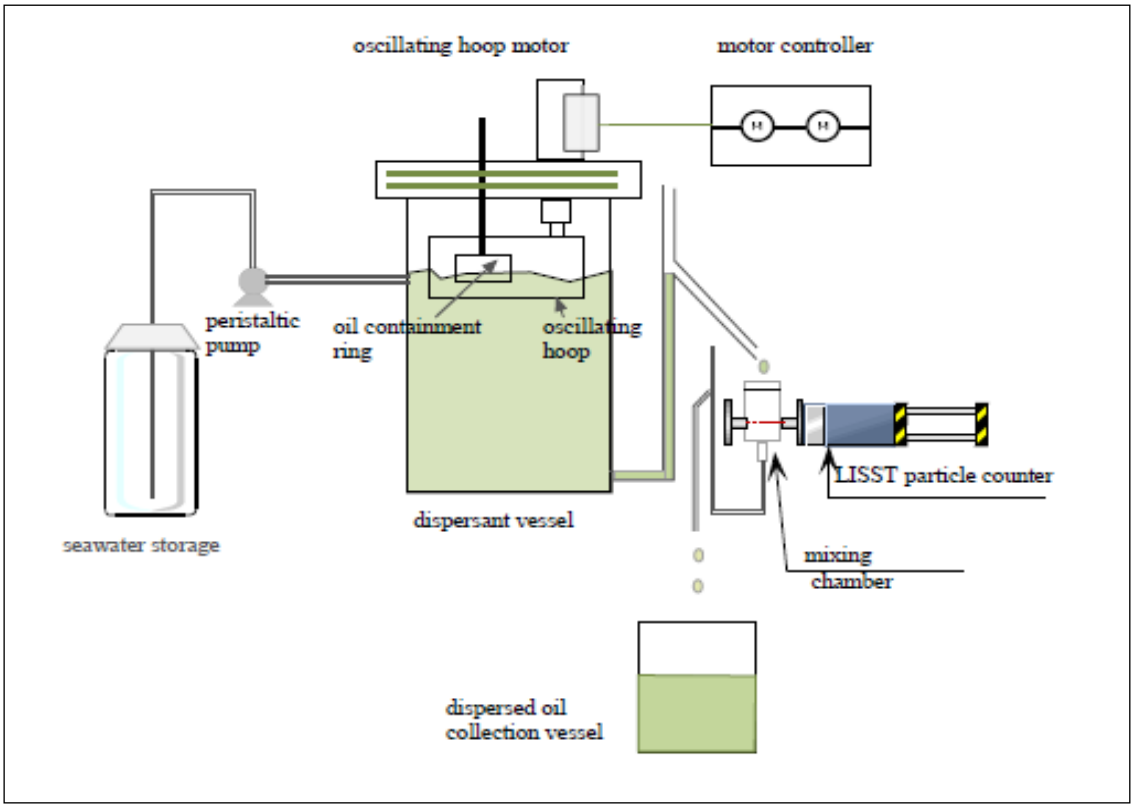

Figure 27: Schematic diagram of the experimental setup of IFP tests in CEDRE, France

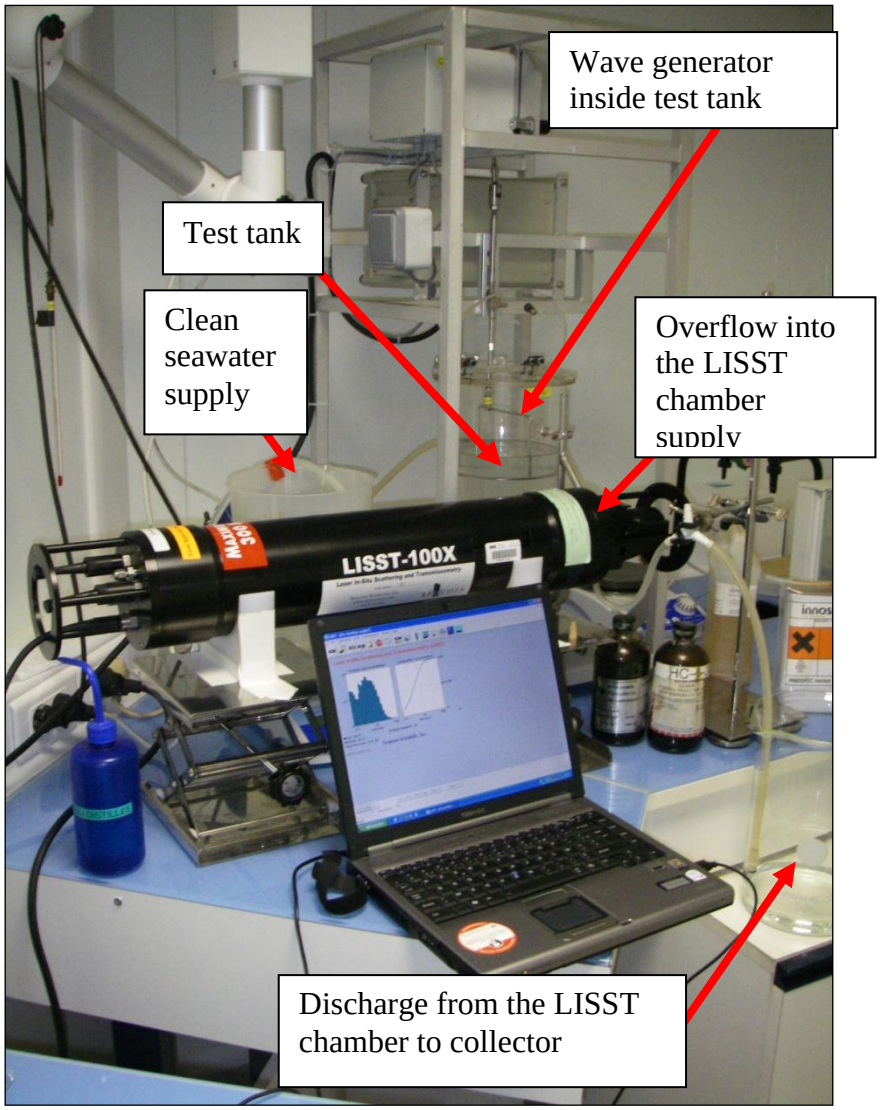

Figure 28: Photograph of modified IFP test setup in CEDRE, France, in which effluent from the IFP test is diverted to the mixing chamber of a LISST-100X for particle size analysis

In order to simulate the actual situation in the field of a treatment combining dispersant and mineral fines, it was preferable to apply dispersant to the oil first, followed by the mineral fines a few minutes later, allowing enough time for the dispersant to act. This procedure simulated a field response to an oil spill. In this protocol, the influent of the flow-through test unit consists of clean, particle-free seawater, and mineral particles were added only once after the chemical dispersant had been applied to the oil. This protocol was used during the first test. It was observed that this protocol produced an uncontrolled and uneven concentration of mineral fines in the water.

To avoid these difficulties it was decided to add the fines to the water (water supply and in the test tank) in order to achieve a known and more homogeneous concentration in the water. The quantities of minerals to be used were kept reasonably low to make field application practical and realistic. Using a high dose of mineral fines (such as MOR at 1:2) could

quickly become problematic in the event of a real-world pollution remediation situation. Tests were carried out with 4 clay concentrations: 0.24 g/L, 0.12 g/L, 0.08g/L and 0.04g/L. This means that for 5 g of test oil in the 5 L tank, clay additions of 24, 12, 8 and 4% of the oil were carried out, respectively.

Tests were carried out under three mixing regimes: (a) very low energy for the first two tests (it was determined that the wave generator was too deep and this regime was later abandoned); (b) standard agitation (wave generator speed = 77 rpm, stroke = 30 mm) and depth of 20 mm (in the highest position) ; and (3) high agitation (wave generator speed = 98 rpm for the first ten minutes of the test, then adjusted to 77 rpm, stroke = 30 mm) and depth of 20 mm.

The test procedure was as follows:

a) Addition of the appropriate concentration of clay to the test tank and to the clean water supply tank.
b) The clean seawater pump was started and allowed to run until the water level in the test tank was stabilized, and then the stirrer in the bottom of the test tank was started.
c) The test oil was added to the confinement ring within the test tank; this was time zero or T = 0.
d) At T = 1.5 min the LISST was started.
e) At T = 3 min the dispersant was applied to the oil slick with a syringe.
f) At T = 4 min the agitation was started (wave generator/oscillating ring) and the overflow from the LISST was directed into a separatory funnel to collect the seawater with dispersed oil.
g) At T = 1 hour 4 min, the clean water pump and the LISST were stopped.
h) The system was allowed to stand for another hour to settle before the sampling procedure.
i) The sampling was completed as follows: a. In the separatory funnel, the oil which had settled was first drained to collect the lowest 40 to 50 mL as the decanted fraction. b. The oil in the water column, around 2500 mL, was collected as the suspended fraction. c. The oil at the surface and very close to the surface was collected as the re-coalesced and resurfaced fraction. d. The oil found in the LISST cell was collected and considered as part of the coalesced fraction and was added to the coalesced fraction.

3.4.2 Experimental Design

Testing factors and their levels included two types of oil (Alberta Sweet Mix Blend and IFO40); dispersant type (no dispersant control, Corexit 9500, and GAMLEN OD 4000); clay type (no clay control, ATC/NA, C2t, and kaolin), and clay dose (30, 15, 10 and 5%, and no-clay control). These parameters were investigated following an experimental design as shown

in Table 4. Experiments were conducted by two operators to assess the additional factor of mixing energy at three levels.

Table 4: Experimental design of the IFP test conditions

Oil	Dispersant	Clay	Clay (%)	Replicates
Alberta Sweet Mix Blend	GAMLEN OD 4000	without	0	2
		ACT/NA	10	3
			30	2
	Corexit 9500	without	0	10
		ACT/NA	30	2
		C2t	30	2
		kaolin	5	2
			10	2
			15	2
			30	9
	No dispersant	kaolin	30	2
IFO 40	C9500	without	0	4
		ACT/NA	30	2
		C2t	30	2
		kaolin	30	4

3.4.3 Particle Size Distribution

A LISST-100X particle size analyzer was used for each test to measure droplet size. The measurements often stopped before the end of the tests (sometimes a few minutes after the test began) possibly due to the relatively high concentration of dispersed oil in the water column. This was probably caused by the high concentration of OMA particles that had passed the optical detection upper limit of the LISST instrument.

3.5 Results and Discussion

3.5.1 IFP Test Results

The IFP test results are given in Table 5. There were 51 independent IFP tests conducted. Among them, three were pretests which were conducted at ambient room temperature (20^{o}C) and two out of these three tests were conducted with clay addition in a different fashion from the remaining 48 tests. Since the primary goal was to evaluate oil dispersion at low temperature conditions, data analysis was performed for the 48 tests that were conducted at low temperature only. Of these 48 tests, the average oil dispersion efficiency was 47 ± 21%.

Table 5: IFP test results

test #	oil	dispersan	clay	clay %	clay addition	pumped	m_0 oil	dispersed oil (g)			oil lost	disperd	% oil	% oil			decantatio	disp oil		Efficacy	energy	tempe	operato
	type	brand	type		mode	water (g)	(g)	settled	in suspen	on surface	on ring	oil (g)	isperse	on surf.	in suspens	settled	time (h)	théor %	actual %		mode	°C	
100	1	1	1	30	before	2499	4,06	0	0,12	0,14	0,11	0,26	7	54	46	0	1	39,3	6,6	17	1	5	2
101	1	1	0	0	-	2945	3,36	0	0,14	0,03	0,15	0,17	5	17	83	0	0,5	44,5	5,3	12	1	5	2
102	1	1	0	0	-	2769	3,54	0	0,59	0,17	0,07	0,77	22	23	77	0	1	42,5	22,1	52	2	5	2
103	1	1	1	30	before	2565	3,86	0,004	0,08	0,59	0,21	0,67	18	88	11	0,66	1	40,1	18,4	46	2	5	2
104	1	1	0	0	-	2854	3,67	0	0,66	0,35	0,20	1,01	29	34	66	0	1	43,5	29,1	67	2	5	2
105	1	1	1	30	before	2844	3,77	0,0089	0,25	0,66	0,05	0,92	25	72	27	0,97	1	43,4	24,6	57	2	5	2
106	2	1	0		-	2867	4,74	0	0,25	1,09	0,06	1,34	29	81	19	0	1	43,6	28,6	65	2	5	2
107	2	1	1	30	before	2837	4,17	0,001	0,10	0,23	0,01	0,32	8	70	30	0,31	1	43,3	7,8	18	2	5	2
108	2	1	0	0	-	2835	3,74	0	0,10	0,26	0,18	0,37	10	72	28	0	1	43,3	10,3	24	2	5	2
109	2	1	1	30	befoe	2841	4,15	0	0,12	0,43	0,01	0,56	13	78	22	0	1	43,3	13,5	31	2	5	2
110	1	1	1	10	before	2867	3,79	6E-04	0,58	0,38	0,11	0,96	26	40	60	0,06	1	43,6	26,2	60	2	5	2
111	1	1	1	10	befoe	2858	3,67	0	0,33	0,28	0,05	0,61	17	46	54	0,00	1	43,5	16,9	39	2	5	2
112	1	0	1	30	before	2842	3,91	0	0,00	0,00	0,04	0,00	0	100	0	0,00	1	43,4	0,1	0	2	5	2
113	1	0	1	30	before	2888	3,98	0	0,00	0,00	0,03	0,00	0	100	0	0,00	1	43,9	0,0	0	2	5	2
114	1	1	0	0	-	2885	3,75	0	0,70	0,57	0,08	1,27	35	45	55	0,00	1	43,8	34,6	79	3	5	2
115	1	1	1	30	before	2875	3,86	0,003	0,63	0,39	0,04	1,02	27	38	62	0,25	1	43,7	26,9	61	3	5	2
116	1	1	0	0		2853	4,01	0	0,34	0,19	0,06	0,53	13	36	64	0,00	1	43,5	13,4	31	3	5	2
117	1	1	1	30	before	2863	3,92	0,016	0,52	0,42	0,03	0,96	25	44	55	1,72	1	43,6	24,6	56	3	5	2
118	1	1	0	0		2857	3,55	0	0,82	0,43	0,07	1,25	36	34	66	0,00	1	43,5	35,9	83	3	5	2
119	1	1	1	5	before	2825	4,41	0	0,42	0,51	0,13	0,93	22	55	45	0,00	1	43,2	21,8	50	2	5	2
120	1	1	1	5	before	2921	4,19	0	0,23	0,88	0,08	1,11	27	79	21	0,00	1	44,2	27,0	61	2	5	2
121	1	1	1	15	before	2921	3,71	0	0,15	0,75	0,12	0,90	25	83	17	0,00	1	44,2	25,2	57	2	5	2
122	1	1	1	15	before	2873	3,67	0	0,39	0,59	0,06	0,97	27	60	40	0,00	1	43,7	27,0	62	2	5	2
123	1	2	3	10	before	2754	3,92		1,17		0,12	1,17	31				1-2	42,4	30,9	73	2	20	1
124	1	2	3	10	premix after	2621	3,91		1,06		0,05	1,06	27				1-2	40,8	27,4	67	2	20	1
125	1	2	3	20	premix after	3164	3,98		1,22		0,08	1,22	31				1-2	46,9	31,4	67	2	20	1
126	1	2	0	0	-	2851	4,20		0,40	0,20	0,11	0,60	15	33	67	0	1-2	43,5	14,6	33	2	5	1
127	1	2	3	10	before	2627	3,85	0,06	0,01	0,22	0,12	0,29	8	75	5	21	2	40,9	7,8	19	2	5	1
128	1	2	3	30	before	2781	3,78	0,01	0,14	0,56	0,04	0,71	19	79	20	1	2	42,7	19,0	45	2	5	1
129	1	2	3	30	before	2864	3,76	0,01	0,07	0,12	0,14	0,19	5	60	36	4	1-2	43,6	5,4	12	2	5	1
130	1	2	0	0	-	2916	3,96		0,72	0,32	0,04	1,05	27	31	69	0	1-2	44,2	26,7	60	2	5	1
131	1	2	3	10	before	2881	3,87	0,00	0,74	0,27	0,06	1,01	27	27	73	0	1-2	43,8	26,6	61	2	5	1
132	1	1	0	0	-	2916	3,89		0,38	0,36	0,07	0,74	19	48	52	0	1	44,2	19,4	44	2	5	1
133	1	1	3	30	before	2438	3,75	0,01	0,55	0,07	0,06	0,63	17	11	86	2	1	38,6	17,1	44	2	5	1
134	1	1	0	0	-	2492	3,91		0,85	0,22	0,06	1,08	28	21	79	0	1	39,2	28,0	71	2	5	1
135	1	1	3	30	before	2487	3,99	0,01	0,26	0,21	0,07	0,47	12	45	54	1	1	39,2	12,1	31	2	5	1
136	2	1	0	0	-	3024	3,87		0,05	0,54	0,01	0,59	15	91	9	0	1	45,4	15,3	34	2	5	1
137	2	1	3	30	before	3021	3,95	0,01	0,21	0,49	0,00	0,70	18	70	29	1	1	45,3	17,8	39	2	5	1
138	2	1	0	0	-	2946	3,73		0,16	0,51	0,00	0,67	18	76	24	0	1	44,5	18,0	41	2	5	1
139	2	1	3	30	before	3014	3,93	0,00	0,08	0,45	0,00	0,53	14	83	16	1	1	45,3	13,6	30	2	5	1
140	2	1	2	30	before	3038	3,90	0,01	0,17	0,56	0,01	0,74	19	76	23	1	1	45,5	19,0	42	2	5	1
141	2	1	2	30	before	3024	4,00	0,00	0,12	0,45	0,00	0,58	14	78	21	1	1	45,4	14,4	32	2	5	1
142	1	1	2	30	before	2957	3,92	0,01	0,63	0,45	0,11	1,09	29	41	58	1	1	44,6	28,6	64	2	5	1
143	1	1	2	30	before	2936	3,92	0,01	0,67	0,47	0,03	1,15	30	41	58	1	1	44,4	29,6	67	2	5	1
144	1	1	0	0	-	2889	3,81		0,77	0,51	0,06	1,29	34	40	60	0	1	43,9	34,3	78	2	5	1
145	1	1	0	0	-	2898	3,77		0,87	0,39	0,03	1,26	34	31	69	0	1	44,0	33,8	77	2	5	1
146	1	1	1	30	before	2888	3,88	0,21	0,29	0,30	0,07	0,80	21	38	36	26	1	43,9	21,0	48	2	5	1
147	1	1	1	30	before	2998	3,91	0,25	0,60	0,17	0,03	1,02	26	17	59	24	1	45,1	26,4	58	2	5	1
148	2	1	1	30	before	2836	4,02	0,07	0,19	0,39	0,00	0,66	16	59	30	11	1	43,3	16,3	38	2	5	1
149	2	1	1	30	before	2923	3,99	0,07	0,25	0,51	0,01	0,82	21	62	30	8	1	44,3	20,7	47	2	5	1
150	1	1	1	30	before	2879	3,99	0,27	0,83	0,28	0,03	1,37	35	20	60	19	1	43,8	34,7	79	3	5	1
151	1	1	1	30	before	2992	3,93	0,36	0,82	0,26	0,03	1,44	37	18	57	25	1	45,0	36,8	82	3	5	1

3.5.2 Measurements of particle size with LISST

The LISST was used during each test to measure the oil droplet and OMA diameter. The measurements often stopped before the end of the tests, sometimes a few minutes into the test, perhaps because the concentration of dispersed oil in the water column was excessive. Figures 29 and 30 show representative LISST measurements of ASMB oil. Figures 31 and 32 are for IFO40.

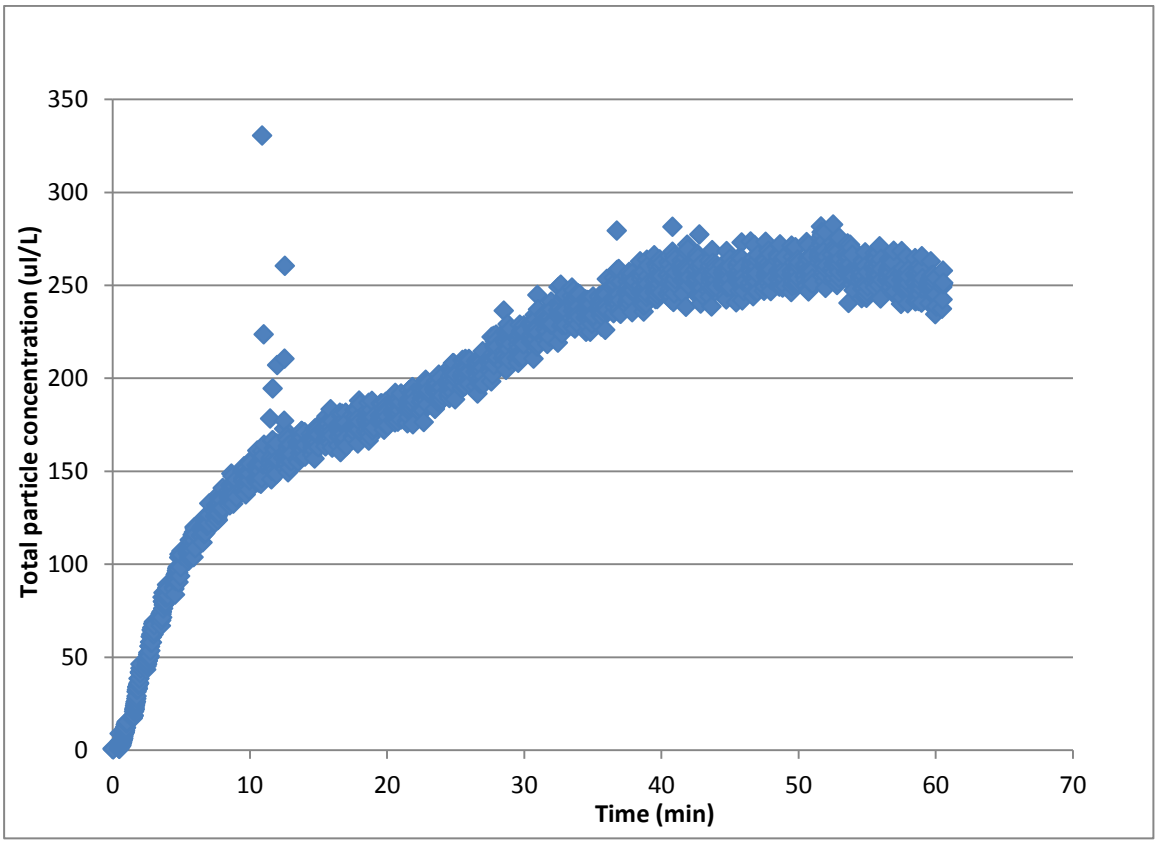

Figure 29: Representative total particle concentration as a function of time for ASMB oil with OD400, 10% ACT/NA, and regular mixing energy

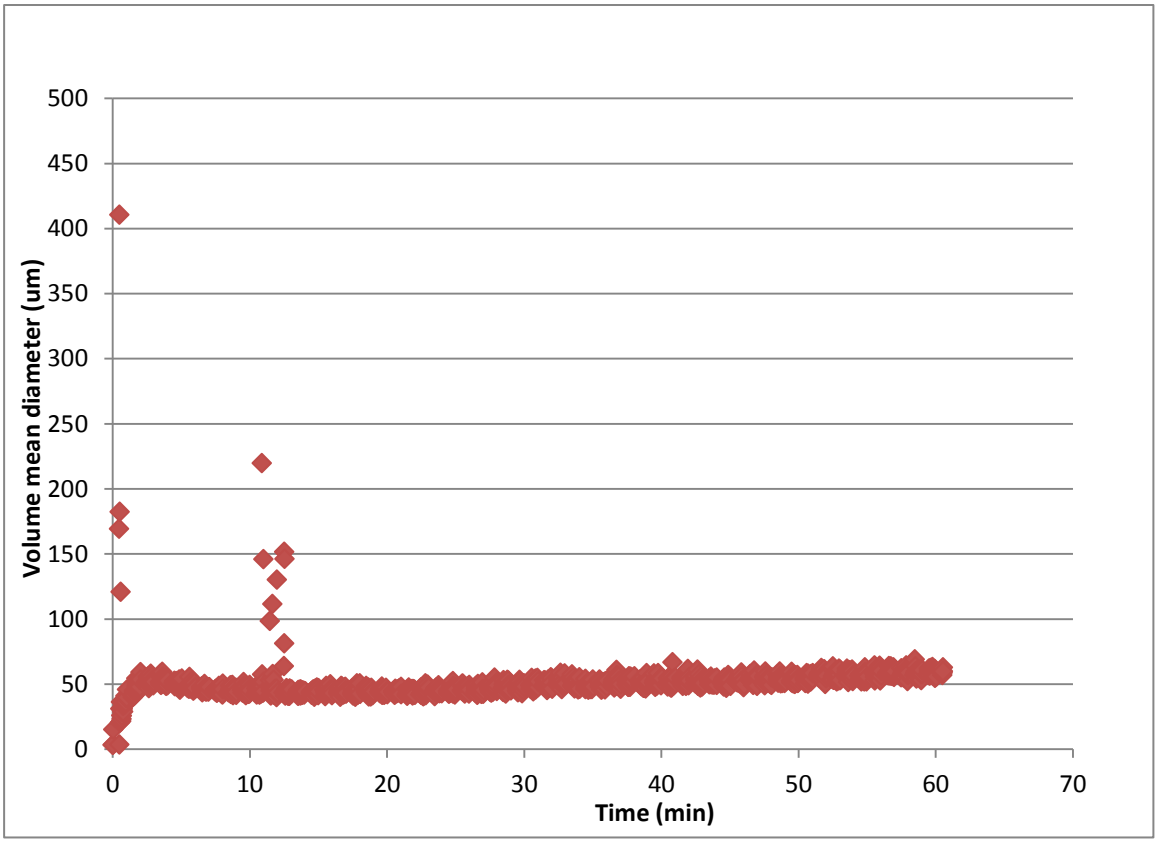

Figure 30: Representative volume mean diameter as a function of time for ASMB oil with OD400, 10% ACT/NA, and regular mixing energy

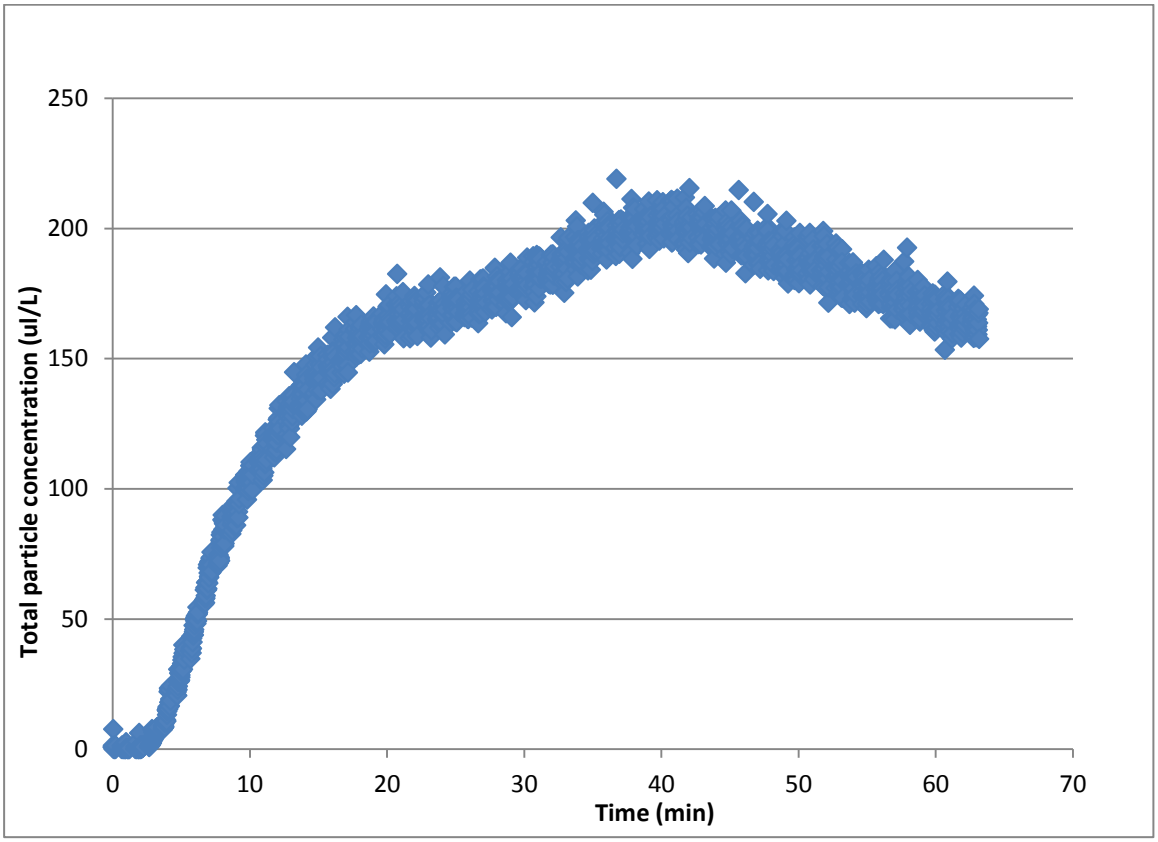

Figure 31: Representative total particle concentration as a function of time for IFO40 oil with Corexit 9500, no clay, and regular mixing energy

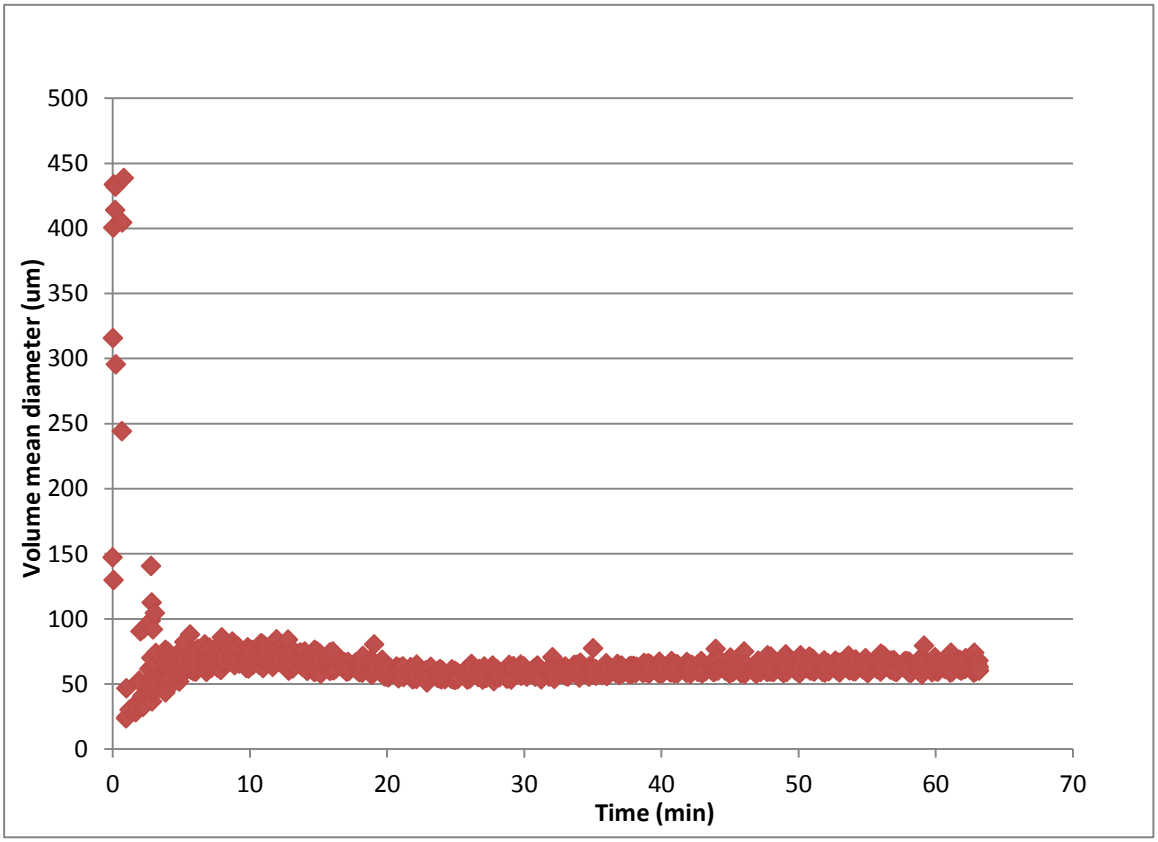

Figure 32: Representative volume mean diameter as a function of time for IFO40 with Corexit 9500, no clay, and regular mixing energy

3.5.3 Statistical Analysis

The results were analyzed using the multivariate software package, Statgraphics, to investigate potential effects of different treatment conditions and operational parameters. Specifically, a multivariate analysis of variance (ANOVA) was performed to evaluate the effects of the main test factors and their interactions on the overall dispersion efficiency of test oil in the modified IFP testing system, the coalesced and resurfaced fraction of the dispersed oil after it was diluted from the IFP testing system, the more stable fraction of the dispersed oil that remained suspended in the water column, and the fraction of the dispersed oil that diffused or settled to the bottom of the separatory flask. Dispersion efficiency was also evaluated through the dispersed oil and OMA particle size distribution data acquired with the LISST-100X.

<u>Effects of test factors on the dispersion efficiency of oil in the IFP system</u>

A 6-way analysis of variance of the IFP tests (Figure 33, Table 6) indicated that three main factors, namely oil type ($p = 0.0128$), dispersant type ($p = 0.0001$), and mixing energy ($p = 0.0009$) had significant effects on the dispersion efficiency of oil from the modified IFP test

system. Other factors including clay type, clay dosage and operator had insignificant effects on the overall dispersion efficiency. None of the multi-factor interaction effects had a significant effect on dispersion efficiency. The significant effects of the three main factors are expected. IFO-40 is an intermediate fuel oil with higher viscosity than the tested crude oil, so the apparent dispersion effectiveness of IFO-40 is lower. The use of dispersants enhanced the dispersion of oil, hence the significant effect of dispersant type. Higher mixing energy also improved dispersion.

Figures 33 to 35 present results of the analysis of variance (ANOVA) for the evaluated factors and levels which are as follows:

Factor	**Level**
i. Test oils	1 = Alberta Sweet Blend 2 = IFO-40
ii. Energy level	1 = Low energy (mode #1) 2 = Standard mixing energy (mode #2) 3 = Higher mixing energy (mode #3)
iii. Dispersant	0 = No dispersant 1 = Corexit 9500 2 = Gamlen OD 4000
iv. Clay type	0 = No clay 1 = ACT/NA 2 = C2t 3 = Kaolin
v. Clay Dosage	0 = No clay 5 = 5% MOR 10 = 10% MOR 15 = 15% MOR 30 = 30% MOR (Tests were carried out with a clay dosage of 30% except tests #110, 111, 123, 124, 125, 127, 131, 150 & 151.)
vi. Operator	#1 #2

Table 6: ANOVA of the effects of main factors and their interactions on DE of the IFP test system

	Degree of freedom (Df)	Sum of Square (SS)	Mean Square (MS)	F Value	P(F)
OilType	1	1703.97	1703.97	7.1817	0.0128*
DispType	2	6920.17	3460.08	14.5831	0.0001*
ClayType	3	918.83	306.28	1.2909	0.2993
ClayDose	3	50.42	16.81	0.0708	0.9750
EnergyMode	2	4454.35	2227.17	9.3868	0.0009*
Operator	1	667.27	667.27	2.8123	0.1060
OilType:ClayType	3	265.31	88.44	0.3727	0.7734
DispType:ClayType	1	117.83	117.83	0.4966	0.4875
DispType:ClayDose	1	99.70	99.70	0.4202	0.5227
ClayType:EnergyMode	2	199.78	99.89	0.4210	0.6610
OilType:Operator	1	32.49	32.49	0.1369	0.7145
ClayType:Operator	1	187.88	187.88	0.7919	0.3820
EnergyMode:Operator	1	71.95	71.95	0.3033	0.5867
OilType:ClayType:Operator	1	262.43	262.43	1.1061	0.3030
Residuals	25	5931.66	237.27		

* Denotes statistically significant effect at 95% confidence interval ($P < 0.05$).

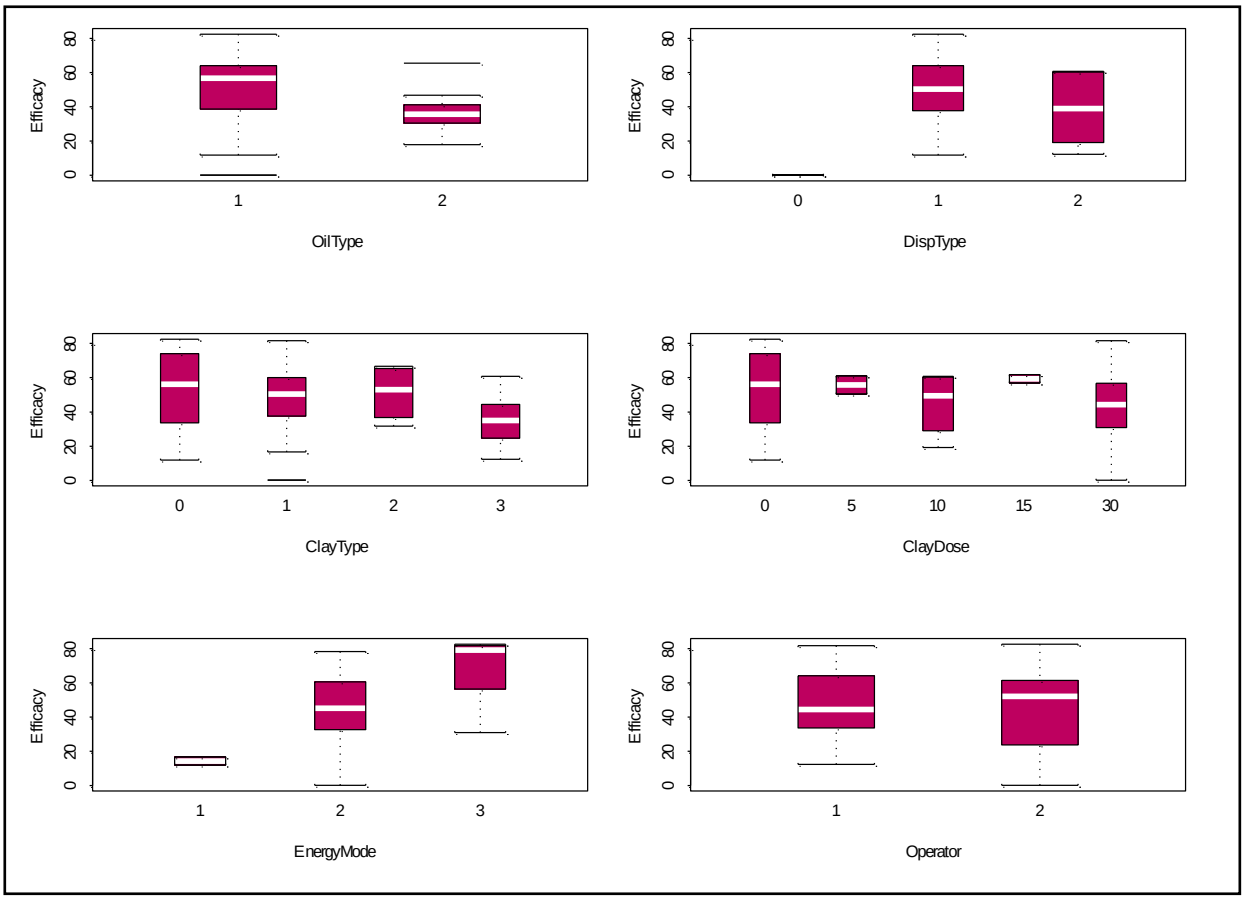

Figure 33: Factorial effects on the overall dispersion efficiency of oil in the IFP test

Table 7: ANOVA of the factorial effects on the coalesced and resurfaced fraction of the dispersed oil

	Df	Sum of Sq	Mean Sq	F Value	P(F)
OilType	1	7154.47	7154.47	48.7448	0.0000*
DispType	2	6410.75	3205.37	21.8389	0.0000*
ClayType	3	1195.97	398.66	2.7161	0.0661
ClayDose	3	2721.41	907.14	6.1805	0.0027*
EnergyMode	2	157.48	78.74	0.5365	0.5914
Operator	1	1766.19	1766.19	12.0334	0.0019*
OilType:ClayType	3	1099.91	366.64	2.4980	0.0828
DispType:ClayType	1	959.96	959.96	6.5404	0.0170*
DispType:ClayDose	1	5.26	5.26	0.0358	0.8514
ClayType:EnergyMode	2	673.16	336.58	2.2932	0.1218
OilType:Operator	1	334.48	334.48	2.2789	0.1437
ClayType:Operator	1	1559.14	1559.14	10.6228	0.0032*
EnergyMode:Operator	1	248.44	248.44	1.6927	0.2051
OilType:ClayType:Operator	1	396.88	396.88	2.7041	0.1126
Residuals	25	3669.35	146.77		

* Denotes statistically significant effect at 95% confidence interval ($p < 0.05$).

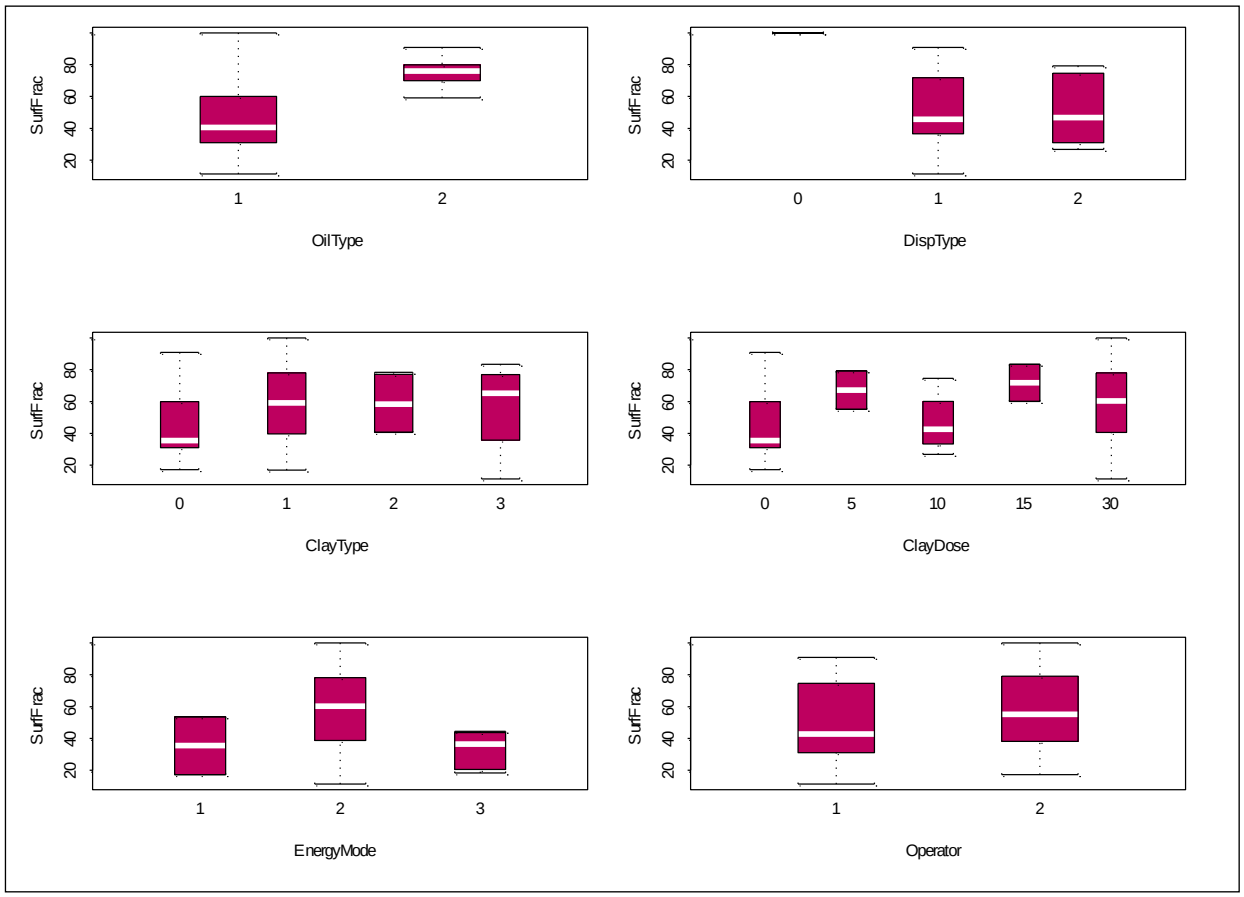

Figure 34: Factorial effects on the coalescence and resurfacing of dispersed oil

3.5.4 Factor effects on coalescence and resurfacing of oil

To clarify factor effects on the dispersion of oil and the formation and stability of OMA in the system, additional investigation was conducted on the fate of oil after dilution from the system. This was done by collecting water samples using a large separatory funnel for each test. After collection, the water sample was allowed to stand for approximately one hour, and then sequentially drained from the funnel for the collection of the settled fraction, the suspended fraction, and the coalesced and surface fraction. The oil that was retained in the small mixing chamber of the LISST-100X particle size analyzer was also counted as the coalesced and surface fraction.

Figure 34 presents the factor effects on the surface fraction of oil after the collected water samples were allowed to stand for one hour. ANOVA data analysis (Table 7) indicated that two interaction terms, clay type and operator interaction, and dispersant and clay type interaction, significantly affected the percentage fraction of dispersed oil that recoalesced and resurfaced. The main factors, oil type, dispersant type, clay dose, and the operator, all had significant effects on coalescence and resurfacing of the dispersed oil. Energy mode and clay type did not.

3.5.5 Factor effects on stable suspension of oil in the water column

Regarding the effects of different factors on the suspended fraction of oil in the water column, ANOVA analysis (Figure 35, Table 8) indicated that the interaction of dispersant type and clay type had a significant effect. The main factors, oil type, dispersant type, and clay type, had significant effects on the stable suspension of dispersed oil in the water column. Clay dose, energy mode and operator did not.

Table 8: ANOVA of the factorial effects on the suspended fraction of the dispersed oil in the water column

	Df	Sum of Sq	Mean Sq	F Value	P(F)
OilType	1	6391.238	6391.238	33.2686	0.0000*
DispType	2	5713.569	2856.784	14.8706	0.0001*
ClayType	3	2831.197	943.732	4.9125	0.0081*
ClayDose	3	1427.39	475.797	2.4767	0.0847
EnergyMode	2	149.113	74.556	0.3881	0.6824
Operator	1	294.156	294.156	1.5312	0.2274
OilType:ClayType	3	1474.14	491.38	2.5578	0.0778
DispType:ClayType	1	1497.206	1497.206	7.7935	0.0099*
DispType:ClayDose	1	68.327	68.327	0.3557	0.5563
ClayType:EnergyMode	2	844.593	422.296	2.1982	0.1320
OilType:Operator	1	70.446	70.446	0.3667	0.5503
ClayType:Operator	1	373.508	373.508	1.9442	0.1755
EnergyMode:Operator	1	262.956	262.956	1.3688	0.2531
OilType:ClayType:Operator	1	150.372	150.372	0.7827	0.3847
Residuals	25	4802.752	192.11		

* Denotes statistically significant effect at 95% confidence interval ($p < 0.05$).

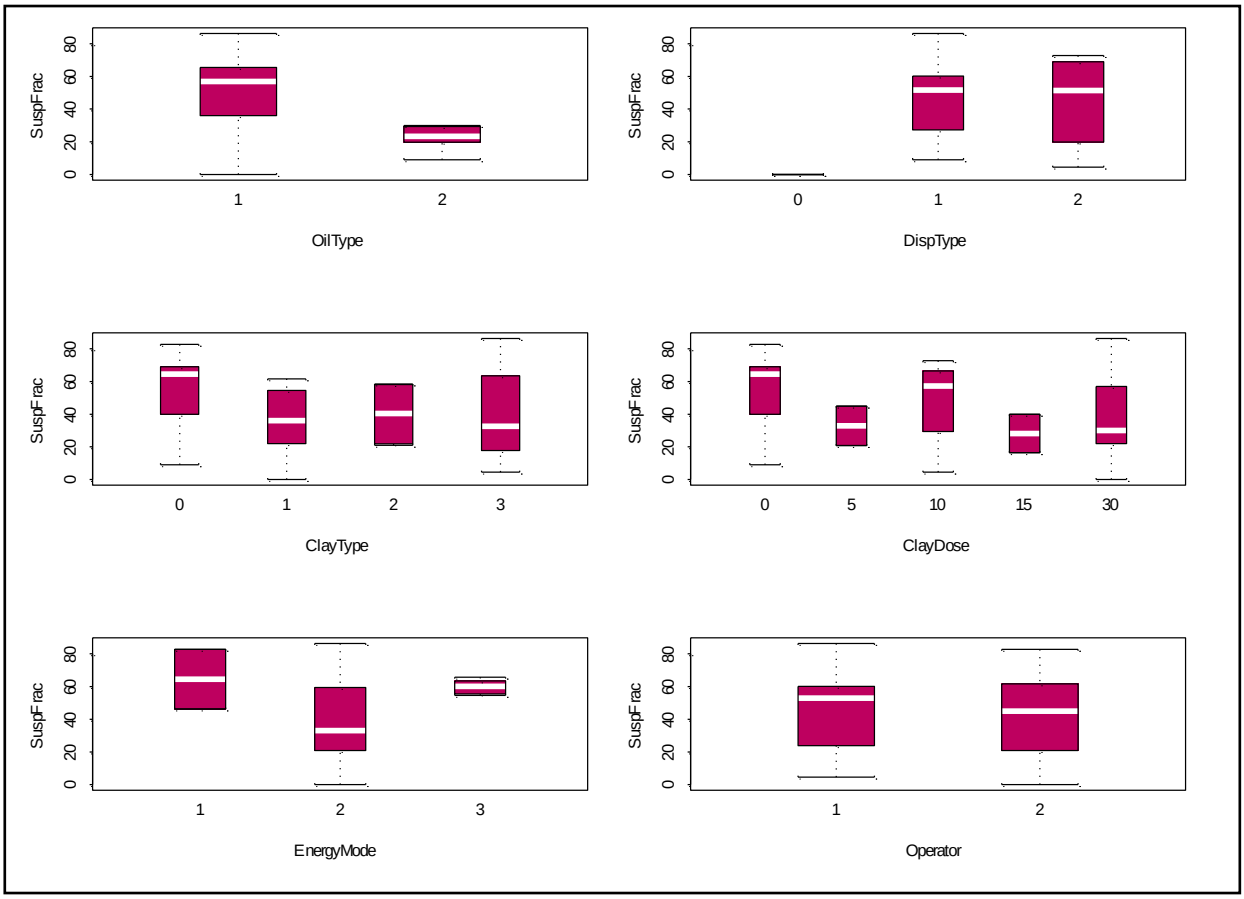

Figure 35: Factorial effects on the stable suspension of dispersed oil in the water column

3.5.6 Factor effects on settling of oil at the bottom

The factorial effects on the settling fraction of oil are complex, as indicated by significant effects of the multi-way interactions (Table 9, Figure 36), including 3-way interaction among oil type, clay type and operator, 2-way interactions between clay type and operator, clay type and energy level, dispersant type and clay dose, and dispersant type and clay type. Besides the multi-way interactions, main factors clay type, clay dose and the operator significantly influenced the settling fraction of oil.

Table 9: ANOVA of the factorial effects on the settling fraction of the dispersed oil

	Df	Sum of Sq	Mean Sq	F Value	P(F)
OilType	1	21.519	21.519	2.2904	0.1427
DispType	2	28.7896	14.3948	1.5321	0.2357
ClayType	3	363.1759	121.0586	12.8849	0.0000*
ClayDose	3	225.0967	75.0322	7.9861	0.0007*
EnergyMode	2	56.5644	28.2822	3.0102	0.0674
Operator	1	618.7696	618.7696	65.8588	0.0000*
OilType:ClayType	3	39.1661	13.0554	1.3896	0.2691
DispType:ClayType	1	59.4533	59.4533	6.3279	0.0187*
DispType:ClayDose	1	111.4846	111.4846	11.8659	0.0020*
ClayType:EnergyMode	2	122.3778	61.1889	6.5126	0.0053*
OilType:Operator	1	97.9194	97.9194	10.4221	0.0035*
ClayType:Operator	1	406.4111	406.4111	43.2564	0.0000*
EnergyMode:Operator	1	0.2061	0.2061	0.0219	0.8834
OilType:ClayType:Operator	1	58.6652	58.6652	6.2440	0.0194*
Residuals	25	234.8851	9.3954		

* Denotes statistically significant effect at 95% confidence interval ($p < 0.05$).

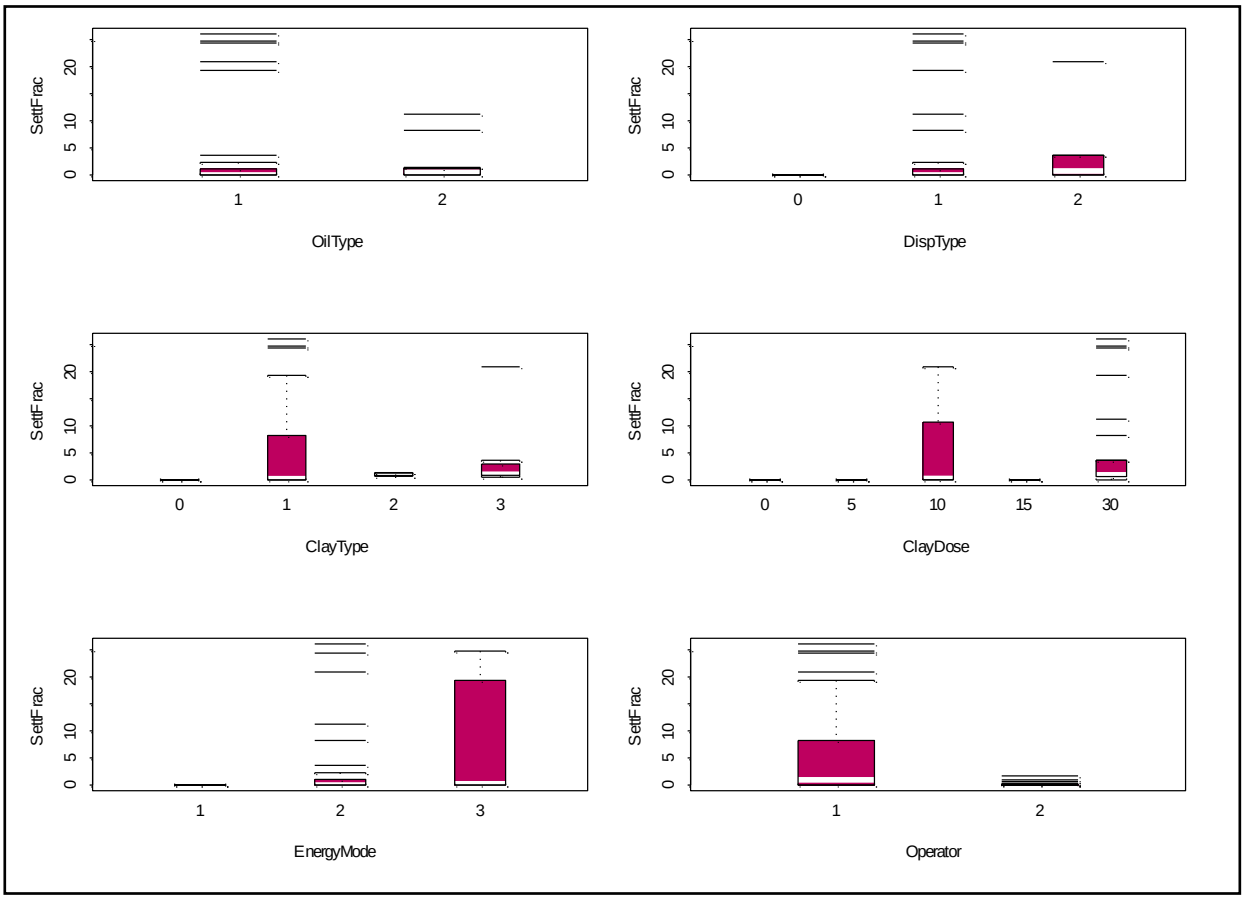

Figure 36: Factorial effects on the settling of the dispersed oil in the IFP test

In order to reduce the variability of the results and to show possible correlations, the data of each oil (ASMB then IFO 40) have been analysed independently.

3.5.7 ASMB coalesced oil on the surface

Figure 37 displays effects of treatment conditions on the percentage of oil coalesced at the surface in the separatory funnel. We observed that there was no clear trend of treatment effects. Nothing is significant. The test remains sensitive to the operator. An effect of dispersant 1 compare to no dispersant (limit to be significant). Possibly, (but it is not significant) an increase in the clay concentration may lead to an increase of the oil coalescence which is unexpected.

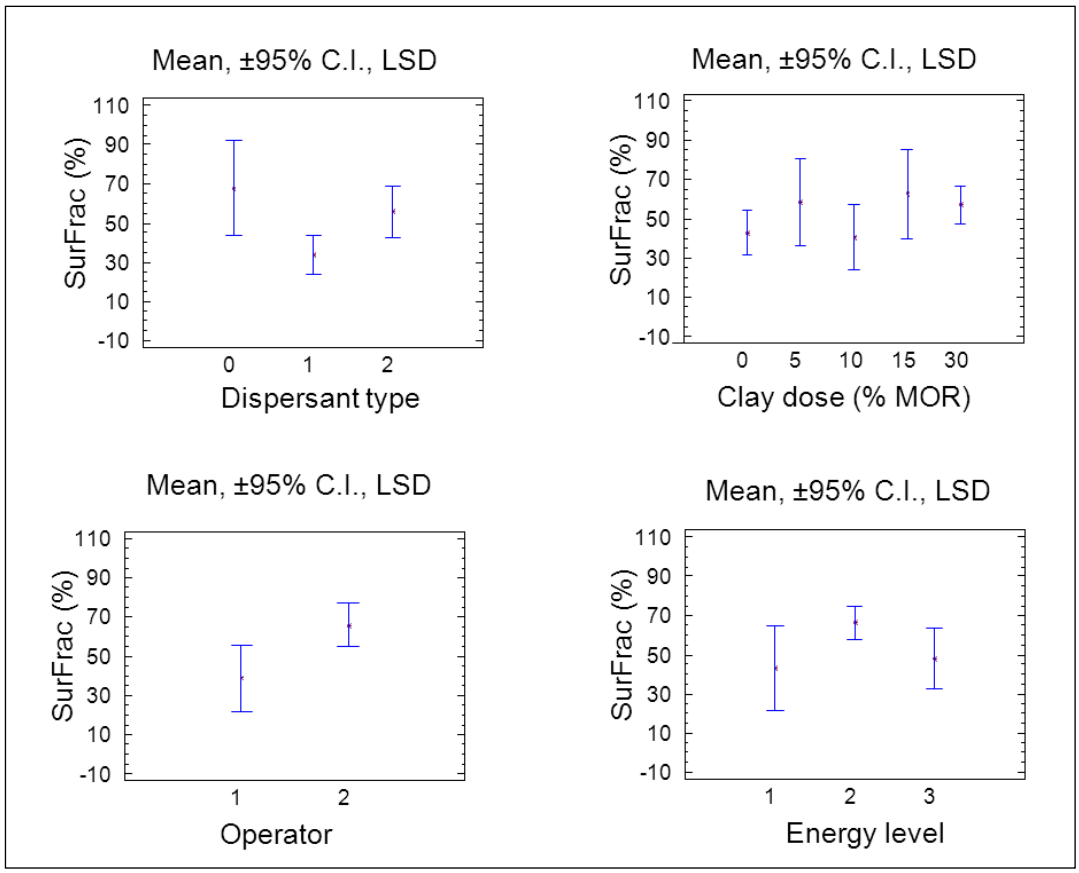

Figure 37: Effects of dispersant type (upper left), clay dose (upper right), operator (lower left), and energy level (lower right) on coalesced oil at the surface

3.5.8 ASMB dispersed oil in suspension in the water column

Figure 38 presents the treatment effects on the percentage of oil suspended in the water column of the separatory funnel. We can observe that the use of dispersant leads to an increase of the dispersed oil in the water column (which makes sense). Otherwise, no clear significant trend, possibly due to an increase in the clay concentration may lead to a decrease of the oil in suspension which is unexpected.

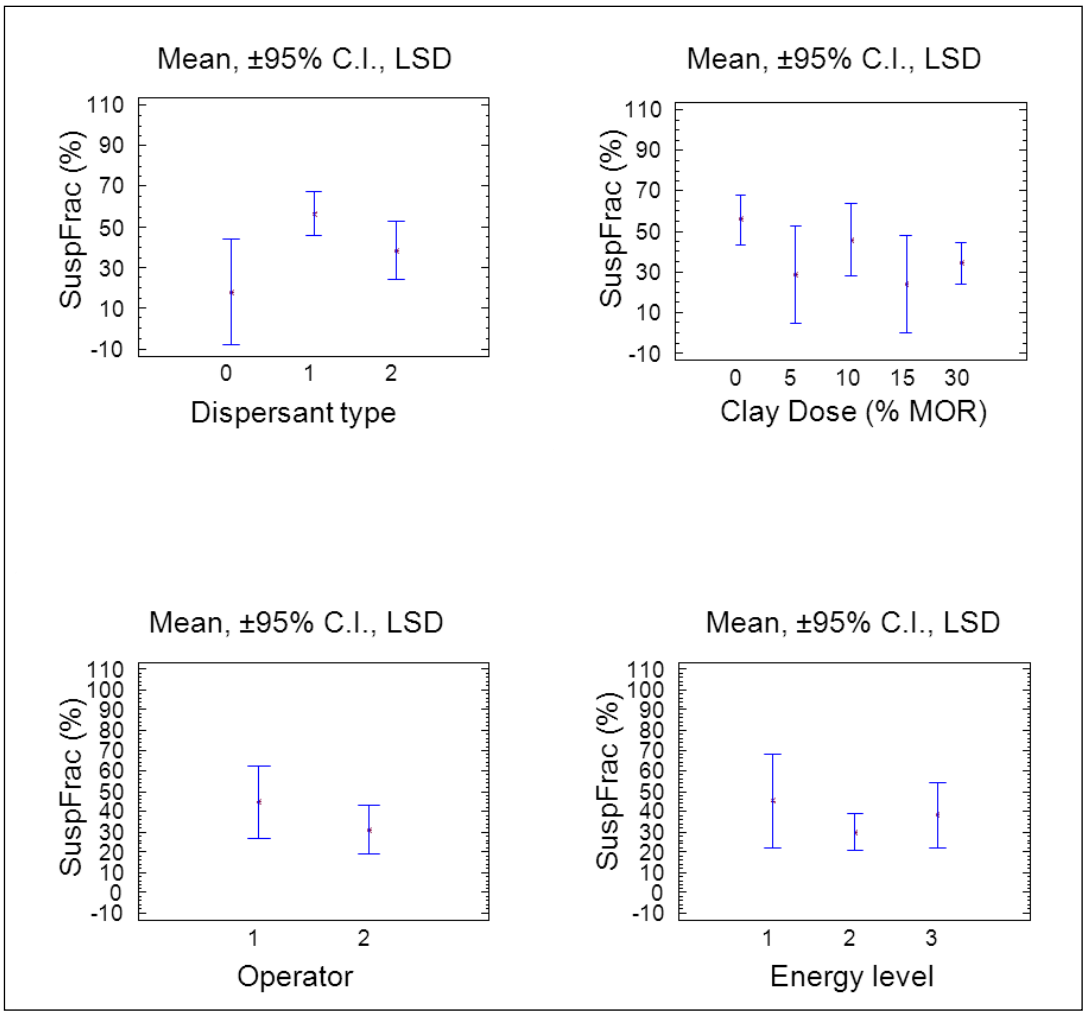

Figure 38: Effect of dispersant (upper left), clay dose (upper right), operator (lower left), and energy (lower right) on oil suspended in the water column

3.5.9 ASMB settled oil and aggregates

Figure 39 shows the treatment effects on the oil settled at the bottom of the separatory funnel. We can observe no clear trend, nothing is significant.

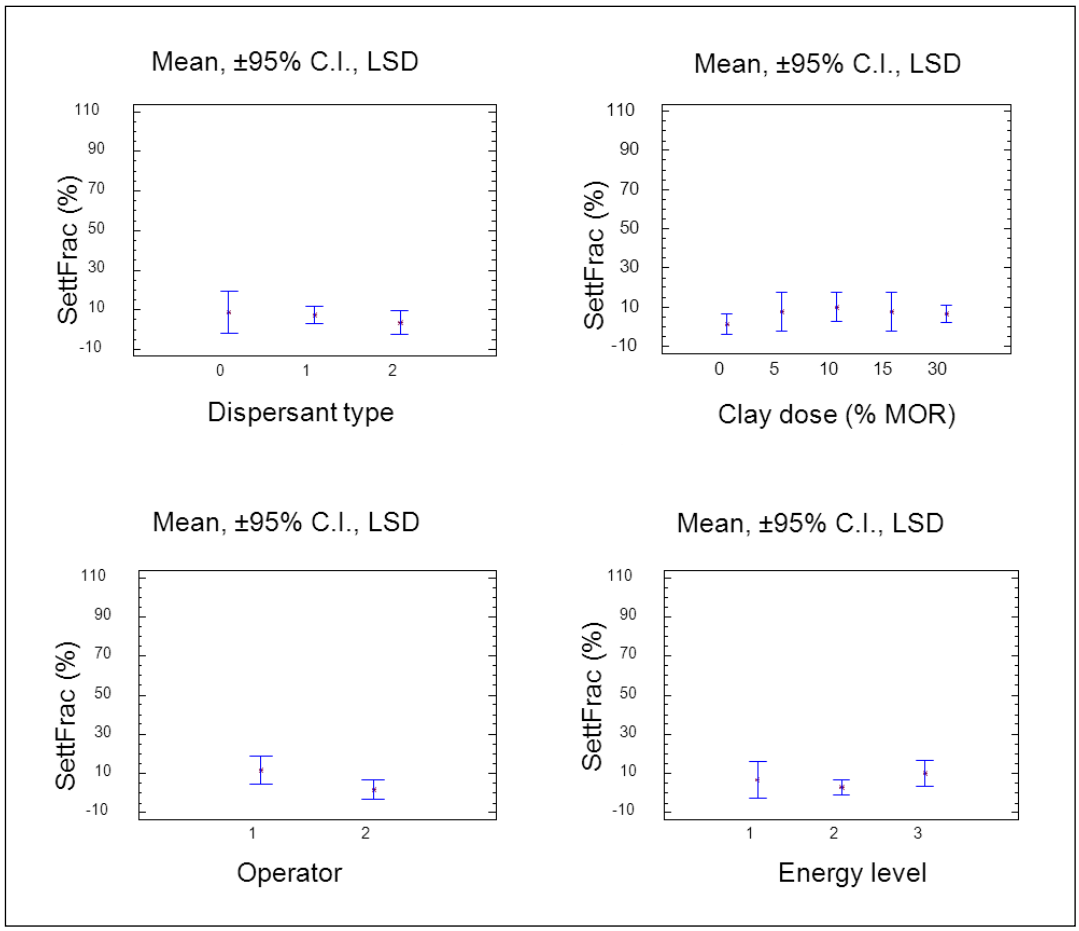

Figure 39: Effect of dispersant (upper left), clay dose (upper right), operator (lower left), and energy (lower right) on oil settled at the bottom

3.5.10 IFO coalesced oil on the surface

Figure 40 displays treatment effects on IFO40 at the surface. No significant effects from the two tested factors.

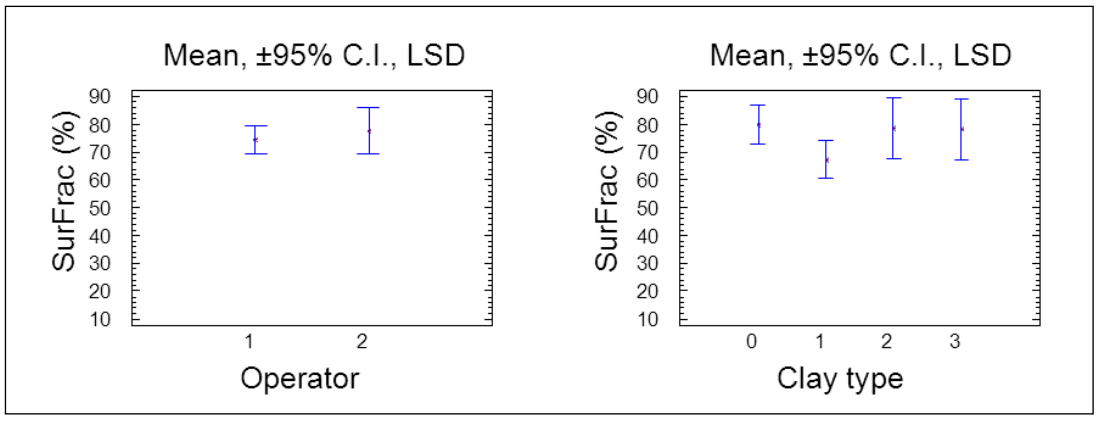

Figure 40: Effect of operator (left) and clay dose (right) on coalesced IFO oil at the surface of the funnel

3.5.11 IFO dispersed oil in suspension in the water column

Figure 41 shows that there were no effects of treatment conditions on the IFO oil suspended in the water column.

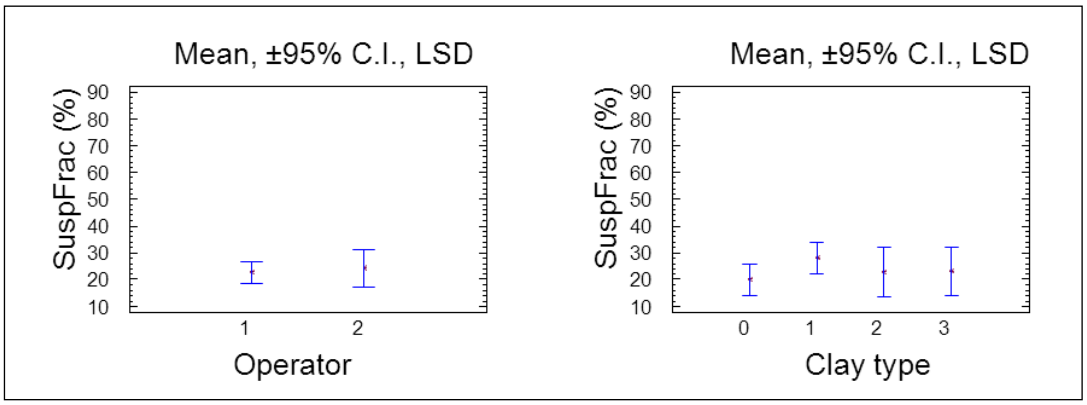

Figure 41: Effect of operator (left) and clay dose (right) on suspended oil in the water column

3.5.12 IFO settled oil at the bottom

We can observe no clear trend, nothing is significant for treatment effects on settled IFO oil (Figure 42).

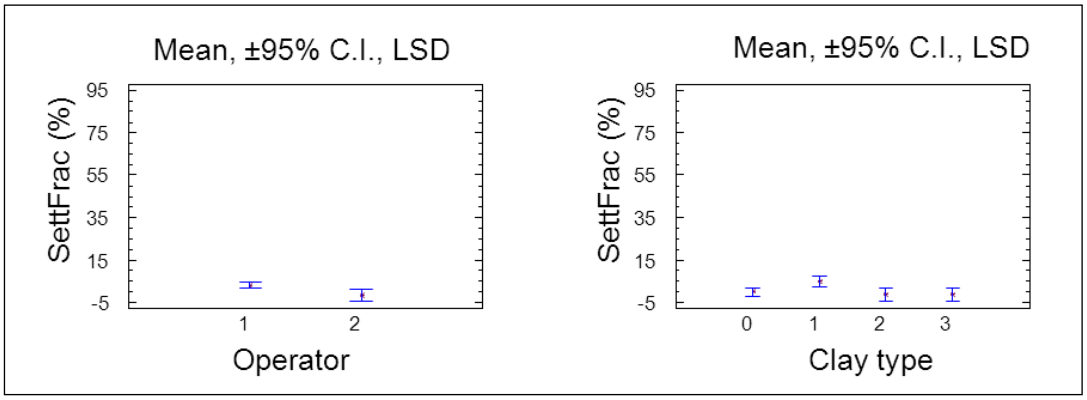

Figure 42: Effect of operator (left) and clay dose (right) on settled IFO oil at the bottom of the funnel

3.5.13 Efficiency of dispersion on both oils

Few analyses were completed on the efficacy considering all the results (both oils) in order to look for possible correlations between factors, especially the oil type (Figure 43). We can observe, as expected, a clear effect of the dispersant on the efficacy of the dispersant, and an influence of the oil type, but below the significant level): the more viscous is the oil; the lower is the efficacy of the dispersion. No difference on the efficiency with and without clay, (possibly a negative effect of the clay: does the clay trap the surfactant?), as well no clear difference between the clays. The energy input is a main factor on the efficiency of the dispersion; the shape of the diagram suggests there could be a threshold energy level to promote the dispersion.

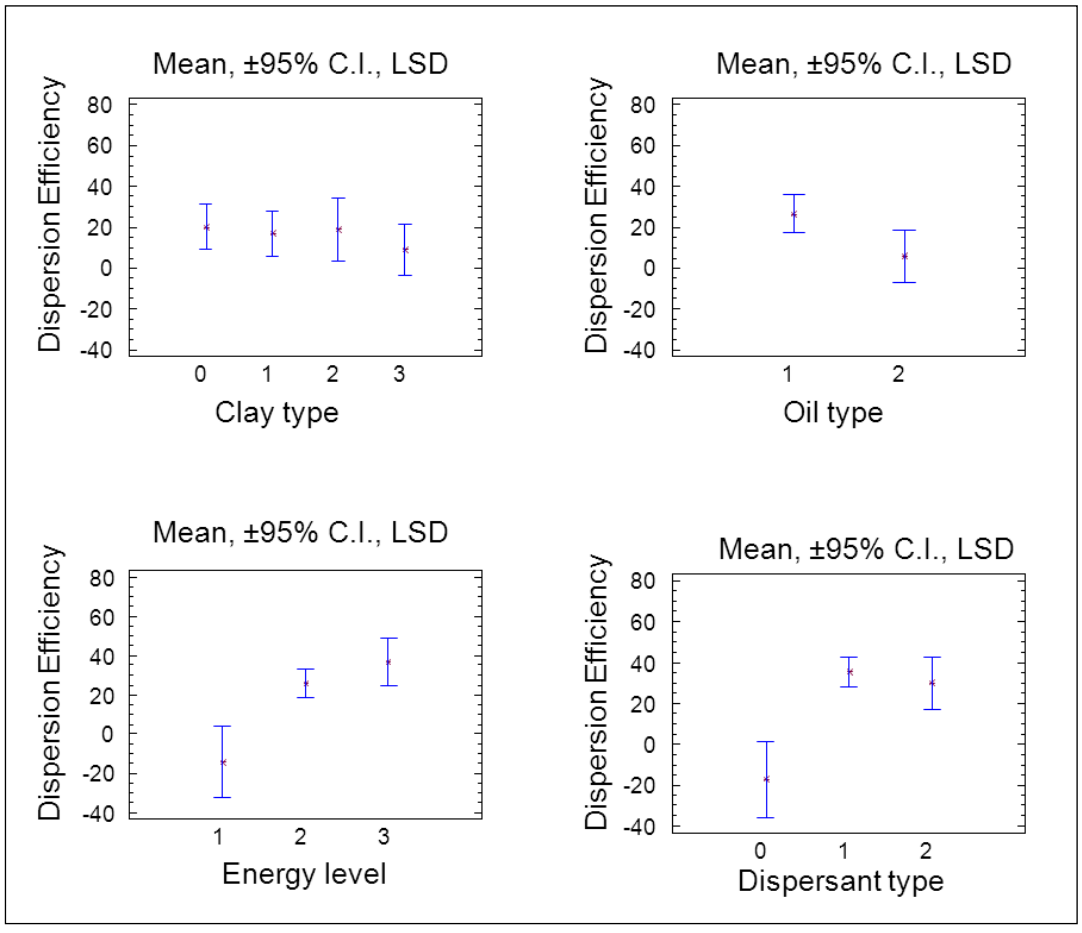

Figure 43: Effect of clay type (upper left), oil type (upper right), mixing energy (lower left), and dispersant (lower right) on oil dispersion efficiency in the IFP test.

3.5.14 Ternary plot

Ternary plots have been drawn (Figure 44) to see if parameters could have impact on the aggregate distribution (coalesced on surface, stabilized, dispersed in the water column and settled to the bottom).

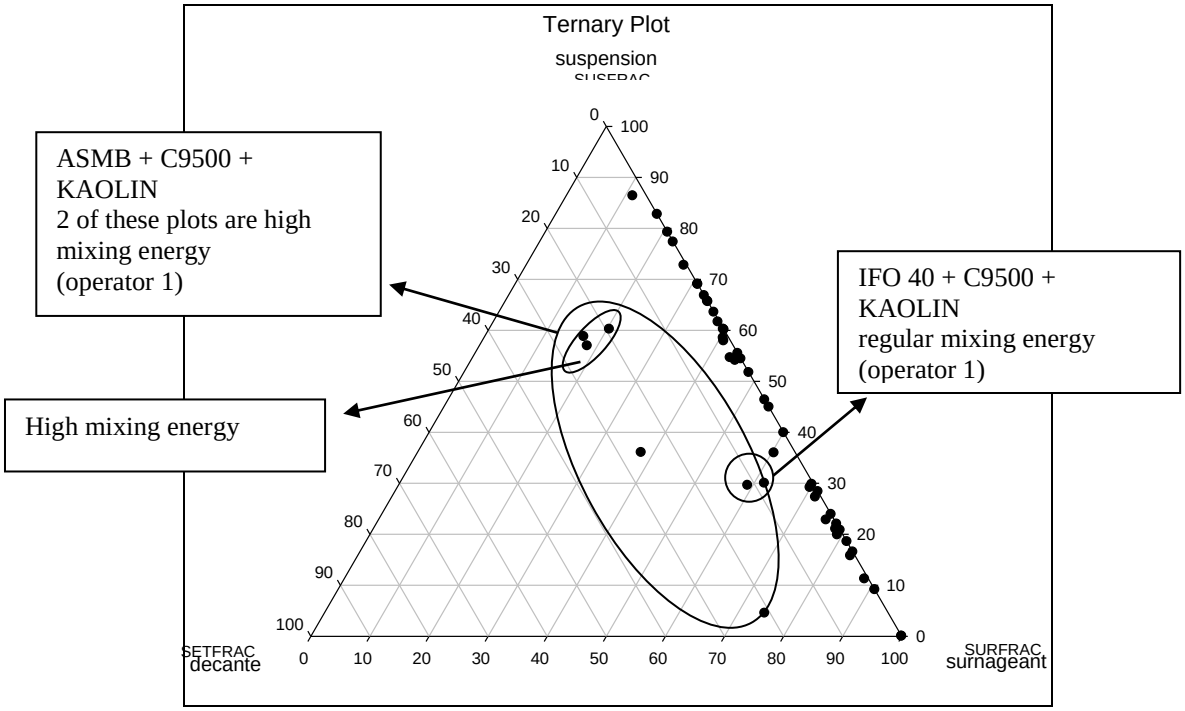

Figure 44: Ternary plot of the treatment effects on distribution of oil in three compartments, suspended in the water column (SUSFRAC), settled to the bottom (SETFRAC), and at the surface (SURFRAC)

After dispersion the oil is mainly on surface and in the water column, the settled oil is quasi none existent; only some tests carried out with Kaolin led to the formation of settled oil (with mineral) which is, nevertheless minority. The mixing energy tended to promote the aggregate formation (which is already known from previous studies).

3.6 Conclusions

This study was conducted to investigate whether the addition of fine minerals can help to stabilize chemically dispersed oil in calm, cold conditions of low turbulence and low mixing energy, with a view to the feasibility of using this technique as an oil spill countermeasure in cold and icy waters such as are encountered in the Arctic. It is based on the formation of chemically dispersed oil-mineral aggregates (OMA) through combining dispersants and

mineral particles to break up oil into droplets, to keep the OMA suspended in the water column as discreet particles, and to dissipate oiled particles in the water so that the oil becomes diluted to a threshold concentration that is lower than the toxic effects level.

In low mixing energy environments the dispersed oil plume, when formed, tends to coalesce towards the sea surface. This could prevent the use of the chemical dispersants in such environments like the Arctic. Yet it is known that oil in the presence of mineral particles tends to form oil-mineral aggregates with lower buoyancy than the oil, which reduces the tendency for oil to coalescence.

Tests were carried out at low temperature (5°C) using the IFP dilution test method (low energy test method). For the purpose of practical application of such a technique in the field, the clay material selected was what is readily available, such as drilling mud additives. Two different mineral products used by the oil industry for the formulation of drilling muds were used in addition to kaolin. In order to better control the operating conditions, the mineral fine was added to the test water in known concentrations before the beginning of each test. Measurements were made of the amount of oil dispersed, the stability of the dispersion, (oil distribution in 3 fractions after one hour settling time, coalesced on surface, stabilized in suspension in the water column, and settled at the bottom). In addition, the size of mineral-oil aggregates was monitored using a LISST-100X.

According to the results, there are no clear advantages to adding mineral particles to the chemically dispersed oil. On the contrary, it seems that the presence of mineral (clay) particles reduced the efficiency of the chemical dispersant perhaps due to the inclusion of surfactant by clay particles in the formation of OMA, although this effect was not statistically significant. It should be noted that the tests with higher mixing energy during the first 10 minutes, and with kaolin, gave better results than the application of lower mixing energy at the start of a test. This observation confirms that the initial mixing energy is an important factor in promoting OMA formation. The question remains, “Was the energy a limiting factor such that operating at higher energy would have led to increased dispersion efficiency?”

4. Wave Tank Experiments: The Influence of Wave Energy and Chemical Oil Dispersants on the Formation and Transport of OMA

The feasibility of oil dispersion in low temperatures and under different mixing energy conditions was evaluated in the wave tank at the Bedford Institute of Oceanography (BIO) to validate laboratory test results. The flow-through wave tank facility is capable of reproducibly generating breaking, and regular non-breaking, wave conditions. The conditions include mixing energy produced by mechanical means to mimic the effects of an energy source such as propeller wash, and natural waves generated by a wave-maker in the test tank. Mineral fines are added together with oil and dispersants at the point of release to simulate a possible on-site remediation procedure.

4.1 Wave Tank Facility and Testing Materials

The BIO wave tank (Figure 45), developed in cooperation with US EPA and NOAA, is used to study dispersion efficiency of various oils with the application of mineral fines under different mixing energy levels in a cold water environment.

Figure 45: The Bedford Institute of Oceanography wave tank facility

Mixing energy levels used in this study are regular (non-breaking) waves and breaking waves. The wave tank is operated in flow-through mode to simulate dilution effects from water currents. The mineral fines used in the experiments were kaolin at three different MOR: 0, 1:10 and 1:5. Tests were conducted using weathered ALC crude oil, ANS crude oil, and IFO-40 fuel oil. In all tests, Corexit 9500 was applied at a DOR of 1:25, the

recommended application rate by the manufacturer. The other experimental conditions are listed in Table 10.

Table 10: Experimental design of wave tank study

Test	Mineral Dose (g)	MOR	Type of Waves
1	0	0	Regular
2	25	1:10	Regular
3	50	1:5	Regular
4	0	0	Breaking
5	25	1:10	Breaking
6	50	1:5	Breaking

4.2 Experiment Procedures

4.2.1 Seawater source for the test tank

Seawater was pumped from the Bedford Basin (Dartmouth, NS, Canada) through triple-layer sock filters (Atlantic Purification Ltd, Dartmouth, NS, Canada) with pore sizes of 25 μm, 5 μm and 5 μm respectively. The wave tank was filled to a depth of 1.5 m. The flow-through system used an influent electric pump to provide a constant current flow rate of 3.8 L/s.

4.2.2 Preparation of Chemically Dispersed Oil-Mineral Aggregates (CDOMA)

In each experiment, mineral fines and oil were pre-mixed in a large flask and released at the surface approximately 10 m downstream of the wave-maker to simulate a remediation procedure that would be used in the field. Designated amounts of kaolin (0, 25 and 50 g) were weighed and added to a 6 L Erlenmeyer flask containing 3 L of filtered seawater. The flask was placed on a reciprocating shaker at 200 rpm for ten minutes. This step is necessary to break down mineral particle agglomerates and facilitate suspension of particles in the seawater. Subsequently, 300 mL of oil were added to the surface of the mixture, followed by 12 mL of dispersant (Corexit 9500) on top of the oil slick. The oil and dispersant were added at a DOR of 1:25. The mixture of minerals, oil and dispersant was then further mixed on the reciprocating shaker at 200 rpm for additional 20 minutes. This mixing stage simulates field remediation operations using the propeller wash from a ship or other artificial mixing strategies.

4.2.3 Background collection

Air temperature, seawater temperature and salinity were recorded prior to the start of each experiment. Background light scattering of the seawater was recorded by a LISST-100X particle size analyzer (Sequoia Scientific, Inc, WA, USA). Water samples (taken prior to introduction of oil, dispersant or mineral fines) were also collected for background chemical analysis of hydrocarbon concentrations.

4.2.4 Transport and dilution of chemically dispersed OMA in the wave tank

The wave-maker was started to provide the required level of mixing energy for each experiment. The chemically dispersed OMA mixture was then released from the surface of the wave tank at 10 m downstream from the wave maker (Figure 46). The duration of each experiment was 60 minutes.

Figure 46: The OMA mixture generated at the point of release

4.2.5 Sampling

Water column samples were collected from the end of the tank furthest from the wave generator (sampling station D, Figure 47) at three depths (5, 75 and 140 cm below the average water level) and location E (effluent port) in a time series of t = 2, 5, 15, 30, 45 and 60 minutes. During each experiment (t = 60 min), additional samples were collected from throughout the wave tank (stations A, B and C) at the same three depths. A total of

36 water column chemistry samples were collected for each experiment, including three background water samples from station D.

The LISST particle counter was deployed approximately 8 m downstream from the initial oil release. It was submerged under water and the optical window positioned 75 cm below the average water surface level. The LISST was started at t = 0 and operated in real-time mode for the entire 60 minutes of each experiment. Particle size distribution data were recorded continually every three seconds throughout the entire duration.

Samples were taken at t = 0 from the release location and t = 5 minutes from location C at a depth of 5 cm for OMA sizing and characterization using a UV Epifluorescent microscope.

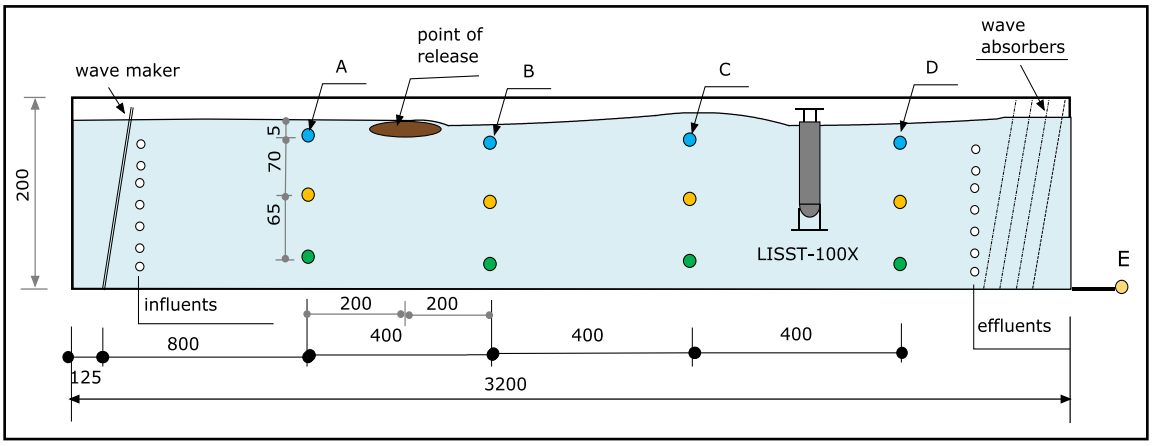

Figure 47: Schematic representation of the BIO wave tank showing initial OMA point of release, sampling locations (A, B, C, D, E), deployment of the LISST-100X and the influent and effluent ports of the flow-through system (all dimensions in cm, not to scale).

Water column samples were collected for oil chemistry analysis following an established protocol (Cole et al., 2007). Briefly, 10 mL of dichloromethane (DCM) was added to each seawater sample (approximately 95 mL sample in a 125 mL amber bottle) to extract hydrocarbons from seawater. Each sample was first shaken vigorously by hand for 30 seconds. Sample bottles were then loaded to a Wheaton R_2P Extraction Roller for 18 hours to ensure complete mixing. Afterward, the solvent layer was pipetted out and transferred to a test tube where the solvent was evaporated through a stream of nitrogen, and condensed to 1 mL. The concentrated sample was then analyzed by gas chromatography coupled to a flame ionized detector (GC-FID) for determination of the total oil concentration in the original seawater (Lee et al., 2009; Li et al., 2009).

4.3 Results and Discussion

4.3.1 Summary of wavetank experimental conditions

Low water temperature is a crucial environmental factor for this study. Wave tank experiments were conducted when the daily temperature was above the freezing point and all facilities were free of the risk of freezing. Figure 48 shows the air temperature, seawater temperature and salinity during one such period. The environmental data show that water temperatures were less than 8^{o}C, and salinity levels were between 28 and 31 ppt, typical for seawater.

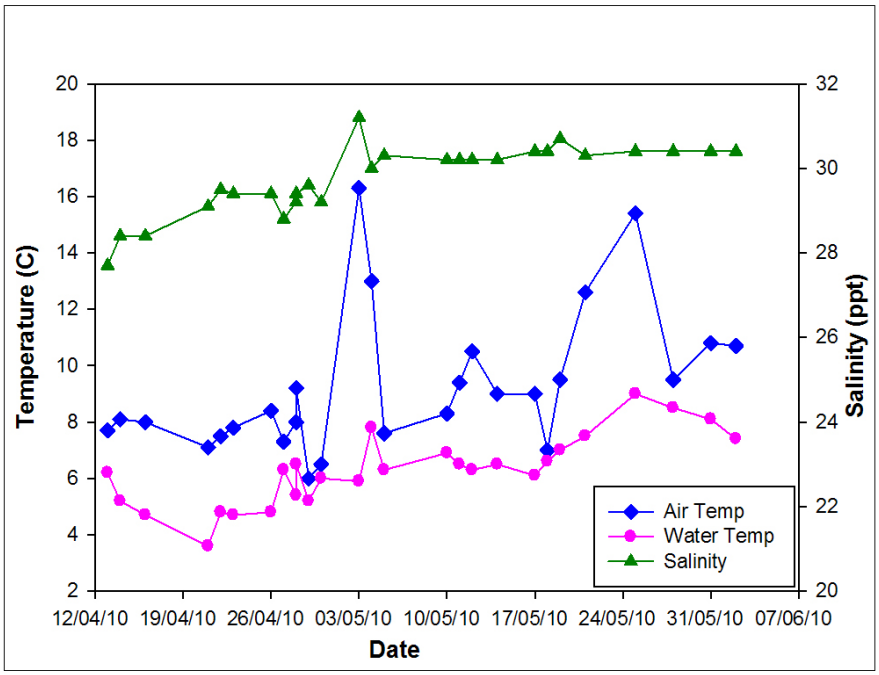

Figure 48: Air temperature, seawater temperature and seawater salinity during the period of wave tank testing.

4.3.2 Analysis of wavetank LISST data

Figures 49 through 60 present the real-time LISST-100X monitoring of oil distribution at the middle depth of the wave tank for all experiments. The data is presented as both the total particle concentration (TPC; sum of all particle concentrations between 2.5-500 μm) and volume mean diameter (VMD; volume weighted mean diameter of all particles). The TPC plot shows the transport of oil droplets and OMA in the wave tank over time. From the initial background levels, TPC concentrations quickly spike between 5-10 minutes as the plume of dispersed oil and OMA reaches the LISST. After the initial plume passes the LISST, concentrations gradually decreased over the remainder of the experiment as the

dispersed oil is pumped out of the tank by the flow-through system. This trend in TPC concentrations was similar for most experiments conducted in the wave tank. Increased noise in the TPC and VMD results for some experiments between 45-60 minutes is likely due to underwater transport of larger droplets formed by coalescence in the wave breakers.

Figure 49 shows TPC results for ALC crude under regular wave conditions. It can be seen that the application of minerals resulted in increased oil-mineral aggregation as shown by elevated particle concentrations in the water column. Particle concentrations varied depending on the mineral dosage, with the 50 g dose producing slightly higher TPC concentrations compared to the 25 g dose. Figure 50 shows theVMD results for the same set of experiments. The highest mineral dose of 50 g (MOR of 1:5) produced the smallest VMD among the three runs, which is in agreement with previous laboratory experiments which showed that the application of minerals stimulated dispersion of oil with higher MOR associated with smaller oil particles. Figures 51 and 52 present the TPC and VMD results for ALC under breaking wave conditions. In general, wave condition did not have a significant effect on OMA distribution in the tank for ALC crude oil. These figures show that increased MOR generally tends to increase total suspended particle concentrations for ALC in the bulk water column but have mixed effects on mean particle diameter.

TPC and VMD results for ANS crude oil are presented in Figures 53 and 54 for regular waves and Figures 55 and 56 for breaking waves. Compared to ALC, the effects of mineral addition on the dispersion of ANS was less apparent under both regular and breaking wave conditions, with TPC plots roughly overlapping for all three different treatments.

The combined effects of mineral addition and wave energy on crude oil dispersion was most evident in the LISST data for IFO-40 oil. Figures 57 and 58 contain the TPC and VMD plots for IFO-40 under regular wave conditions, and Figures 59 and 60 for breaking waves. Under regular wave conditions, the addition of dispersant alone resulted in an increase in dispersed oil concentrations in the water column, with the trend being similar to ALC and ANS. In contrast, the 25 g mineral dose and regular waves resulted in almost no increase in crude oil concentrations in the water column. The experiment with the 50 g dosage was similar to the 25 g treatment, although there was more noise in the TPC plot with several significant spikes in TPC concentrations throughout the entire duration of the experiment. This indicates that the regular waves generated in the tank

lacked sufficient energy to form and maintain small OMA particles using the high viscosity IFO-40 oil, and instead resulted in the formation larger oil-mineral agglomerates as shown by the VMD plots where a significant portion of the particles are greater than 100 µm. Under breaking wave conditions, the 0 g and 25 g treatments resulted in an initial spike in TPC followed by a gradual decrease in concentrations over time. Conversely, with the 50 g treatment there was no initial spike in TPC and instead concentrations gradually increased up to 20 minutes and then remained relatively stable for the duration of the experiment. These findings indicate that for heavier oils such as IFO-40, mineral dosage and wave energy play key roles in the effectiveness of OMA formation and crude oil dispersion.

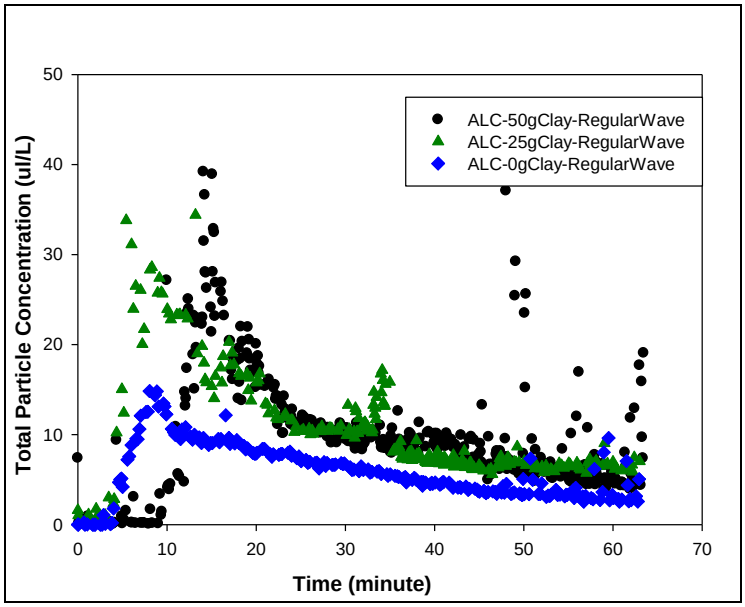

Figure 49: ALC total particle concentrations (TPC) for three doses of minerals at a depth of 75cm under regular waves (RW) as a function of time as measured by the LISST-100X (0 = 0g of fines, 25 = 25g of fines and 50 = 50g of fines).

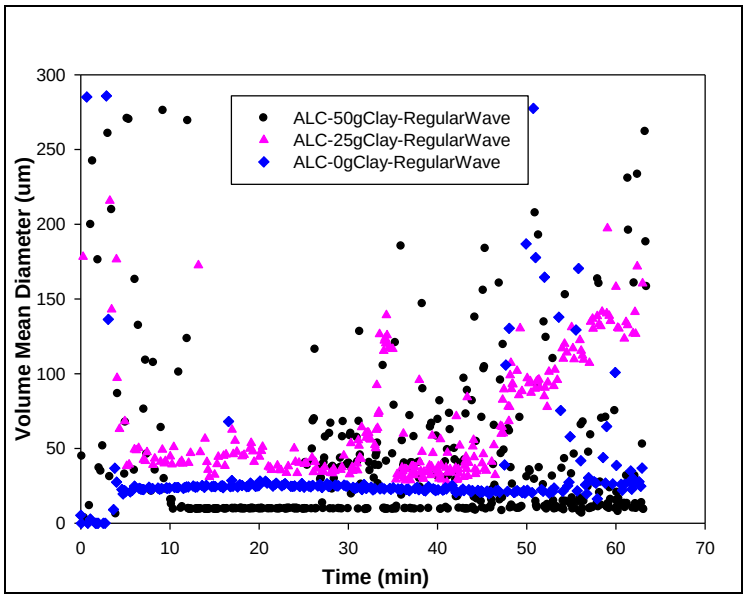

Figure 50: ALC particle volume mean diameters (VMD) at a depth of 75cm under regular waves (RW) as a function of time as measured by the LISST-100X.

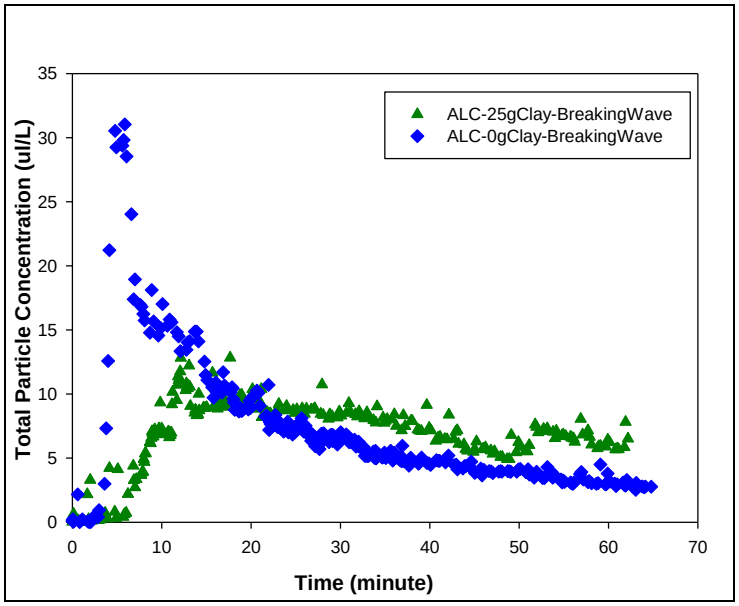

Figure 51: ALC total particle concentrations (TPC) at a depth of 75cm under breaking waves (BW) as a function of time as measured by the LISST-100X. Note that LISST data for the experiment with 50g minerals is not available due to an instrument problem.

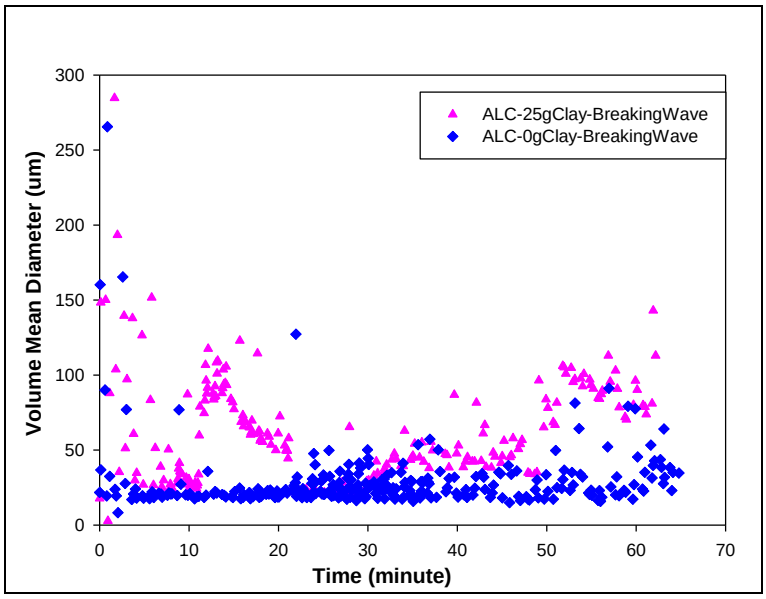

Figure 52: ALC particle volume mean diameters (VMD) at a depth of 75cm under breaking waves (BW) as function of time as measured by the LISST-100X. Note that LISST data for the experiment with 50g minerals is not available due to an instrument problem.

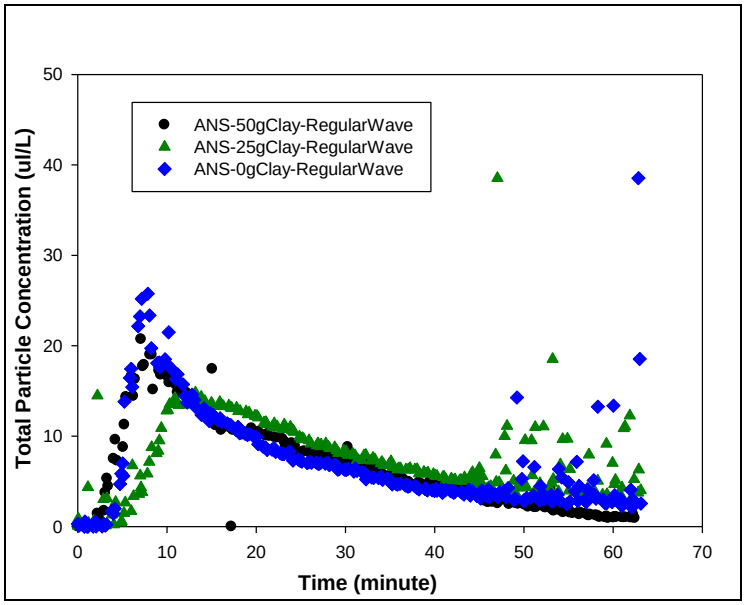

Figure 53: ANS total particle concentrations (TPC) for three doses of minerals at a depth of 75cm under regular waves (RW) as a function of time as measured by the LISST-100X (0 = 0g of fines, 25 = 25g of fines and 50 = 50g of fines).

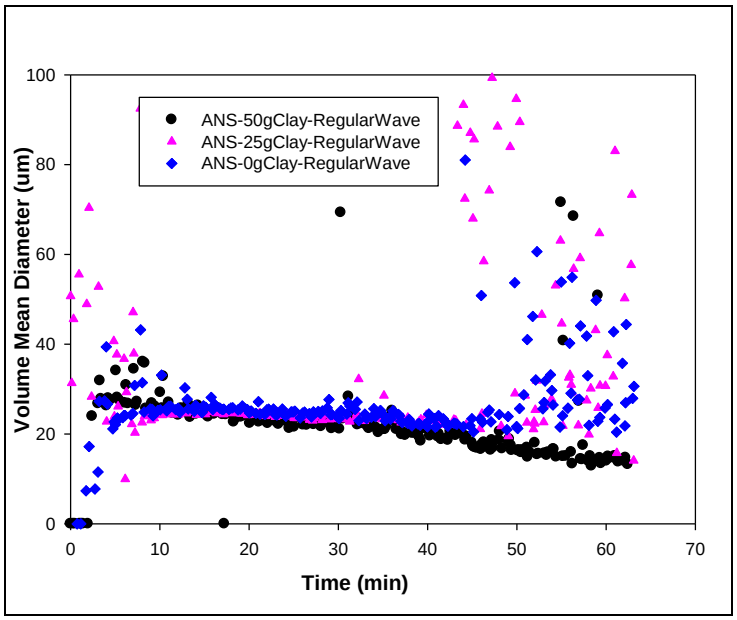

Figure 54: ANS particle volume mean diameters (VMD) at a depth of 75cm under regular waves (RW) as a function of time as measured by the LISST-100X.

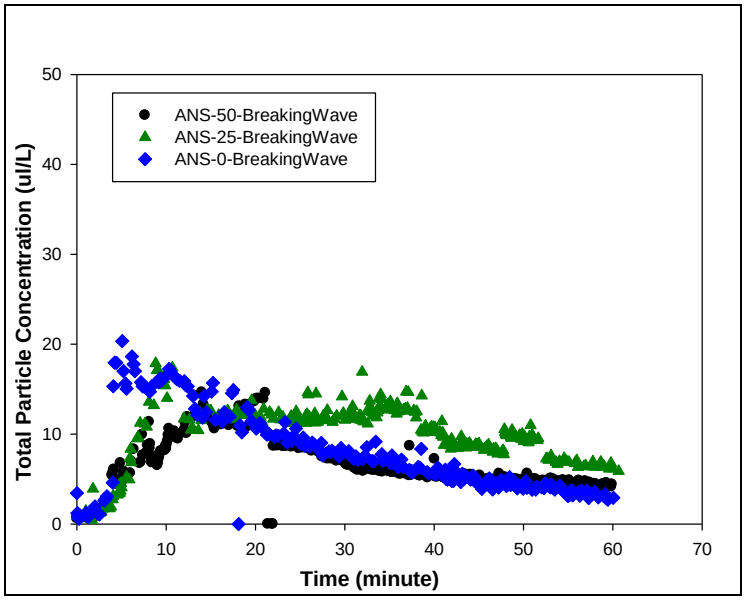

Figure 55: ANS total particle concentrations (TPC) at a depth of 75cm under breaking waves (BW) as a function of time as measured by the LISST-100X.

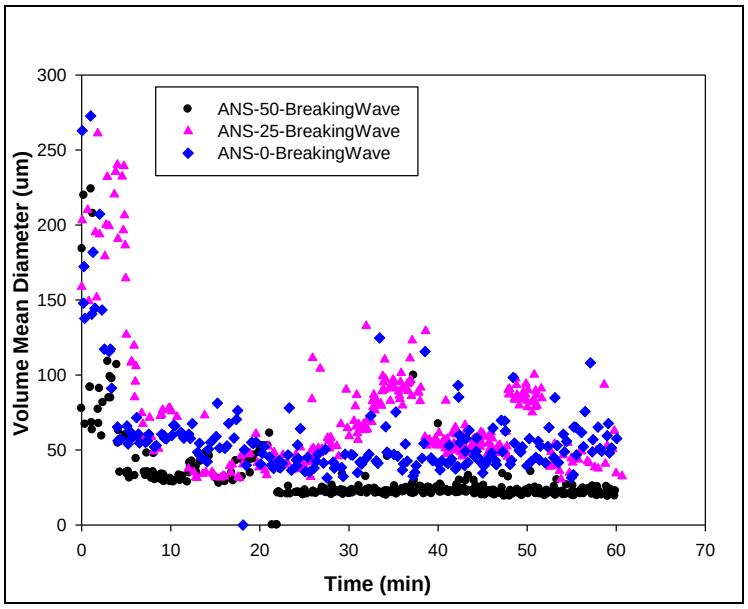

Figure 56: ANS particle volume mean diameters (VMD) at a depth of 75cm under breaking waves (BW) as function of time as measured by the LISST-100X.

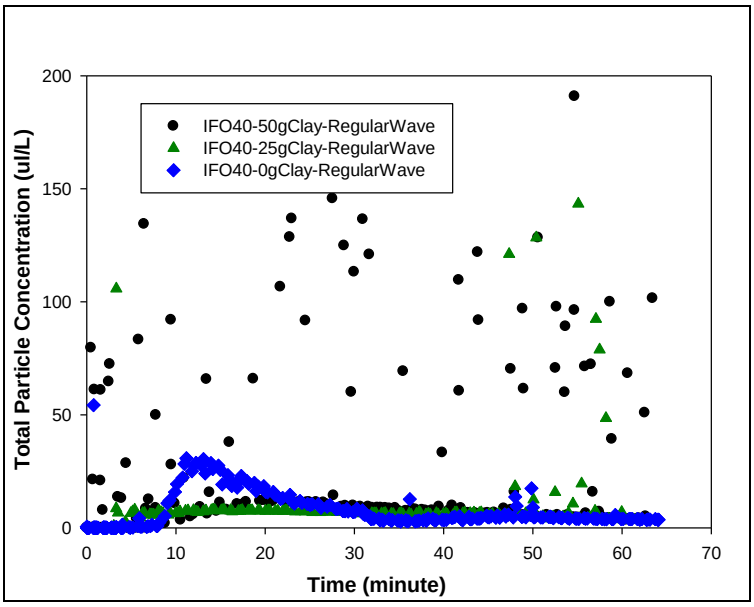

Figure 57: IFO-40 total particle concentrations (TPC) for three doses of minerals at a depth of 75cm under regular waves (RW) as a function of time as measured by the LISST-100X (0 = 0g of fines, 25 = 25g of fines and 50 = 50g of fines).

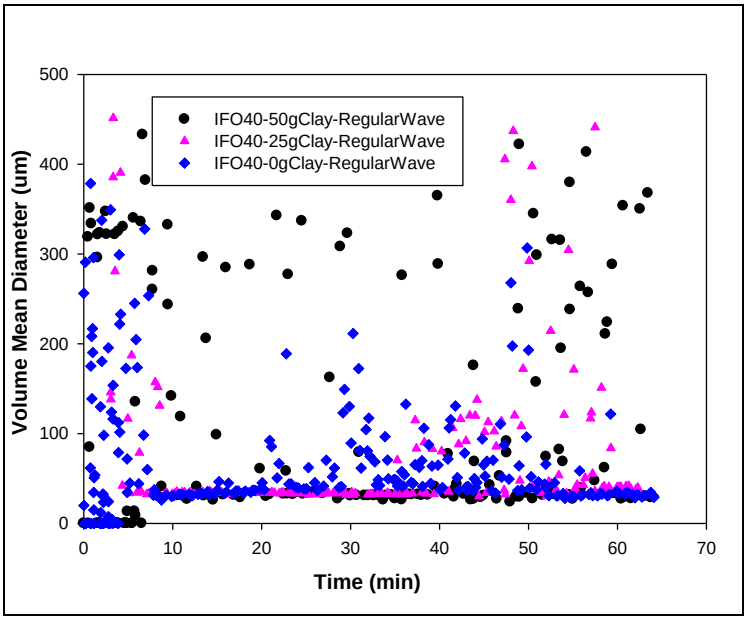

Figure 58: IFO-40 particle volume mean diameters (VMD) at a depth of 75cm under regular waves (RW) as a function of time as measured by the LISST-100X.

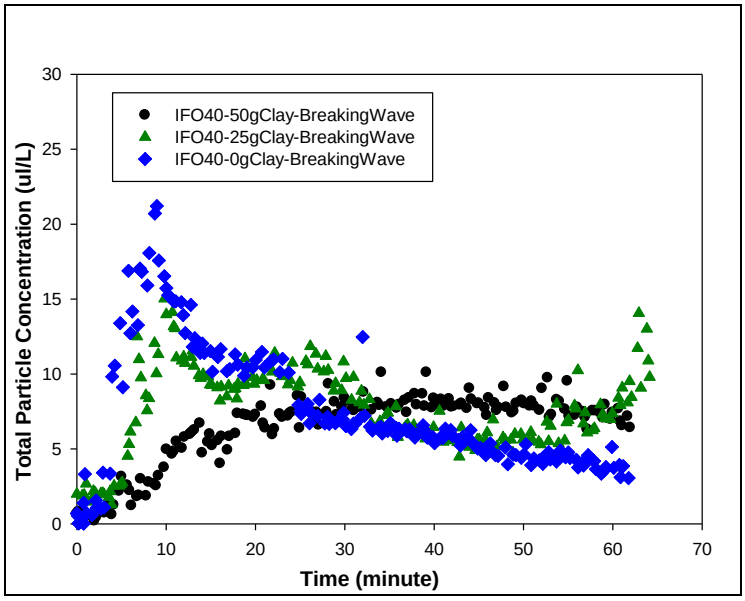

Figure 59: IFO-40 total particle concentrations (TPC) at a depth of 75cm under breaking waves (BW) as a function of time as measured by the LISST-100X.

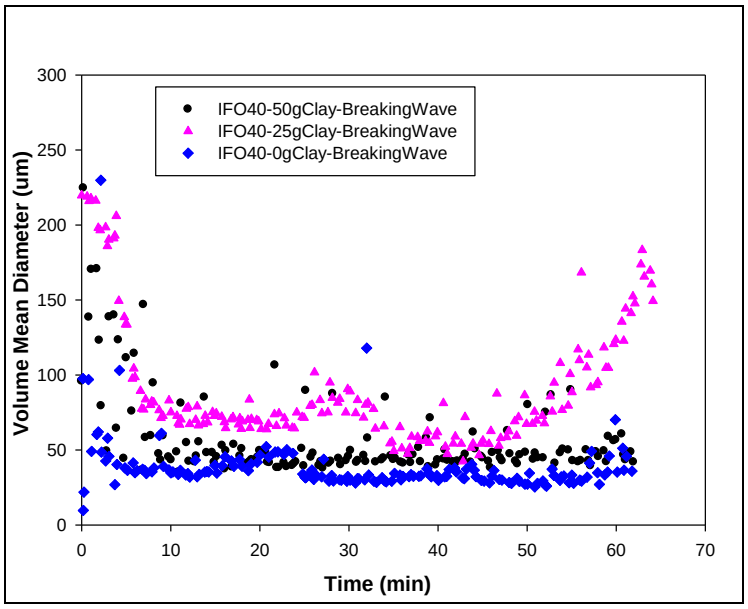

Figure 60: IFO-40 particle volume mean diameters (VMD) at a depth of 75cm under breaking waves (BW) as function of time as measured by the LISST-100X.

Figures 61 and 62 show the dispersed particle size distributions for ALC and ANS under the different treatment conditions including three different clay dosages (50, 25 and 0 g) and two wave conditions (breaking waves and regular waves). The volume median diameter of each sampling point during the one hour experiment is also plotted in each panel. The particle size distributions exhibited multiple modes, whereas under regular waves the size distributions were more mono-modal. Although pre-mixing of oil with dispersant or kaolin or both tend to generate OMA in the flask, additional breakage and transport of particles are shown by the time-series change in volume median diameter. The overall trend in VMD was a decline as a function of time. Significant variation of the median sizes of the particles, however, was observed particularly under regular wave conditions and in the absence of mineral fines. The same results were obtained for IFO-40 (Figure 63).

Breaking waves had significant effects on the dispersion and transport of oiled particles in the flow-through wave tank. The increased energy dissipation rates and turbulent diffusion coefficients associated with the breaking wave conditions enhanced oil dispersion and the particle concentrations were more stable as a function of time.

The presence of clay mineral fines, either at 25 g or 50 g, appears to have enhanced the spreading the OMA particles more widely over time. In the meantime, there appears to be coalescence of dispersed oil particles after 30 min during each experiment under regular

wave conditions. The coalescence of small particles into larger ones seems to be enhanced in the presence of mineral fines as well. This is probably caused by the hydrodynamic conditions at the downstream end of the wave tank attributable to the wave absorbing area. In the open ocean environment, the coalescence of small particles into larger ones may not be significant given a sufficient dilution rate so that the particle collision frequency can be dramatically reduced.

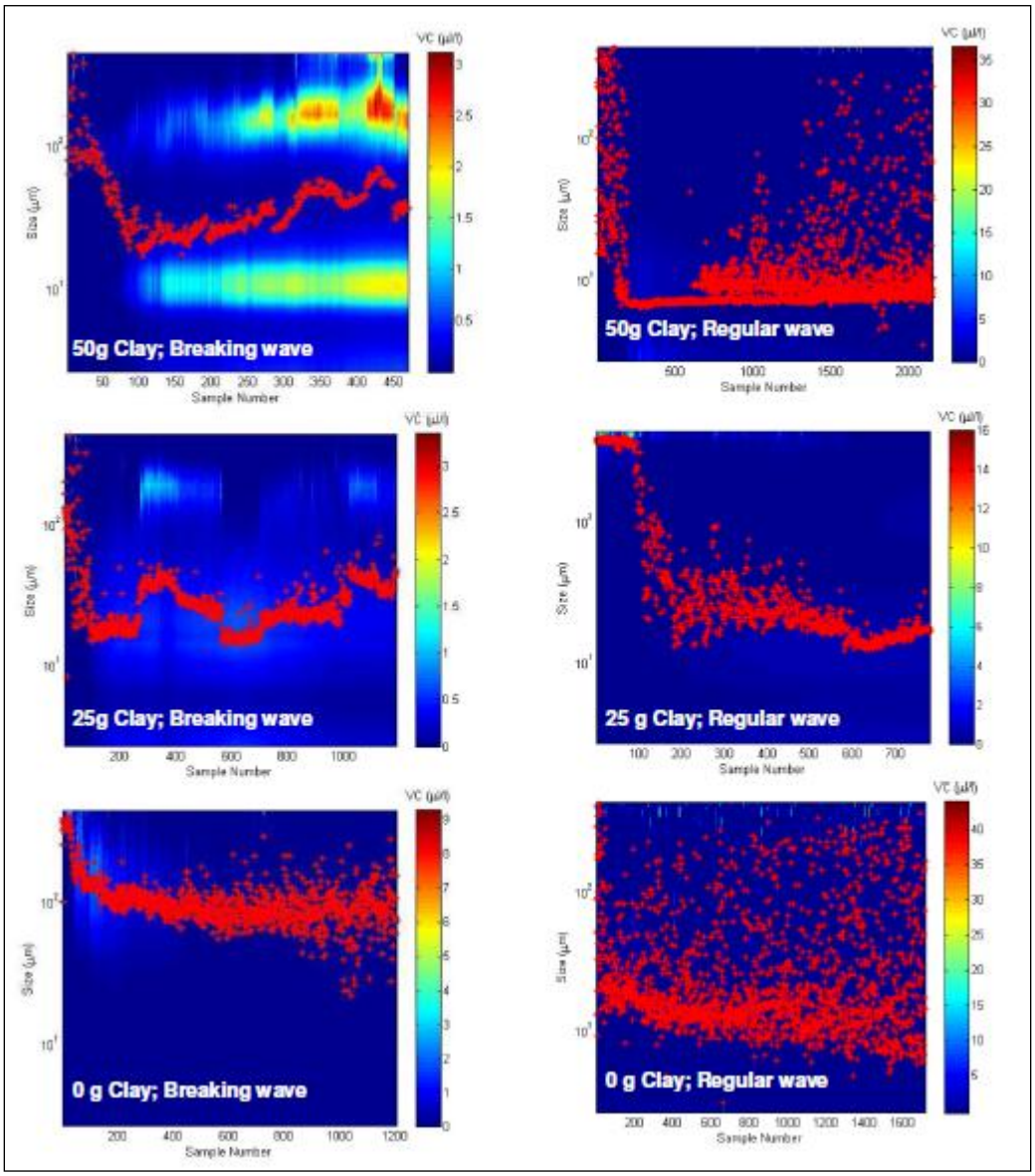

Figure 61: ALC dispersed oil droplet size distribution as a function of clay dosage under different wave conditions; contour plots are droplet size distribution for each snap shot over the one hour experiments and the red dots represent the volume median diameter of each sampling point

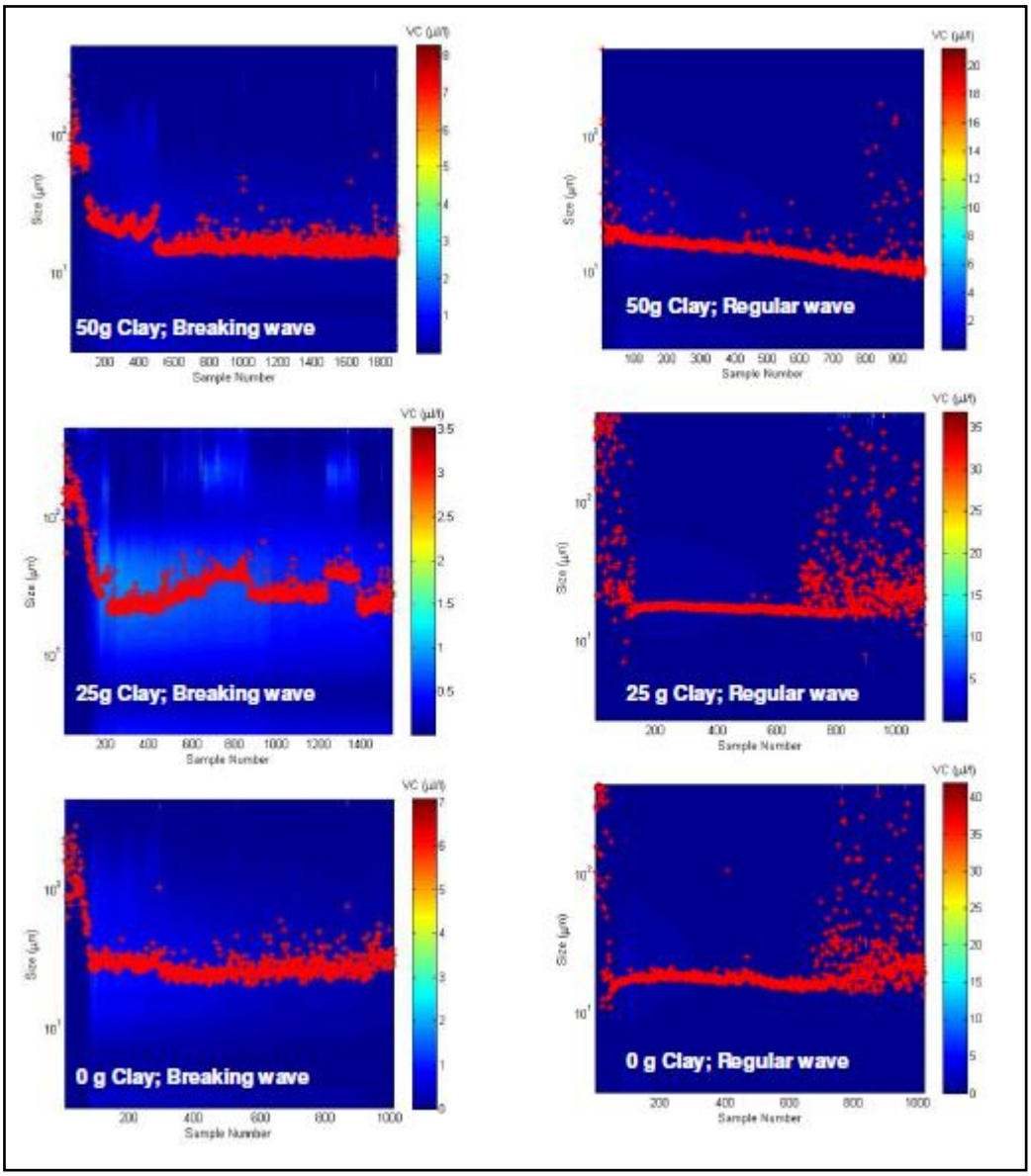

Figure 62: ANS dispersed oil droplet size distribution as a function of clay dosage under different wave conditions; the contour plots are droplet size distribution for each snap shot over the one hour experiments and the red dots represent the volume median diameter of each sampling point

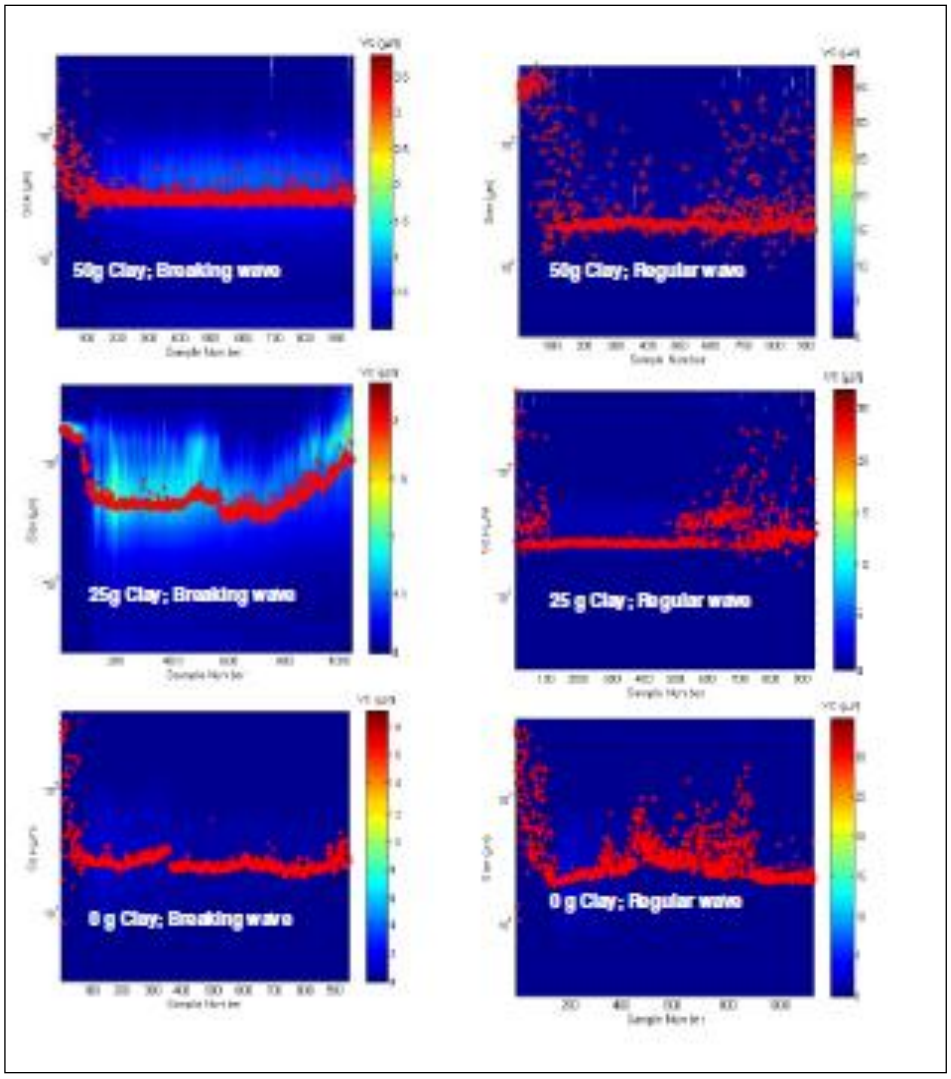

Figure 63: FO40 dispersed oil droplet size distribution as a function of clay dosage under different wave conditions; contour plots are droplet size distribution for each snap shot over the one hour experiments and the red dots represent the volume median diameter of each sampling point

4.3.3 Analysis of Total Petroleum Hydrocarbons

Figures 64 and 65 show the total petroleum hydrocarbon (TPH) concentrations of ALC and ANS at three depths (5, 75 and 140 cm) and the effluent with application of different mineral doses under different wave conditions. The data are averaged from duplicate wave tank experiments for each treatment condition. Oil concentrations were plotted as a function of time for different treatment conditions. This was done to compare the dispersion efficiency with different mineral doses and at different mixing energy levels. Under regular waves, high concentrations of oil were measured at the surface when there was no mineral applied. Higher mineral dosage transferred more oil from the surface to

within the water column. The treatment using 50 g clay, which is equivalent to a MOR of 1:5, showed homogeneous oil concentrations at different water depths throughout the experiment. The oil concentrations observed from the samples collected at the surface and the water column under breaking waves were very similar to those under regular wave conditions. The oil concentration from the effluent exhibited a similar pattern as in the water column, but with a delay in the peak oil concentration in agreement with the flow pattern. This suggests that with premixing, the dispersion of oil with the combined usage of chemical dispersants and mineral fine particles to enhance the formation and transport of OMA would probably be as effective under high mixing energy breaking wave conditions as in low mixing energy regular wave conditions.

Compared to the previous experiments with ANS and ALC, no obvious trends between the different mineral treatments or wave conditions were observed in the hydrocarbon results from the wave tank experiments using IFO-40 Figure 66. Moreover, the results displayed more variability compared to the ANS and ALC experiments, especially with the 25 g mineral treatment under breaking waves. Despite the fact that the addition of minerals did not appear to affect the dispersion of IFO-40, a significant amount of oil was still detected in the water column at all sampling depths, with total petroleum hydrocarbon concentrations similar to those obtained with ANS and ALC.

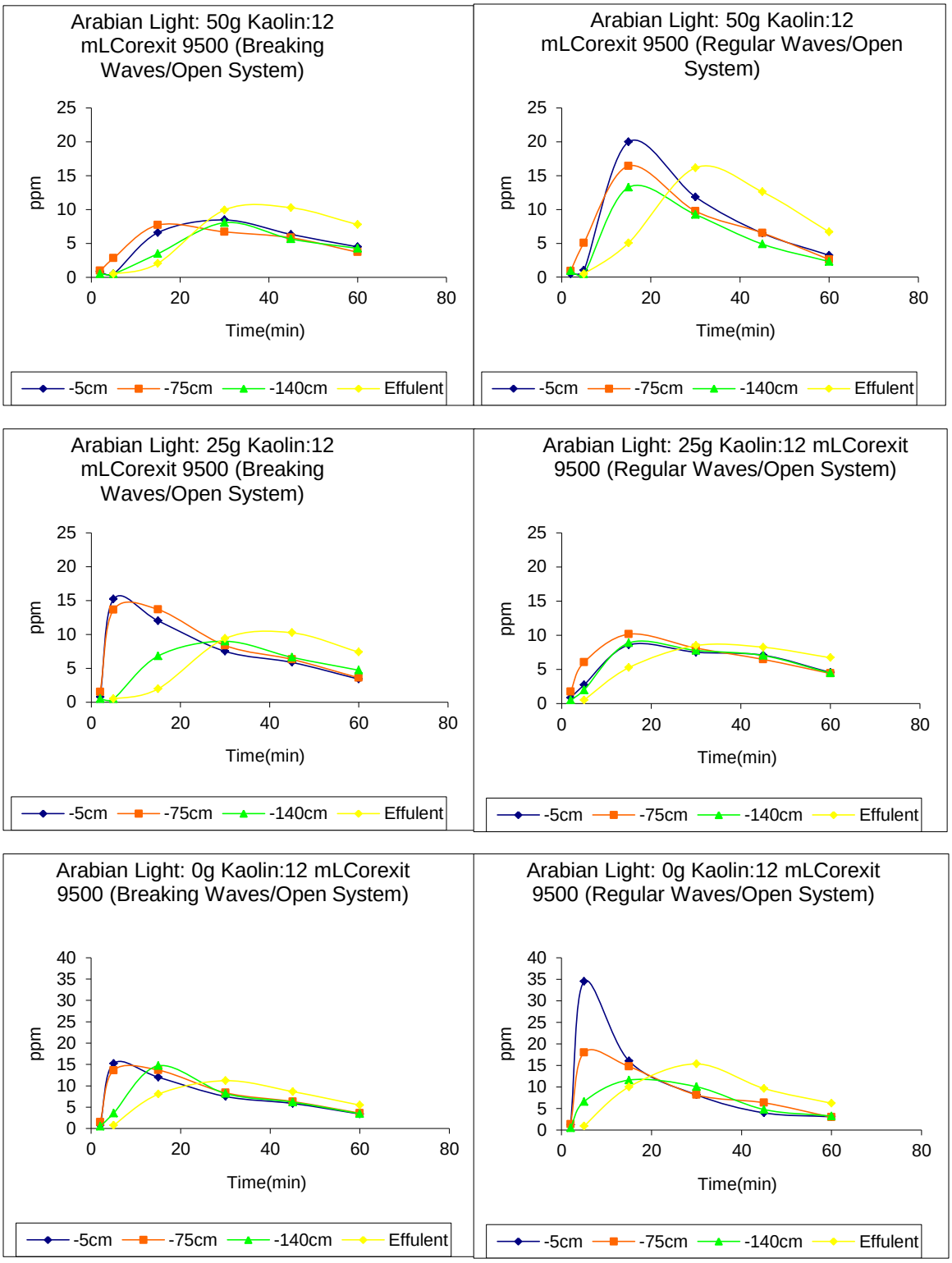

Figure 64: ALC oil concentration as a function of time at different mineral doses, and measured at different depths including the effluent of the wave tank, under breaking waves (left) and regular waves (right) with data averaged from duplicate wave tank experiments

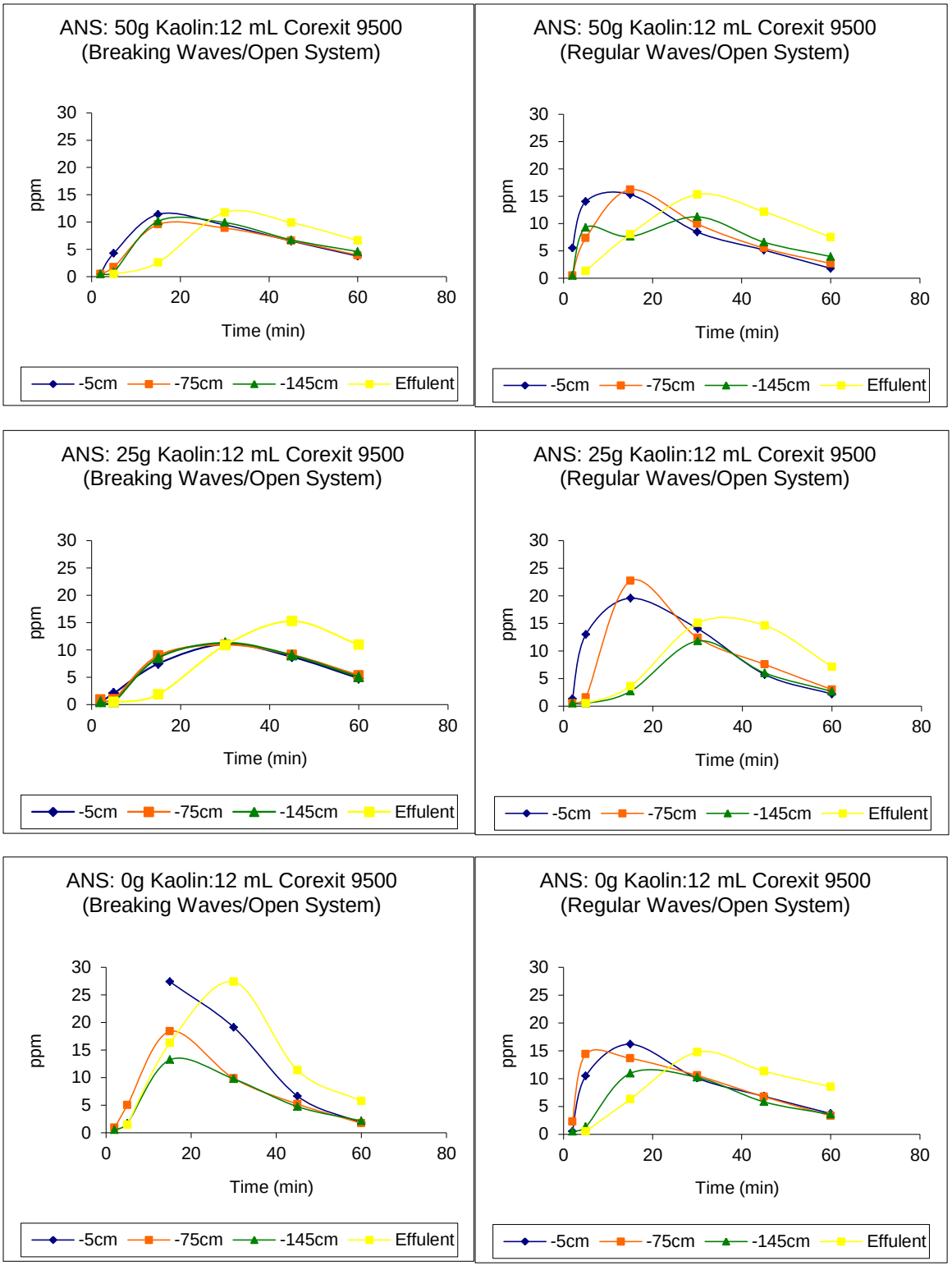

Figure 65: ANS oil concentration as a function of time at different mineral doses measured in the effluent and at different depths of the wave tank under breaking waves (left) and regular waves (right).

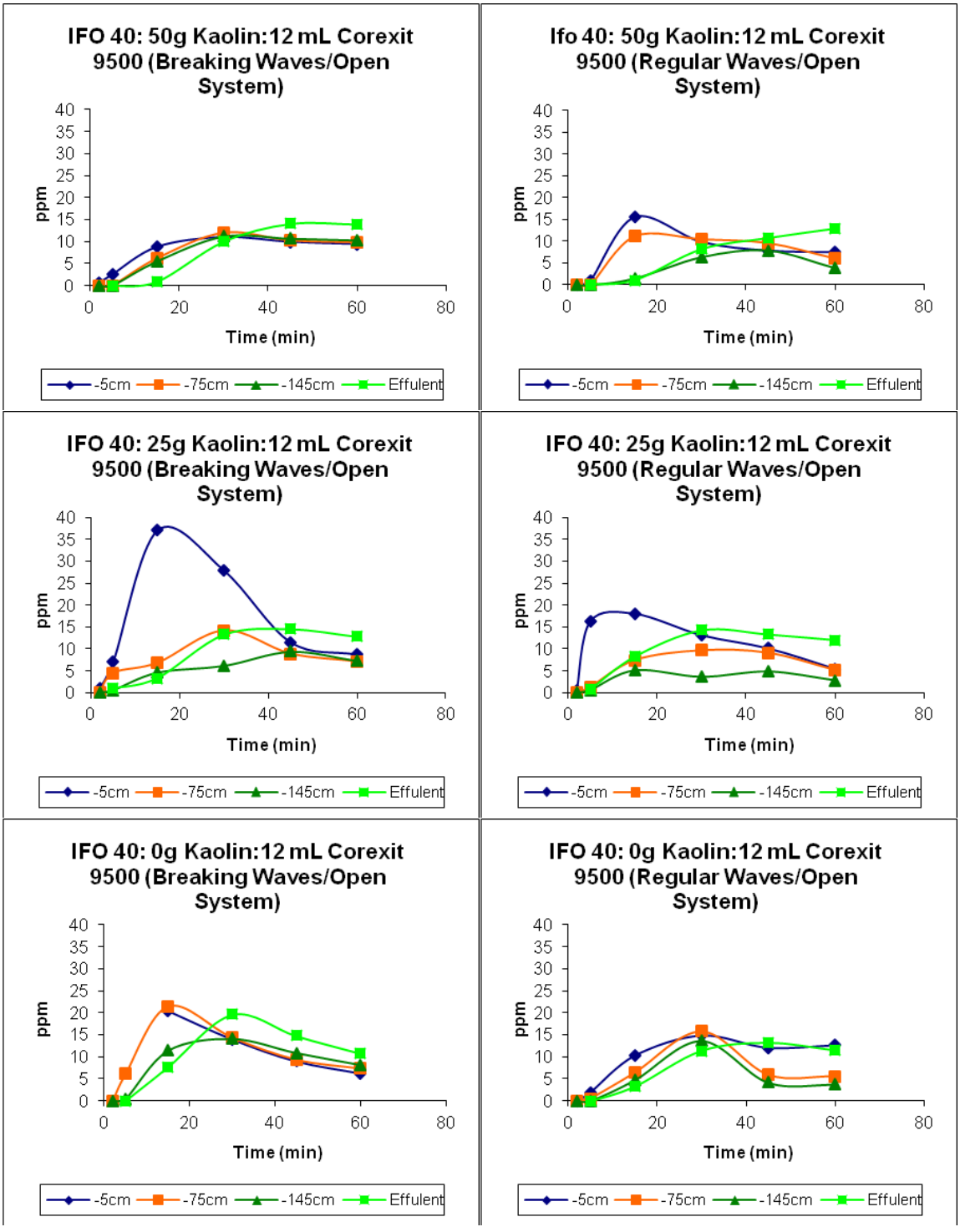

Figure 66: IFO-40 oil concentration as a function of time at different mineral doses, and measured at different depths including the effluent of the wave tank, under breaking waves (left) and regular waves (right) with data averaged from duplicate wave tank experiments.

4.3.4 Interfacial tension in the flow-through wave tank

Figures 67-69 present the measured interfacial tension of water samples collected from different depths, including the effluent of the wave tank, at different time points under breaking and regular wave conditions. The general trend for all treatment conditions corresponds to a relatively high interfacial tension of approximately 74 dyne/cm at time zero, followed by a drop of the interfacial tension to a minimum of 65-70 dyne/cm, and then ascending to initial levels. This pattern is coincident with the transport of dispersed oil and likely the chemical dispersant associated with the oil. The use of clay particles under breaking wave conditions appears to most effectively enhance dispersion of oil and dispersant throughout the depths of the tank, resulting in an even distribution of interfacial values as a function of time.

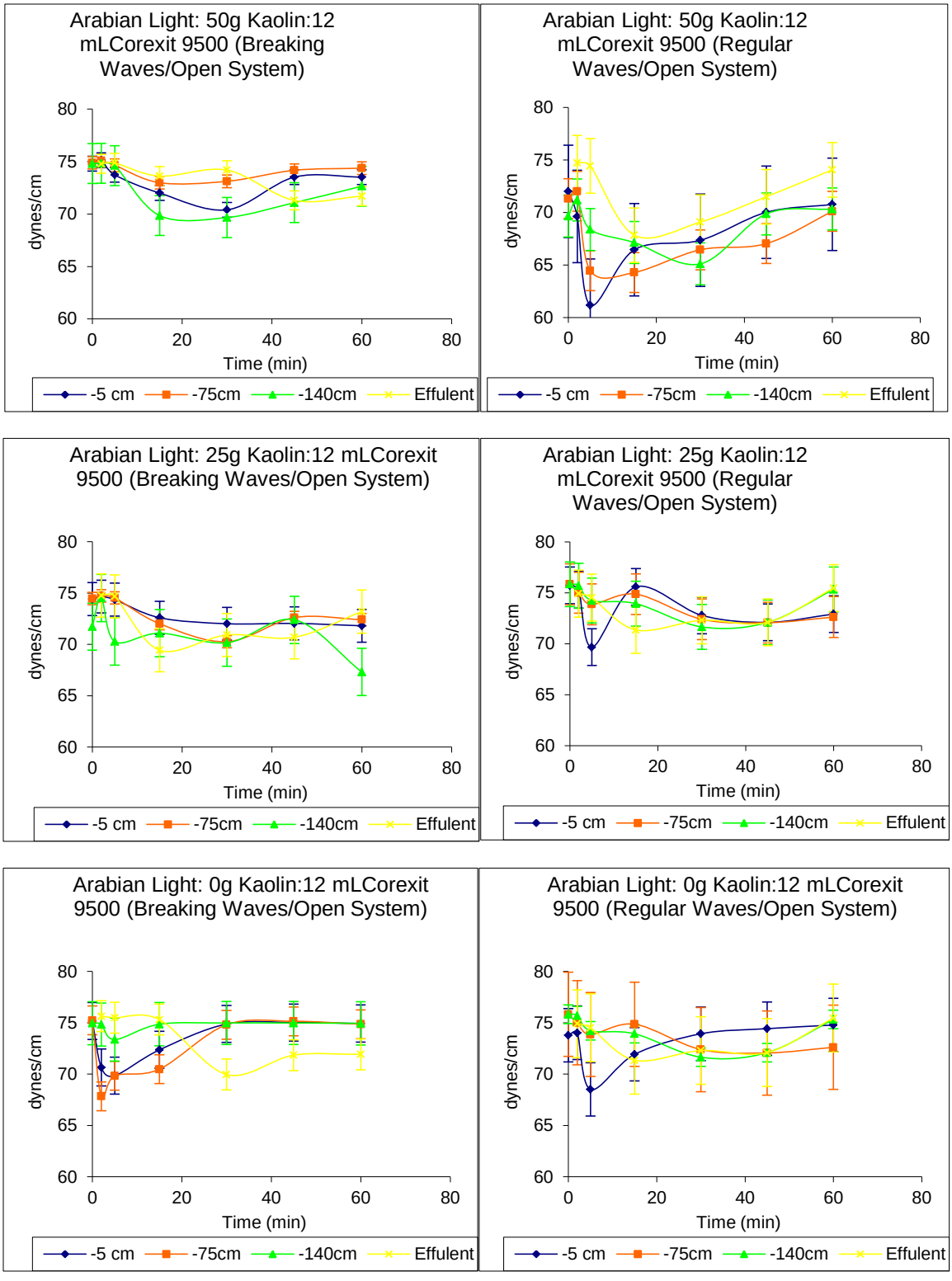

Figure 67: Dynamic interfacial tension of ALC oil measured in the effluent and at different depths of the wave tank as a function of mineral dosage and wave conditions.

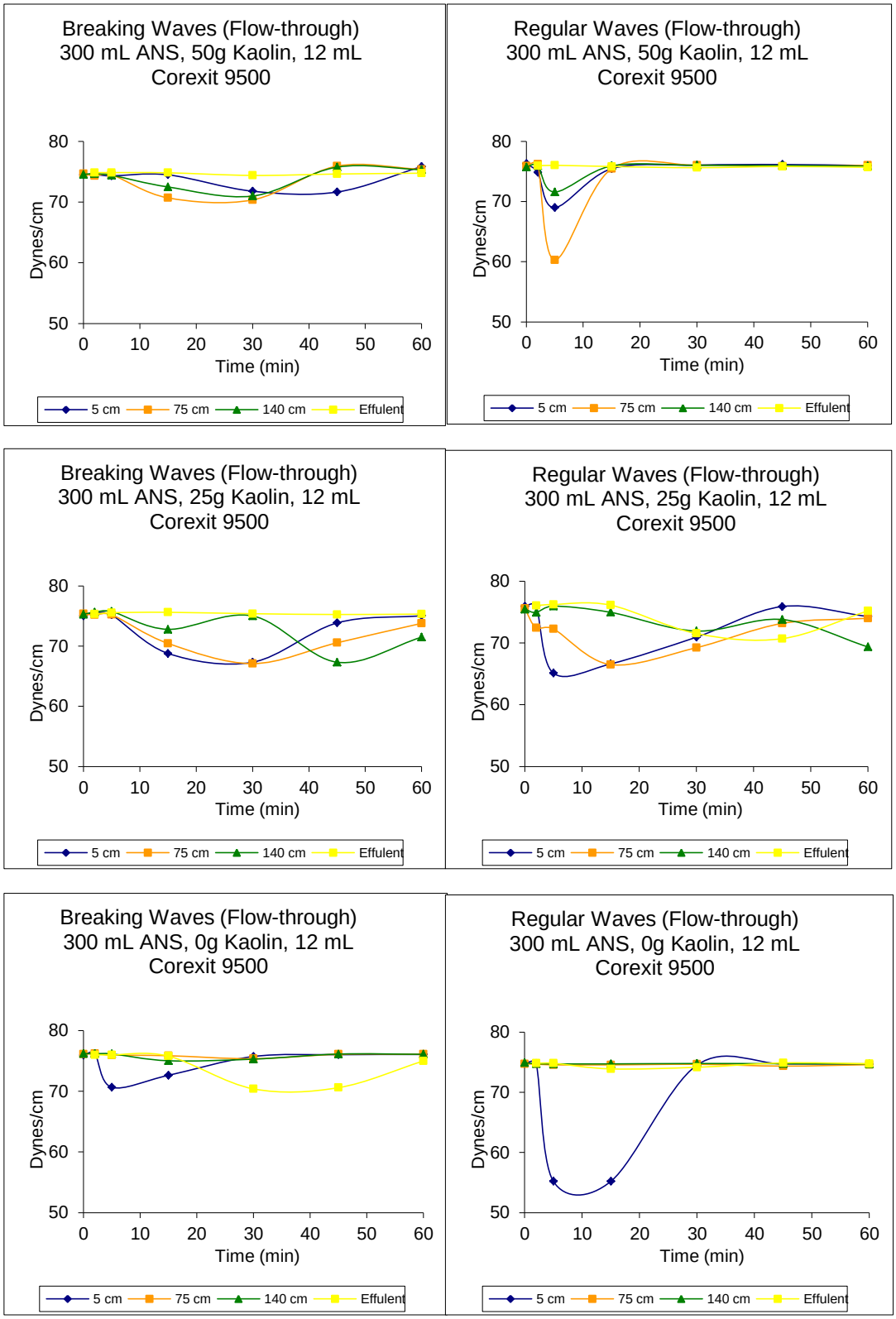

Figure 68: Dynamic interfacial tension of ANS oil measured in the effluent and at different depths of the wave tank as a function of mineral dosage and wave conditions.

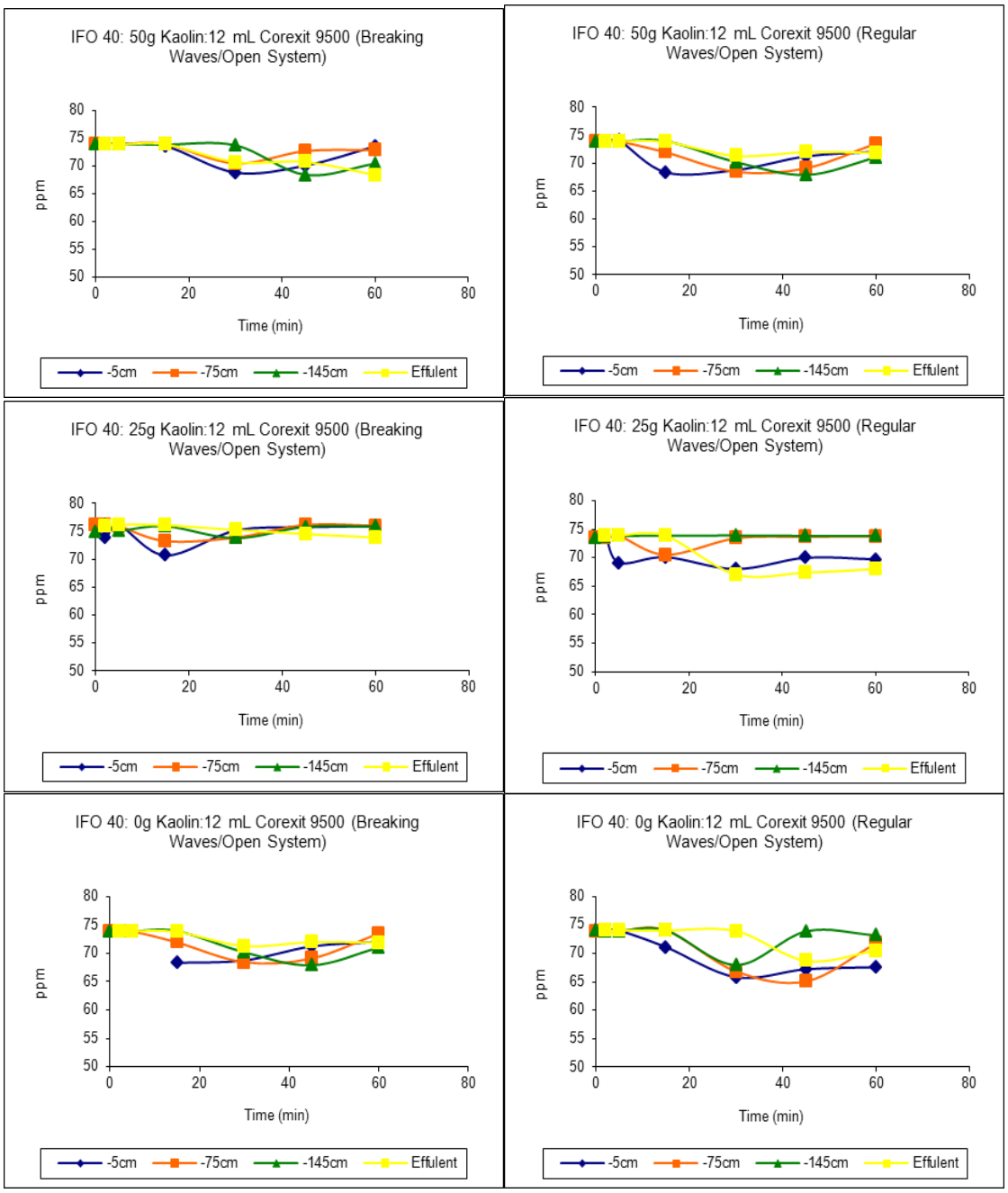

Figure 69: Dynamic interfacial tension of IFO-40 measured in the effluent and at different depths of the wave tank as a function of mineral dosage and wave conditions.

4.3.5 Dynamic Dispersion Effectiveness

The combined effects of chemical dispersants and mineral fines under different wave conditions on dynamic dispersion effectiveness (DDE) over the duration of the entire

experiment can be evaluated by computing the fraction of dispersed oil flowing out of the wave tank and the residual dispersed oil in the water column at the end of each experiment:

$$DDE(\%) = \frac{\overline{C}_{effluent} Q_{effluent} T + \overline{C}_{sample} V_{wt}}{\rho_{Oil} V_{Oil}} \times 100 \quad (3)$$

where $\overline{C}_{effluent}$ is the time-averaged oil concentration in the effluent carried out of the wave tank ($g \cdot L^{-1}$); $Q_{effluent}$ is the flow rate of the current ($L \cdot min^{-1}$); V_{wt} is total effective water volume of the wave tank (27,000 L); T is the duration of each wave tank experiment (60 min); $\overline{C}_{sample}$ represents the average concentration of oil remaining in the water column after T; ρ_{oil} is the density of the test oil ($g \cdot mL^{-1}$), and V_{oil} is the volume of oil used in the experiment (300 mL).

Dynamic dispersion efficiency (DDE) of oil in the tank as a result of applying chemical dispersant and mineral fines is summarized in Figure 70. DDE data indicated that dispersion of ANS and ALC oils was relatively effective under both regular and breaking wave conditions. Under regular waves, the high dose (50 g) of mineral fines slightly increased the total concentration of dispersed oil remaining in the water column. From these data it appears that to achieve a high rate of DDE, adding mineral fines is probably not necessary under the high mixing energy of breaking waves because the chemical dispersant on its own leads to good dispersion efficiency.

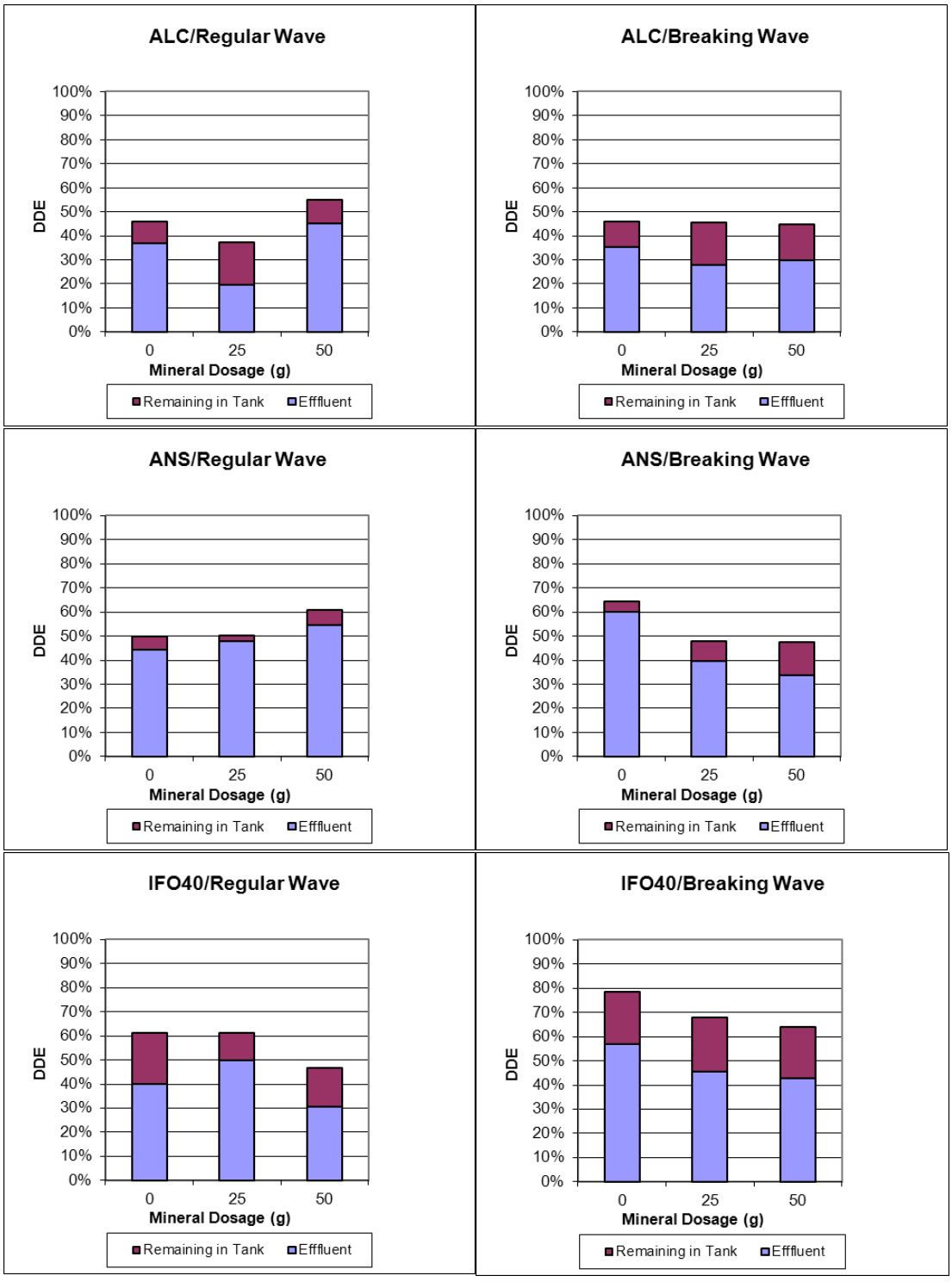

Figure 70: Dynamic dispersant effectiveness (DDE) of ALC and ANS oils as a function of mineral dosage and wave conditions (RW = regular waves, BW = breaking waves).

5. Modelling of OMA: Predicting Fate and Potential Biological Effects in Spill Response Operations

Spilled oil can interact with suspended particles (mineral or organic) in marine environments and form aggregates, including OMA. Some OMA with densities greater than seawater can settle to the seabed and pose potential risks to benthic organisms. To understand the transport and fate of oil associated with OMA and evaluate their potential risks, researchers recently developed an integrated hydrodynamic, fate/transport and risk assessment modeling system, and conducted several case studies. One of the limitations of these studies was the use of a conservative approach which neglected biodegradation processes. Although this approach is acceptable for the study of short term effects of settled oil, the long term effects cannot be studied. The objective of this project is to improve the existing modelling approach in order to simulate the long term fate, transport, and potential risk of settled oil associated with OMA. The improved approach used the DREAM model developed by SINTEF and a number of case studies under different combinations of oil, sediment type, wave and current conditions.

5.1 Modelling approach

The new approach in this study takes into consideration the following fates for OMA in the water column: 1) advection; 2) diffusion; 3) settling; and 4) biodegradation of oil. The fates in sediment are: 5) deposition of OMA; 6) burial; 7) oxygen depletion; 8) biodegradation; and 9) re-suspension.

Governing equations for hydrodynamics (Sørensen et al., 2006; Sørensen et al., 2004) and fate processes 1-3 and 5 (Reed and Hetland, 2002; Rye et al., 2006a; Rye et al., 2006b) have been described before in Niu et al. (2010b; 2010c). Process 4, the reduction of concentration due to biodegradation of the oil in the water column, is calculated by (Rye et al., 2006a):

$$PEC_{water} = C_{discharge} \exp(-K_w t) / \mathrm{DILUTION} \qquad (4)$$

where PEC*water* is the local concentration in water column, C*discharge* is the initial oil concentration, K*w* is the first order biodegradation factor, *t* is time, and DILUTION is the dilution factor calculated from advection and diffusion processes.

The biodegradation process of oil associated with OMA in sediment is modeled using diagenetic equations 5 and 6 (Rye et al., 2006b):

$$\frac{\partial C_1}{\partial t} = \frac{\partial}{\partial z}\left(D_B \frac{\partial C_1}{\partial z} - wC_1 \right) - \left[K_s C_1 \right] \frac{O_2}{K_{O_2} + O_2} \tag{5}$$

where C1 is the concentration of oil in sediment, D_B is a bioturbation coefficient, K_s is the biodegradation rate in sediment, K_{O2} is the "Monod-type" saturation constant and O_2 is the free oxygen pore-water concentration, and

$$\frac{\partial O_2}{\partial t} = \frac{D_0}{\theta^2} \frac{\partial^2 O_2}{\partial z^2} - \frac{1-\varphi}{\varphi} \left[K_s C_1 \right] \frac{O_2}{K_{O_2} + O_2} \tag{6}$$

where D_0 is the diffusion coefficient for oxygen in pore water, θ is tortuosity of sediment, φ is the porosity of the sediment, and γ is the Redfield number. The potential risk of settled oil on benthic organisms in terms of Hazard Quotient (HQ) was evaluated using the same method as Niu et al. (2009; 2010a; 2010b) HQ is the ratio of a contaminant's environmental concentration to a screening value selected for risk assessment of that substance (US EPA, 2009):

$$HQ = PEC / BC \tag{7}$$

where the PEC is the predicted environmental concentration in sediment of eight hydrocarbon groups (8-HCG), and the BC is the benchmark concentration (Battelle, 2007). If HQ is greater than 1.0, harmful effects can be expected; if HQ is less than 1.0, harmful effects are unlikely to occur. It should be noted that although oxygen depletion is considered in the computation of PEC, its effect is not included in the HQ calculation.

5.2 Modelling Results and Discussion

The mass balances of oil, represented by eight hydrocarbon groups (8-HCG), associated with OMA that would form from Cook Inlet (CI) sediment (sedimentation rates described by Khelifa et al., 2008) are plotted in Figure 71.

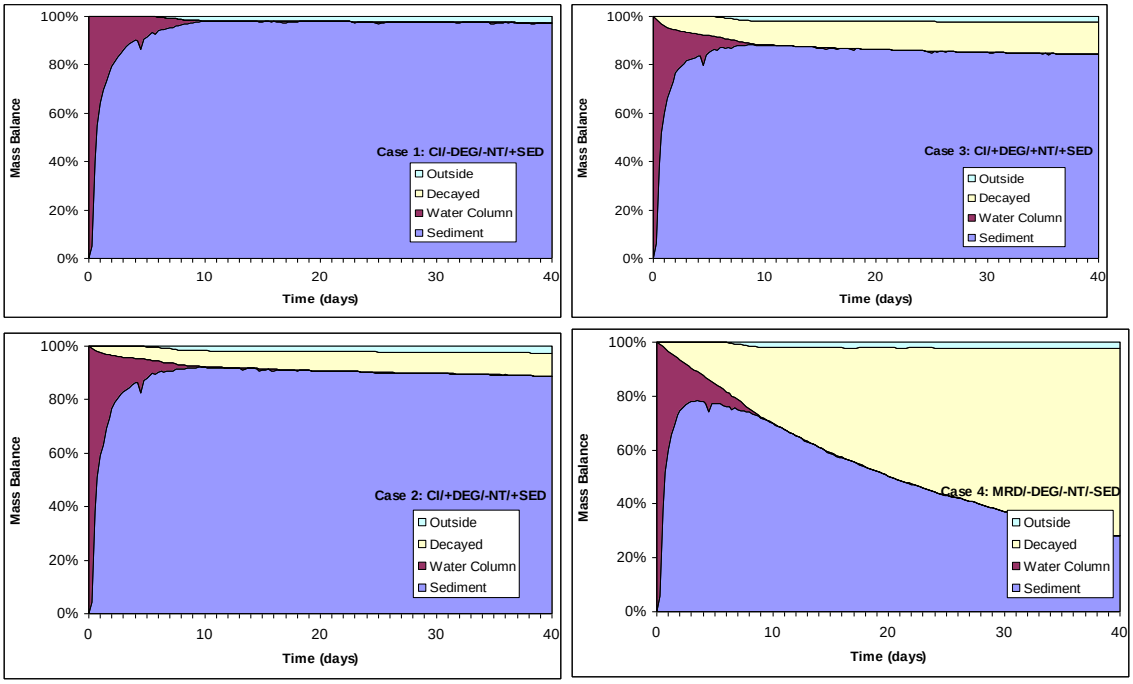

Figure 71: Mass balance for oil associated with OMA (CI); +DEG/-DEG is with/without degradation; +NT/-NT is high or low nutrient regime; +SED/-SED is with/without the use of the sediment model

For case 1, the OMA rapidly settled from the water column to the sediment and the amount settled was about 98% at 10 days. Due to the exclusion of the degradation mechanism, the amount of the 8-HCG associated with OMA in sediment changed little (97%) until the end of simulation for this case. With the inclusion of biodegradation (case 2), the amount of 8-HCG associated with OMA in sediment was reduced to 92% and 5.9% was biodegraded at ten days. After the first ten days, the rate of loss due to biodegradation becomes quite slow. The amount remaining in sediment at the end of the simulation was 88.8%. With higher nutrient concentration and increased biodegradation rate (case 3), the trend was similar to that of case 2 but with increased decay, such that at ten days, the amount in sediment was 88% and the amount degraded was 9.7%. The amount remaining in sediment at the end of the simulation was 84.5%.

The increase in degraded 8-HCG with higher nutrient concentrations is plotted in Figure 72 (left). It can be seen that the rate is much higher at the beginning (or in water column) than during the later stage (in sediment). This implies that the sediment model (equations 2 and 3) realizes a decrease in degradation as a result of oxygen depletion. This was confirmed by a comparison of cases 2 and 4 (in which the sediment model was not used) in Figure 72 (right). Notice that the amount in the water column is almost the same which indicated that it was unaffected by the inclusion of the sediment model. However, if the sediment model was excluded, the degradation in sediment became much higher. The

amount remaining in sediment for case 4 was 28% while the amount for case 2 was 88.8%.

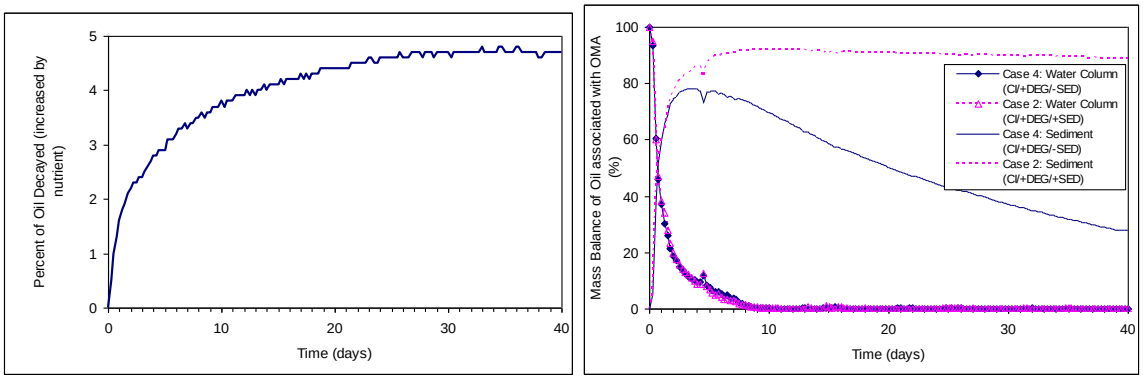

Figure 72: Effects on degradation under higher nutrient regime (case 2, at left), and with inclusion of the sediment model (case 2 vs. case 4, at right)

The results using Mississippi River Delta (MRD) sediment are depicted in Figure 73. A comparison of Figure 73 with Figure 71 shows that the deposition rates are much higher for MRD than CI. The time for 90% of the 8-HCG associated with OMA to be transported to the sediment was from 0.5 to 1.25 days for MRD, while the time required for CI was from four to six days. Rates for the cases with chemical dispersant were also higher than those without dispersant. This was due to higher oil fractions being associated with the larger MRD sediment particles (based on laboratory measurements by Khelifa et al., (2008), but it may not be the same for OMA generated from other oil or sediment types. Despite the deposition rate, the general trends of case 6 to 9 (MRD) are similar to that of case 2 and 3 (CI). Without chemical dispersant, the percentages of 8-HCG associated with OMA in sediment at the end of simulation were 94% and 89% at 5^{o} and 20^{o}C respectively. The amounts decayed were 5.1% and 10% at 5^{o} and 20^{o}C respectively. The higher degradation rate at 20^{o}C resulted in a 5% decrease of the total oil associated with OMA in sediment. The amount of 8-HCG decayed for the two cases with chemical dispersant at the end of simulation were 4.4% and 10.6% at 5^{o} and 20^{o}C respectively. Although the percentages in the presence of chemical dispersant were not significantly different from percentages without dispersant, the total amount of oil decayed or in sediment were different because oil associated with OMA was 16% of the total spilled oil without chemical dispersant as opposed to 23% with it (Figure 74).

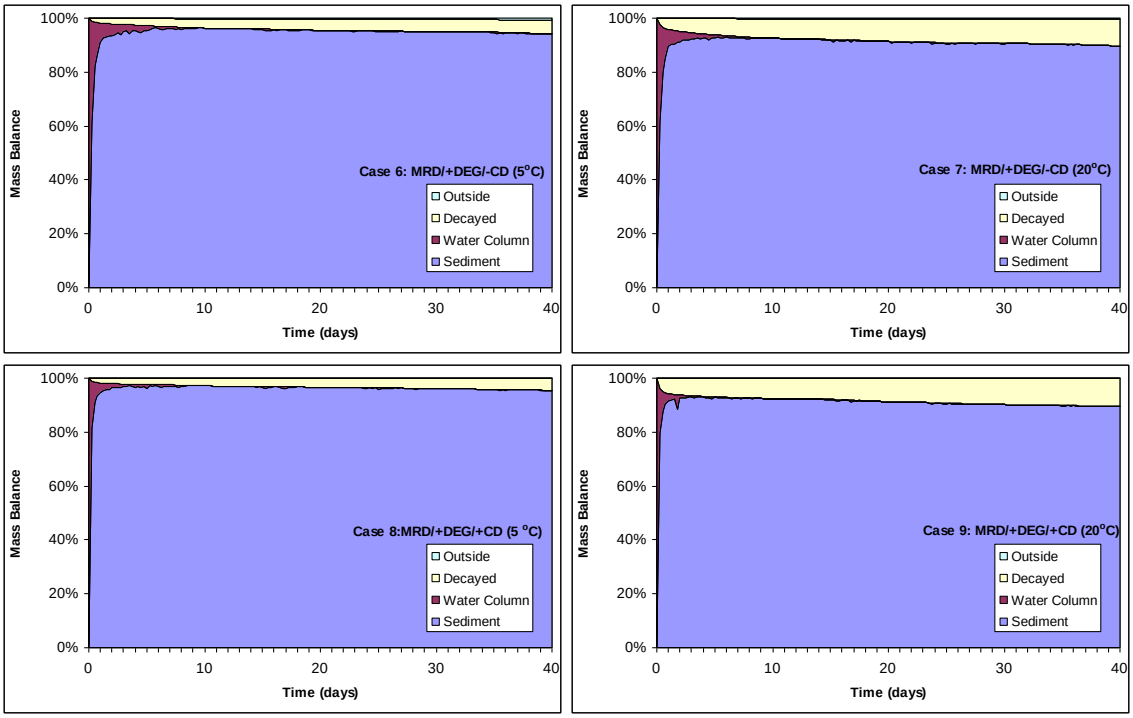

Figure 73: Mass balance for oil associated with OMA (MRD); +DEG/-DEG is with/without degradation; +CD/-CD is with or without chemical dispersant

The temperature effect for the case with chemical dispersant was more dramatic than the case without dispersant. The total amount of oil decayed due to increased temperature was 1.4% for cases with chemical dispersant while the amount was only 0.74% for those cases without dispersant. The effect of including the degradation process (cases 6 and 7 vs. case 5) can also be seen in Figure 74.

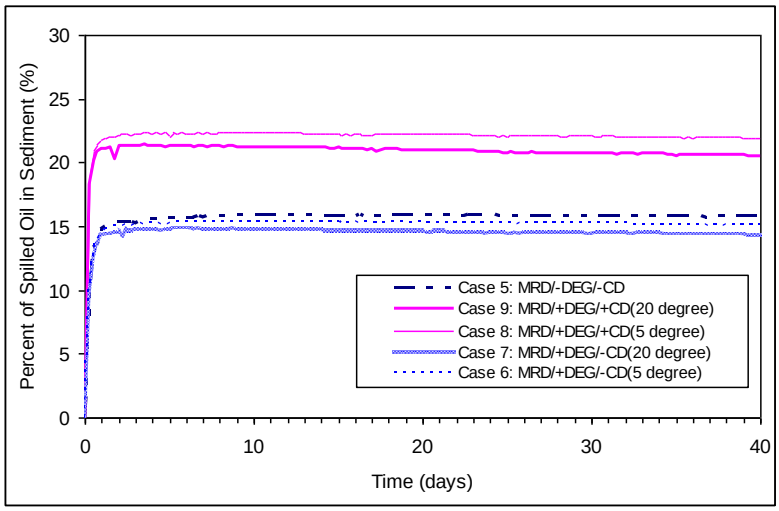

Figure 74: Percentage of spilled oil in sediment

6. Summary and Conclusions

This research project was focused on evaluating the feasibility of a cold water and Arctic marine oil spill countermeasure strategy based on the stimulation of (Oil-Mineral-Aggregates) OMA formation in combination with chemical dispersant. The project was an international collaborative effort between the Centre for Offshore Oil, Gas and Energy Research (COOGER), Fisheries and Oceans Canada, the Department of Chemical Engineering, University of New Brunswick, Canada, and the Center of Documentation, Research and Experimentation (CEDRE) on Accidental Water Pollution (Brest, France). The scope of work included bench studies on the formation and oil dispersion efficacy of OMA using different types of mineral fines; laboratory tests to determine how mineral fines affect chemical dispersant efficiency; and wave tank experiments to validate laboratory results at the mesoscale. A preliminary model was also developed to evaluate the level of environmental risk associated with the application of the spill response technologies under consideration.

Following consultation with the Scientific Authority of MMS (now the Bureau of Safety and Environmental Enforcement (BSEE)), three reference oils, Alaska North Slope (ANS), Arabian Light Crude (ALC), and an Intermediate Fuel Oil (IFO-40) were used in the laboratory Baffled Flask Test (BFT) protocol developed by the US EPA, and in a flow-through wave tank facility located at the Bedford Institute of Oceanography, Dartmouth, Nova Scotia, Canada. The petroleum hydrocarbons selected for evaluation were deemed to be representative of the range of crude oils and refined products that may be encountered in cold water and harsh environmental oil spill response operations, including the Arctic. The chemical dispersants used in the baffled flask tests were Corexit 9500 and Corexit 9527, the two most commonly stocked commercial chemical dispersants in North America. Alberta Sweet Blend, (ABS) and the chemical oil dispersant formulation, GAMLEN OD 4000, a product commercially available in Europe was also added to the study conducted by CEDRE (France) using the modified Institut Français du Pétrole (IFP) test protocol that has been accepted as "the standard" in Europe.

The layered silicate, kaolin, with chemical composition $Al_2Si_2O_5(OH)_4$, was used as the reference mineral fine in this study. Screening in previous studies (Lee, 2002; Stoffyn-Egli and Lee, 2002), had identified it to be among the most effective products involved in the formation of OMA. For comparison with previous studies conducted at higher

temperatures (Lee et al., 2009; Zhang et al., 2010), various samples of kaolin were chemically altered to provide test materials with higher levels of hydrophobicity (Molphy et al. 1994). CEDRE included bentonite and sepiolite in their screening of mineral fines using their modified IFP test apparatus. In the event of emergency spill response operations, these mineral fines should be readily available on many offshore oil and gas platforms as they are used in drilling mud formulations.

The objective of this research was to assess the feasibility of enhanced formation of OMA using a combination of mineral fines and chemical dispersants in a cold water environment. During the first phase of this study the potential role of dispersant and mineral fines in the enhancement of oil dispersion under low temperature conditions (2^{o}C) was investigated by the use of the BFT protocol. The results confirmed that a combination of dispersant and mineral fines could be the basis of an effective approach to remediate oil spills in cold environments. The data resolved the presence of optimal mineral-to-oil ratio (MOR) and dispersant-to-oil ratios (DOR) that facilitated the transport of oil from the surface into the water column. OMA morphology and size distributions revealed a correlation which indicates that the addition of more minerals could also result in a greater abundance of larger OMA. However, the laboratory observations also showed that excess additions of mineral fines (MOR >1:3) could be counterproductive in oil spill countermeasure operations due to an accumulation of OMA at the water surface. Consistent with the results of previous studies conducted at higher temperatures, chemically modified kaolin with higher levels of hydrophobicity than untreated kaolin exhibited a stronger interaction with oil droplets compared to the original kaolin. For this interaction an optimal maximum was also found to exist. The presence of dispersants can lower the hydrophobic nature of oil droplets and thus improve their interaction with hydrophilic minerals. Direct microscopic examinations showed that dispersant additions generally reduced the size of OMA and enhanced the effectiveness of the original, unaltered kaolin. There appeared to be no net advantage in adding dispersants to improve the interaction between modified kaolin and test oils.

The IFP test apparatus was modified for the conduct of experiments under low mixing energy with the integration of a LISST particle size analyzer to determine the efficacy of OMA formation using various types of mineral fines. In addition to the size distribution of mineral fines, the efficiency of oil dispersion was monitored by measurements of the amount of oil dispersed, and the stability of the dispersed oil in the water column. These factors are of importance as the proposed OMA/oil dispersant countermeasure procedure

is based on the transport of oil into the water column and its subsequent dilution to concentrations below toxicity threshold limits.

Low mixing energy conditions were used in this study to simulate Arctic conditions. There was evidence that the plume of dispersed oil would eventually coalesce and rise to the surface, thus preventing the effective use of chemical dispersants. As a result, there was interest in evaluating the addition of mineral fines which could facilitate the formation of OMA with a greater density than the oil itself to reduce its tendency to coalesce and rise to the surface. To test this hypothesis, low temperature experiments (5°C) were conducted using the IFP dilution test method (a low energy test procedure) with various types of mineral fines. Measurements were made of the amount of oil dispersed, the stability of the dispersion, oil distribution in 3 fractions after one hour settling time (coalesced on surface, stabilized in suspension in the water column, and settled at the bottom), and particle size (LISST-100X analysis of oil droplets and OMA).

Under the experimental conditions used in this study there was no clear advantage gained by the addition of mineral particles to the chemically dispersed oil. On the contrary, it appeared that the presence of mineral fines reduced the efficiency of the chemical dispersant. This may be due to the binding of the surfactant to the mineral fine particles associated with the formation of OMA, although this effect was not statistically significant. It should be noted that the tests with kaolin provided better results at the higher mixing energy levels within the first 10 minutes of the test assay. This observation confirms that the initial mixing energy is an important factor in promoting OMA formation. In response to the question, "Was the energy a limiting factor such that operating at higher energy would have led to increased dispersion efficiency?" it is important to note that preliminary field trials on the use of OMA in the Arctic have proposed using "propeller wash" to provide mixing energy to facilitate both oil droplet and OMA formation (Lee et al., 2011).

To evaluate the effectiveness of oil dispersion under different mixing energy regimes at low temperatures ($<8^{o}C$), studies were conducted in a flow-through wave tank facility located at the Bedford Institute of Oceanography, Dartmouth, Nova Scotia. This wave tank, constructed under a partnership between Fisheries and Oceans Canada (DFO) and the US Environmental Protection Agency (US EPA), is capable of reproducibly generating breaking and regular non-breaking wave conditions. Mixing energy levels used in the current study included both regular (non-breaking) waves and breaking waves. The wave tank was operated in flow-through mode to simulate dilution effects

from water currents. Fine mineral particles of kaolin were evaluated for their potential to form OMA at three different MORs: 0, 1:10 and 1:5. The test oils included weathered ALC crude oil, ANS crude oil, and IFO-40 fuel oil. In all tests, Corexit 9500 was applied at a DOR of 1:25, as recommended by the manufacturer.

Oil, dispersant and mineral fines were premixed and added to the wave tank in a manner that would mimic the mixing of oil, fines, and dispersant by mechanical means during response operations. The dispersed oil concentration, dispersed particle size distribution, and the interfacial tension were measured to track the performance of dispersant in the presence and absence of mineral fines, and to evaluate the overall oil dispersion efficiency under the different mixing energy conditions.

Experimental data showed that all of the tested oils could be dispersed in cold water conditions (<8^{o}C) given sufficient mixing energy levels. Consistent with the results of a preliminary field study conducted in ice-infested waters (Lee et al., 2011), high mixing energy, particularly in the initial stages, appeared beneficial to the overall efficiency of OMA formation. Adding chemical dispersants stimulated the droplet formation rate at low temperature in a manner similar to that observed at normal seawater temperature. Both the type and concentration of mineral fines influenced the final concentration and stability of OMA formed in the water. Adding mineral fines in the absence of sufficient mixing energy did not improve oil dispersion efficiency. This is consistent with the theory that OMA formation is predominantly based on the stabilization of oil droplets by mineral fines. As reported in the laboratory studies, an excess of mineral fines under high mixing energy may have a negative impact to the overall stability of dispersed oil in the water. This is because the excess mineral fines promote the aggregation of oil droplets into larger OMA which might resurface or settle, therefore reducing the amount oil suspended in the water column.

Real-time LISST-100X analysis of ALC crude oil distribution within the wave tank expressed as both total particle concentration (TPC; sum of all particle concentrations between 2.5-500 μm) and volume mean diameter (VMD; volume weighted mean diameter of all particles) showed that the application of minerals under regular wave conditions resulted in increased oil-mineral aggregation. The highest mineral dose of 50 g (MOR of 1:5 – a value lower than the highest values evaluated in the laboratory studies) produced the lowest VMD values. Compared to ALC, the effects of mineral addition on the dispersion of ANS was less apparent under both regular and breaking wave conditions, with TPC plots roughly overlapping for all three treatments.

The combined effects of mineral addition and wave energy on crude oil dispersion were most evident in the LISST data for IFO-40 oil. This was due to that fact that regular waves lacked sufficient energy to generate and maintain small OMA particles from the higher viscosity IFO-40 oil, and instead formed oil-mineral agglomerates >100 μm as evidenced by the VMD plots. These findings indicate that for heavier oils such as IFO-40, mineral dosage and wave energy play key roles in the effectiveness of OMA formation and crude oil dispersion.

Breaking waves had significant effects on the dispersion and transport of oiled particles in the flow-through wave tank. The increased energy dissipation rates and turbulent diffusion coefficients associated with the breaking wave conditions enhanced oil dispersion and the particle concentrations were more stable as a function of time. The observed coalescence of small particles into larger ones within the wave tank seems to be enhanced in the presence of mineral fines, however this may be an artifact associated with hydrodynamic conditions linked to the design of the test system which has a wave absorbing section downstream of the area of experimental data collection. In the open ocean environment, the coalescence of small particles into larger ones may not be significant given a sufficient dilution rate so that the particle collision frequency is dramatically reduced.

The combined effects of chemical dispersants and mineral fines under different wave conditions on dynamic dispersion effectiveness (DDE) over the duration of the entire experiment can be evaluated by computing the fraction of dispersed oil flowing out of the wave tank and the residual dispersed oil in the water column at the end of each experiment. The DDE data indicated that dispersion of ANS and ALC was relatively effective in both regular and breaking waves. In regular waves, the high dose (50 g) of mineral fines slightly increased the total concentration of dispersed oil remaining in the water column. From these data it appears that to achieve a high rate of DDE, adding mineral fines is probably not necessary under the high mixing energy of breaking waves, because the chemical dispersant on its own leads to good dispersion efficiency. There is considerable concern that OMA with densities greater than seawater can settle to the seabed and pose potential risks to benthic organisms. To understand the transport and fate of oil associated with OMA and evaluate their potential risks, a preliminary integrated hydrodynamic, fate/transport and risk assessment modeling system was developed and evaluated under two test conditions within this study. To fully predict long-term effects this new approach considered the following fates for OMA in the water column: 1) advection, 2) diffusion, 3) settling, and 4) biodegradation of oil. The fates in sediment

were: 5) deposition of OMA, 6) burial, 7) oxygen depletion, 8) biodegradation, and 9) re-suspension. The application of this model is currently limited by the availability of field data. Proposed field trials in the future will support application and validation testing of this system, for which development is ongoing.

References

Battelle. 2007. *Sediment Toxicity of Petroleum Hydrocarbon Fractions*. Report prepared for Massachusetts Department of Environmental Protection. Duxbury, MA. 52 pp.

Bragg, J. R. and S. H. Yang. 1995. Clay-oil flocculation and its effects on the rate of natural cleansing in Prince William Sound following the Exxon Valdez oil spill. In Wells, P.G., Butler, J.N. and Hughes, J.S. (eds.), *Exxon Valdez Oil Spill - Fate and Effects in Alaskan Waters*. American Society for Testing and Materials, Philadelphia, PA.

Cole, M. G., T. L. King and K. Lee. 2007. Analytical technique for extracting hydrocarbons from water using sample container as extraction vessel in combination with a roller apparatus. Canadian Technical Report on Fisheries and Aquatic Science. 2733: vi + 12p.

Cui, Y. N., M. Threlfall and J. S. van Duijneveldt. 2011. Optimizing organoclay stabilized Pickering emulsions. *Journal of Colloid and Interface Science* 356: 665-671.

Delvigne, G. A. L., J. A. Van del Stel and C. E. Sweeney. 1987. *Measurements of Vertical Turbulent Dispersion and Diffusion of Oil Droplets and Oil Particles*. US Department of the Interior, Minerals Management Service, Anchorage, Alaska. 501 pp.

Garrett, R. M., I. J. Pickering, C. E. Haith and R. C. Prince. 1998. Photooxidation of crude oils. *Environmental Science & Technology* 32: 3719-3723.

Khelifa, A., M. Fingas and C. Brown. 2008. *Effects of dispersants on oil-SPM aggregation and fate in US coastal waters*. Report for Coastal Response Research Center at University of New Hampshire, NH.

Lee, K., Z.Li, B. Robinson and P.E. Kepkay 2011. Oil spill countermeasures in the Arctic. N. Bellefontaine and Olof Linden (eds,), WMU Publications, Malmo, Sweden. pp. 93-108.

Lee, K., Z. Li, B. Robinson, P. E. Kepkay, M. Blouin and B. Doyon. 2011. Field trials of *in-situ* oil spill countermeasures in ice-infested waters. *Proceedings of the 2011 International Oil Spill Conference*, May 23-26, Portland, OR, USA. 16 pp.

Lee, K. 2002. Oil-particle interactions in aquatic environments: Influence on the transport, fate, effect and remediation of oil spills. *Spill Science & Technology Bulletin* 8: 3-8.

Lee, K., Z. Li, H. Niu, P. Kepkay, Y. Zheng, M. Boufadel and Z. Chen. 2009. *Enhancement of oil-mineral-aggregate formation to mitigate oil spills in offshore oil and gas activities*. Final Report (Contract No. M07PC13035) submitted to Minerals Management Service. 91p. March 30, 2009.

Lee, K. and P. Stoffyn-Egli. 2001. Characterization of oil-mineral aggregates. In: *Proceedings of the 2001 International Oil Spill Conference*. American Petroleum Institute, Washington D.C. pp. 991-996

Lee, K., P. Stoffyn-Egli and E. H. Owens. 2001. Natural dispersion of oil in a freshwater ecosystem: Desaguadero Pipeline Spill, Bolivia. In: *Proceedings of the 2001 International Oil Spill Conference*. American Petroleum Institute, Washington, DC, Publication no. 14710B, pp. 1445-1448.

Lee, K., P. Stoffyn-Egli and E. H. Owens. 2002. The OSSA II pipeline oil spill: Natural mitigation of a riverine oil spill by oil-mineral aggregate formation. *Spill Science & Technology Bulletin* 7: 149-154.

Lee, K., P. Stoffyn-Egli, G. H. Tremblay, E. H. Owens, G. A. Sergy, C. C. Guenette and R. C. Prince. 2003. Oil-mineral aggregate formation on oiled beaches: Natural attenuation and sediment relocation. *Spill Science & Technology Bulletin* 8: 285-296.

Lee, K., A. M. Weise and S. St-Pierre. 1996. Enhanced Oil Biodegradation with Mineral Fine Interaction. *Spill Science & Technology Bulletin* 3: 263-267.

Lessard, R. R. and G. Demarco. 2000. The significance of oil spill dispersants. *Spill Science & Technology Bulletin* 6: 59-68.

Li, Z., P. Kepkay, K. Lee, T. King, M. C. Boufadel and A. D. Venosa. 2007. Effects of chemical dispersants and mineral fines on crude oil dispersion in a wave tank under breaking waves. *Marine Pollution Bulletin* 54: 983-993.

Li, Z., K. Lee, T. King, M. C. Boufadel and A. D. Venosa. 2009. Evaluating crude oil chemical dispersion efficacy in a flow-through wave tank under regular non-breaking wave and breaking wave conditions. *Marine Pollution Bulletin* 58: 735-744.

Menon, V. B. and D. T. Wasan. 1988. A review of the factors affecting the stability of solids-stabilized emulsions. *Separation Science and Technology* 23: 2131-2142.

Muschenheim, D. K. and K. Lee. 2002. Removal of oil from the sea surface through particulate interactions: Review and prospectus. *Spill Science & Technology Bulletin* 8: 9-18.

Nciri, H., M. Benna-Zayani, M. Stambouli, N. Kbir-Ariguib, M. Trabelsi-Ayadi, V. Rosilio and J. L. Grossiord. 2009. Influence of clay addition on the properties of olive oil in water emulsions. *Applied Clay Science* 43: 383-391.

Niu, H., Z. Li, P. Kepkay, K. Lee and J. Mullin. 2009. Lagrangian simulation of the transport of oil-mineral-aggregates (OMAs) and assessment of their potential risks. In: *Proceedings of the 32nd AMOP Technical Seminar on Environmental Contamination and Response*, Vancouver, Canada, pp.705-721.

Niu, H., Z. Li, K. Lee, P. Kepkay and J. Mullin. 2010a. A method for assessing environmental risks of oil-mineral-aggregate to benthic organisms. *Human and Ecological Risk Assessment*. 16:762-782.

Niu, H., Z. Li, K. Lee, P. Kepkay and J. Mullin. 2010b. Modeling the transport of oil-mineral aggregates (OMAs) in the marine environment and assessment of their potential risks. *Environmental Modeling and Assessment.* In Press.

Niu, H., Z. Li, K. Lee, P. Kepkay and J. Mullin. 2010c. The effects of waves and currents on the transport of oil-mineral-aggregates (OMAs) and their potential risks to benthic organisms. In: *Proceedings of the 33rd AMOP Technical Seminar on Environmental Contamination and Response*. June 7-9, 2010, Halifax, NS, Canada, pp.623-634.

Omotoso, O. E., V. A. Munoz and R. J. Mikula. 2002. Mechanisms of crude oil-mineral interactions. *Spill Science & Technology Bulletin* 8: 45-54.

Owens, E. H., G. A. Sergy, C. C. Guenette, R. C. Prince and K. Lee. 2003. The reduction of stranded oil by *in situ* shoreline treatment options. *Spill Science and Technology Bulletin* 8: 257-272.

Reed, M. and B. Hetland. 2002. DREAM: a dose-related exposure assessment model, Technical Description of physical-chemical fates components. In*: Proceedings of the SPE Internayional Conference on Health, Safety and Environment in Oil and Gas Exploration and Production*. Kuala Lumpur, Malaysia, 23 pages.

Richter-Menge, J., J. Overland, M. Svoboda, J. Box, M. J. J. E. Loonen, A. Proshutinsky, V. Romanovsky, D. Russell, C. D. Sawatzky, M. Simpkins, R. Armstrong, I. Ashik, L.-S. Bai, D. Bromwich, J. Cappelen, E. Carmack, J. Comiso, B. Ebbinge, I. Frolov, J. C. Gascard, M. Itoh, G. J. Jia, R. Krishfield, F. McLaughlin, W. Meier, N. Mikkelsen, J. Morison, T. Mote, S. Nghiem, D. Perovich, I. Polyakov, J. D. Reist, B. Rudels, U. Schauer, A. Shiklomanov, K. Shimada, V. Sokolov, M. Steele, M.-L. Timmermans, J. Toole, B. Veenhuis, D. Walker, J. Walsh, M. Wang, A. Weidick and C. Zöckler. 2010. Arctic Report Card. Accessed 14 April 2011: http://www.arctic.noaa.gov/reportcard/.

Rye, H., M. Reed, I. Durgut and M. K. Ditlevsen. 2006a. *Documentation report for the revised DREAM model*. ERMS Report No. 18, SINTEF Marine Environmental Research, Trondheim, Norway.

Rye, H., M. Reed, I. Durgut and M. K. Ditlevsen. 2006b. The use of diagenetic equations to predict impact on sediment due to discharge of drill cuttings and mud. In: *Proceedings of International Marine Environmental Modeling Seminar*, Rio, 9-11 October, 2006.

Sørensen, O. R., H. Kofoed-Hansen and O. P. Jones. 2006. Numerical modeling of wave-current interaction in tidal areas using an unstructured finite volume technique. In: *Proceedings of the 30th International Conference on Coastal Engineering (ICCE 2006)*. San Diego, USA.

Sørensen, O. R., H. Kofoed-Hansen, M. Rugbjerg and L. S. Sørensen. 2004. A third-generation spectral wave model using an unstructured finite volume technique. In: *Proceedings of the 29th International Conference on Coastal Engineering (ICCE 2004).* Lisbon, Portugal.

Stepaniyan, O. 2008. Effects of crude oil on major functional characteristics of macroalgae of the Barents Sea. *Russian Journal of Marine Biology* 34: 131-134.

Stoffyn-Egli, P. and K. Lee. 2002. Formation and characterization of oil-mineral aggregates. *Spill Science & Technology Bulletin* 8: 31-44.

US EPA. 2009. Ecological risk assessment step 2 exposure estimation/risk calculations. Available from http://www.epa.gov/region5superfund/ecology/html/erasteps/erastep2.html#hazquot.

Yan, N. X., M. R. Gray and J. H. Masliyah. 2001. On water-in-oil emulsions stabilized by fine solids. *Colloids and Surfaces a-Physicochemical and Engineering Aspects* 193: 97-107.

Zhang, H., M. Khatibi, Y. Zheng, K. Lee, Z. Li and J. V. Mullin. 2010. Investigation of OMA formation and the effect of minerals. *Marine Pollution Bulletin 60*: 1433-1441.